



UNIVERSITÀ
DEGLI STUDI
DI PADOVA

Head Office: Università degli Studi di Padova

Department of Comparative Biomedicine and Food Science

DOCTORAL COURSE IN VETERINARY SCIENCE

XXXI CYCLE

**STUDY ON NORMAL AND TUMORAL CELL
SUBPOPULATIONS AND THEIR INTERACTIONS IN THE
MAMMARY GLAND CANCER OF HUMANS AND ANIMALS**

Coordinator: Prof. Valentina Zappulli

Supervisor: Prof. Valentina Zappulli

Ph.D. student: Dr. Alessandro Sammarco

CONTENTS

ABSTRACT	5
INTRODUCTION	7
MAMMARY GLAND MORPHOLOGY	7
MAMMARY GLAND CANCER IN WOMEN, DOGS, AND CATS	8
INTRA-TUMOR HETEROGENEITY AND CANCER STEM CELLS	10
SIGNALING PATHWAYS IN CANCER STEM CELLS	12
MAMMARY CANCER METASTASIS	14
INTERCELLULAR COMMUNICATION THROUGH EXTRACELLULAR VESICLES	16
AIMS	21
MATERIALS AND METHODS	23
Phase I: isolation and characterization of human, canine, and feline cancer stem cells	23
Phase II: epithelial-to-mesenchymal transition and Wnt/ β -catenin and Hippo pathways	25
Phase III: <i>in vivo</i> model of mammary cancer metastasis	28
Phase IV: intercellular communication through extracellular vesicles	31
RESULTS	37
Phase I: isolation and characterization of human, canine, and feline cancer stem cells	37
Phase II: epithelial-to-mesenchymal transition and Wnt/ β -catenin and Hippo pathways	44
Phase III: <i>in vivo</i> model of mammary cancer metastasis	50
Phase IV: intercellular communication through extracellular vesicles	55
DISCUSSION	59
CONCLUSIONS	85
ACKNOWLEDGEMENTS	87
REFERENCES	89
SUPPLEMENTARY DATA	115

ABSTRACT

Human breast cancer (HBC), canine (CMT), and feline mammary tumors (FMT) are extremely common and are characterized by a remarkable both inter- and intra-tumor heterogeneity. Intra-tumor heterogeneity is due to the coexistence of cancer cells that differ between each other in terms of phenotypic, genetic, behavioral characteristics, and metastatic potential. Cancer stem cells (CSCs) are thought to be responsible for such heterogeneity, resistance to therapy, and metastasis development. Several pathways are altered in CSCs, such as the oncogenic Wnt/ β -catenin and Hippo pathways, and CSCs are associated to the epithelial-to-mesenchymal transition (EMT) process.

The aims of this study were to i) isolate and characterized mammary CSCs; ii) investigate EMT process and Wnt/ β -catenin and Hippo pathways in mammary cancer of the three species; iii) establish a metastatic mouse model of breast cancer seeking for genes responsible of metastatic dissemination; iv) isolate and characterize extracellular vesicles (EVs), which is one of the main forms of intercellular communication, from canine and feline mammary tumors as well as study the role that EVs play during tumor development.

CSC-like cells were isolated from established canine and feline mammary tumor cell lines (CYPp and FMCp, respectively) and phenotypically and molecularly characterized for common CSC markers: CD44, CD24, CD133, SOX2, OCT4. Moreover, gene (qPCR) and protein (IHC and WB) expression of Wnt/ β -catenin and Hippo pathways-related molecules (β -catenin, CCND1, YAP, TAZ, CTGF, ANKRD1) as well as protein expression (IHC) of EMT-related molecules (E-cadherin, SNAIL, TWIST, ZEB) were evaluated in a subset of human, canine, and feline mammary cancer tissues, that were also phenotypically characterized for the following markers: CK8/18, CK5/6, CK14, CD44, and vimentin. Additionally, triple negative breast cancer (TNBC) cell line MDA-MB-231 was used to establish a clinically relevant *in vivo* metastatic model. Finally, EVs were isolated and characterized from CYPp and FMCp and human glioblastoma-derived EVs were used to study tumor angiogenesis.

We found that CD44, CD133, SOX2, and OCT4 expression increase in CSC-like cells (mammospheres) compared to parental adherent cells, therefore they could be used as useful markers in CMTs and FMTs. Wnt/ β -catenin and Hippo pathways seem to be deregulated at a post-transcriptional level in HBCs, CMTs, and FMTs. Interesting similarities were confirmed between TNBCs and FMTs, as well as between ER⁺ HBC and CMTs. In our metastatic model, mice developed distant metastases and we found a few genes that might play a role during metastatic dissemination. Among these, caspase 3 seems to be involved in brain metastases. Additionally, EVs were isolated from CYPp and FMCp, visualized by transmissible electron microscopy, counted using nanoparticle tracking analysis, and characterized by immunogold and WB (Alix, CD63, TSG101). Finally, using a human glioblastoma cell line (GBM8) we demonstrated that EVs are directly involved in tumor angiogenesis.

Overall, this study confirms the use of dogs and cats as spontaneous models of mammary cancer development due to highly interesting biological similarities among the three species. Also, identification of EVs in CMTs and FMTs opens an interesting unexplored field in veterinary medicine.

INTRODUCTION

MAMMARY GLAND MORPHOLOGY

The mammary gland is an exocrine gland present in mammals that produces milk. It develops along the "milk line" and parallel to the midline in the abdominal wall. The number and positioning of mammary glands varies among different animals. The number of teats varies from 2 (in most primates, in goats, in sheeps, and in horses), to 4 (in cows), to 8 (in cats), to 10 (in dogs and in mice), to 18 (in pigs) (Nickel et al., 1985).

Generally, in all mammals, the mammary gland is a tubuloalveolar gland, which is divided into lobules by interlobular connective tissue. The anatomical components of the mammary gland are: parenchyma (alveoli), ducts, stroma (connective tissue), blood vessels, and nerves (Silver, 1966; Dellmann and Carithers, 1996; Salomon et al., 2008). Alveoli are composed of simple cuboidal to columnar secretory epithelium, which produces milk. Additionally, the secretory epithelium is lined with myoepithelial cells, which are covered by a basal lamina. The myoepithelial cells possess contractile filaments and are responsible for squeezing the luminal/epithelial cells in order for the milk to be excreted. Alveoli proceed into intralobular ducts, which then continue into the interlobular ducts. The latter convene into lactiferous ducts, that open into a lactiferous sinus, which continues in the teat sinus opening onto the teat surface via the papillary duct. These ducts are covered by slightly different epithelium. The smallest ducts are lined with a simple cuboidal epithelium that might secrete milk in lactating mammary glands. Larger ducts and sinuses have a bistratified cuboidal to columnar epithelium. Papillary ducts are lined by a keratinized stratified squamous epithelium. Myoepithelial cells are typically abundant in the ducts (Dellmann and Carithers, 1996).

Interalveolar stromal tissue is relatively sparse and well vascularized, whereas interlobular septa are formed by dense irregular connective tissue with elastic fibers (Barone, 1990; Dellmann and Carithers, 1996; Salomon et al., 2008).

Different arteries supply the mammary gland with blood and the venous drainage parallels the arterial supply. Each mammary gland has a network of small lymphatic vessels, which joins similar networks in the subcutaneous tissue and conjugates in larger vessels going to the draining regional lymph nodes (Miller et al., 1964; Silver, 1966). The lymphatic circulation is quite different among the species and it depends on the number and location of the mammary glands. The lymphatic system is extremely important in the spread of tumor cells. It is thought that mammary neoplasia can change the lymphatic drainage pattern by forming new drainage channels (Pereira et al., 2003).

In the normal mammary gland, the cell populations can be recognized based on a different immunophenotype easily assessed by immunohistochemistry. With regards to cytokeratins that are intermediate filaments characteristically found in epithelial cells (Moll et al., 1982; Espinosa de Los Monteros et al., 1999), the luminal epithelial layer, is labeled by cytokeratins 7, 8, 18, and 19 (Taylor-Papdimitriou and Lane, 1987). Basal/myoepithelial cells are labeled by cytokeratins 5, 6, 14, 17. Myoepithelial cells also express

other markers, such as p63, vimentin, P-cadherin, CD10, epidermal growth factor receptor (EGFR), maspin, and 14-3-3 sigma protein (Destexhe et al., 1993; Espinosa de Los Monteros et al., 2005; Gama et al., 2003; Gama et al., 2009; Gama et al., 2004; Griffey et al., 1993; Hellmen et al., 1989; Sanchez-Cespedes et al., 2013; Sorenmo et al., 2011; Vos et al., 1993). Additionally, due to their contractile phenotype, myoepithelial cells express smooth muscle-specific proteins such as smooth muscle actin (SMA) and calponin (Destexhe et al., 1993; Espinosa de Los Monteros et al., 2002; Gama et al., 2003).

The different steps of cell differentiation have not been precisely defined (Birnbaum et al., 2004). Bocker and collaborators demonstrated that in the human mammary gland luminal and myoepithelial cells seem to have intermediate stages of maturation, expressing various markers. A small subpopulation of cells that are CK5 positive but negative for CK8, CK18, CK19, and SMA have been identified, these cells have stem cell features and have the ability to differentiate toward either the luminal or the basal phenotype (Bocker et al., 2002).

MAMMARY GLAND CANCER IN WOMEN, DOGS, AND CATS

Human breast cancer (HBC) is the most common neoplasm in women and the second main cause of cancer-related death in America and accounts for roughly 30% of all new cases of cancer diagnosed in female patients (Pearlman et al., 2017). In Europe, 28.2% of women are expected to develop HBC in 2018, with a mortality of 16.2% (Ferlay et al., 2018).

The main predisposing factors of HBC are age, early menarche, late menopause, obesity in postmenopausal women, high concentration of endogenous estrogen, and heredity (Kontomanolis et al., 2018). HBC is a heterogeneous group of disease with variable clinical behavior (Ali et al., 2014). Morphologically, this diversity is reflected in several different histologic types of HBC with their distinct microscopic appearances and associated clinical outcomes. However, 70% to 80% of them are invasive ductal carcinomas (IDC), which show a remarkable heterogeneity with respect to tumor morphology, underlying molecular biology, and prognosis (Lakhani et al., 2012). The classification of breast cancer is still mainly based on the histologic subtype, tumor grade, and stage, which provide an idea of the degree of tumor differentiation and growth rate (Provenzano et al., 2018). The most recent classification system, based on gene expression profiling as well as immunophenotypic markers, classifies HBC into 3 main subtypes, including estrogen receptor (ER)-positive, HER2-positive, and triple-negative (ER, progesterone receptor [PR], and HER2-negative: triple negative breast cancer [TNBC]) groups (Provenzano et al., 2018). This classification is highly clinically relevant because therapeutic regimens are centered on antiestrogen therapy, chemotherapy, and HER2-targeted agents. ER-positive tumors comprise up to 75% of all breast cancer patients and they are typically well-differentiated, less aggressive, and associated with better outcome after surgery (Dunnwald et al., 2007) than ER-negative tumors. HER2-positive tumors are characterized by HER2 gene amplification or protein over-expression and they are associated with poor prognosis and good clinical outcome receiving systemic chemotherapy (Wolff et al., 2007; Bartlett et al., 2003; Chia et al., 2008). TNBC is the most aggressive subtype and tends to have a poor prognosis with a high risk of distant metastasis and death within the first

3-5 years after the diagnosis. Due to the lack of well-defined molecular targets, the treatment of TNBCs relies on chemotherapy, mainly anthracycline, taxanes based regimen (Shi et al., 2018).

Mammary tumors are also the most common neoplasm in most mammalian small animals including felines and canines and the need for appropriate animal models in cancer research has led, over the past 20 years, to the use of pet animals with spontaneous tumors as a valuable and underutilized resource (Abdelmegeed et al., 2018; Wiese et al., 2013; Caliari et al., 2014)

In the feline species, mammary tumor is the third most common cancer in cats, and the most common tumor in queens (Zappulli et al., 2005). It looks like there is an extremely decreased risk of feline mammary tumors (FMT) development in cats neutered between 6 months and 1 year of age. Conversely, the risk of mammary tumor development increases in cats under regular, continued progestin treatment (Adega et al., 2016). Most FMTs are hormone-independent carcinomas (80-90%) of the simple type (proliferation of a single neoplastic cell component: epithelial luminal) that are characterized by an aggressive biological behavior (Nielsen et al., 1967; Hayden et al., 1989; Misdorp et al., 1999; Zappulli et al., 2015). FMTs are frequently high-grade (III) invasive carcinomas (80-90%) and are characterized by rapid progression and metastasis to the lungs (83%), local lymph nodes (83%), liver (25%), and pleura (22%) (Hahn et al., 1977; Hahn et al., 1994). FMTs often lack significant levels of ER, PR, and HER2 positivity (Rasotto et al., 2011), constituting a remarkable spontaneous model for the human TNBC. Additionally, FMTs have been associated with a low expression of basal cytokeratins and vimentin, and a basal-like phenotype has been identified by IHC and molecular analysis (Caliari et al., 2014). FMTs share a broad clinicopathologic, demographic, and epidemiological similarity with the HBC (Siegel et al., 2013), which, beside the hormonal receptor status, are often simple epithelial tumors, as in cats (Adega et al., 2016).

In the adult female dog, spontaneous mammary tumors are the most common neoplasm and malignant tumors account for up to 50% of the cases (Sleeckx et al., 2011; Sorenmo et al., 2003).

Similar to FMTs, different factors, such as age, breed, genetic predisposition, diet, have an influence on the development of canine mammary tumors (CMTs). Ovary(ohtyster)ectomy at an early age, as preventive measure, can significantly reduce the risk of developing CMTs (Sleeckx et al., 2011). CMT is a heterogeneous group of disease and the histological classification is rather intricate (Goldschmidt et al., 2011). Most CMT are of epithelial origin (simple tumors), some consist of both epithelial and myoepithelial tissues (complex tumors), a few tumors are a combination of epithelial, myoepithelial and cartilaginous/bone tissue (mixed tumors). Additionally, tumors of mesenchymal origin can arise in the mammary gland (Goldschmidt et al., 2011). Survival can vary significantly depending on several factors, such as age, tumor size, tumor stage, histopathological subtype, tumor grade, clinical behavior of the tumor, and lymph node involvement, just to name a few (Rakha et al., 2010).

Several recent publications describe the advantages of canine mammary carcinomas (CMCs) as a model of HBC because of their similarities, such as relative age of onset, incidence, risk factors, biological behaviour, metastatic pattern and some histopathological and molecular features (Rivera and von Euler, 2011).

The evidence of these extremely interesting similarities between HBC and feline and canine mammary tumors support the use of dogs and cats as useful spontaneous animal models to investigate tumor biology, to study the clinical behavior, and to predict efficacy as well as side effects of anticancer compounds and treatments for HBC (Weise et al., 2013). Similarities in predisposing factors, clinical behavior, and biological features, such as genetic alterations, between humans and dogs and cats have raised interest even further (Sleekx et al., 2011). In addition, FMCs and metastatic CMCs still lack adequate treatments and often lead to death of the patients (Sleekx et al., 2011; Zappulli et al., 2015).

INTRA-TUMOR HETEROGENEITY AND CANCER STEM CELLS

Mammary gland tumors in humans, dogs, and cats are not a single entity. As already stated, different subtypes are associated with different clinical outcomes. Mammary cancer in the three species exhibits both inter- and intra-tumor heterogeneity as a consequence of genetic and non-genetic alterations (Polyak, 2007).

Inter-tumor heterogeneity reflects the differences between patients, which result in staging systems and morphological classifications of breast cancer (Skibinski and Kuperwasser, 2015). Intra-tumor heterogeneity is defined as the coexistence of cancer cells that differ between each other in terms of phenotypic, genetic, behavioral characteristics or metastatic potential within the primary tumor and between the primary tumor and its metastasis. Such diversity can be due to genetic and epigenetic factors and to non-hereditary mechanisms such as adaptive responses to several stimuli or variation in signaling pathways (Marusyk et al., 2012; Marusyk and Polyak, 2010). Two theories describe the origin and maintenance of intra-tumor heterogeneity: the cancer stem cell (CSC) hypothesis and the clonal evolution model. Initially, these two theories were considered to be mutually exclusive, but are now recognized as potentially complementary (Campbel and Polyak, 2007). Both theories state that tumors originate from single cells that somehow acquire molecular alterations, develop indefinite proliferative potential, and assume that microenvironment might have an impact on the composition of a tumor (Campbel and Polyak, 2007). Specifically, CSC hypothesis suggests a hierarchical organization of tumor cells, with a minority of undifferentiated CSCs that are able to aberrantly differentiate into heterogeneous groups of cells and are therefore responsible for the intra-tumor heterogeneity (Meacham et al., 2013). The clonal evolution model theory suggests that cancer cells acquire genetic aberrations during tumorigenesis and tumor evolution and gives rise to a natural selection eventually leading to the generation of more aggressive subclones (Zardavas et al., 2015; Martelotto et al., 2014).

Human CSCs have several features that are similar to normal tissue stem cells, including i) self-renewal, which is the ability to renew indefinitely in an undifferentiated status; ii) unlimited proliferative potential; iii) slow replication rate; iv) high DNA repair capacity; and v) the ability to differentiate into virtually all cell types found in a tumor (Wicha et al., 2006; Crabtree and Miele, 2018). CSCs are described as those cells that are able to form tumors in a relatively permissive environment (that is, immunosuppressed mice) (Meacham and Morrison, 2013). Moreover, CSCs are thought to be responsible of resistance to chemotherapy/radiotherapy, development of local relapses and metastasis formation (Reya et al., 2001; Wang et al., 2013).

Mammosphere formation assays are widely used to assess the behavior of these cells. In these assays, breast CSCs (BCSCs) are grown in absence of serum, with the addition of epidermal growth factor (EGF) and fibroblast growth factor (FGF) in low adherence tissue culture dishes (Lombardo et al., 2015; Dontu et al., 2004). Growing under these conditions, cells give rise to spheroids, which are commonly called "mammospheres" and contain stem-cell associated features, including activation of stem cell related signaling pathways (Dontu et al., 2003).

The identification of such population in the mammary gland is often defined on the basis of cell-surface markers. Cluster of differentiation 44 (CD44) and cluster of differentiation 24 (CD24) are mainly used to identify BCSCs. In addition to these, over the years, other markers have been identified, such as ALDH1, CD133, and CD49f (Meyer et al., 2010; Shima et al., 2016). These cells are often associated with chemotherapy and radiotherapy resistance (Crabtree and Miele, 2018).

When it comes to HBC, it has been reported that TNBC have the highest expression of these biomarkers when compared to other breast cancer subtypes (Croker et al., 2009). CD44 is a cell surface transmembrane glycoprotein that binds hyaluronic acid and is involved in many cellular functions, such as cellular adhesion, proliferation, survival, and differentiation. CSCs have a strong expression of CD44 (Pham et al., 2011; Crabtree and Miele, 2018). CD24 is a sialoprotein that enhances cellular adhesion, proliferation, and metastasis. Typically, the expression of CD24 is very low or absent in CSCs and *in vitro* studied showed that the upregulation of this molecule inhibited stemness in CSCs (Schabath et al., 2006). ALDH1 is an enzyme, member of the aldehyde dehydrogenase family of proteins that catalyze oxidation of intracellular aldehydes and may play a role in early differentiation of CSCs through the oxidation of retinol to retinoic acid. Elevated expression of this enzyme identifies CSCs and correlates with poor HBC prognosis in TNBC (Ginestier et al., 2007; Charafe-Jauffret et al., 2010). CD133, or prominin-1, is a cell surface glycoprotein that localizes to membrane protrusions such as microvilli and on the apical surface of epithelial cells. CD133⁺ CSCs correlate with poor prognosis and are associated with TNBCs (Liu et al., 2013). CD49f is a $\alpha 6$ integrin that homodimerizes with other integrins (CD24 or CD104) to bind laminin and facilitate epithelial cell adhesion to the extracellular matrix (ECM). CD49f also facilitates communication between the cell and the ECM through the regulation of specific signal transduction pathways. Its expression has been associated with poor prognosis in HBC (Friedrichs et al., 1995; Crabtree and Miele, 2018).

In addition to these cell-surface markers, several studies showed that CSCs are also characterized by an increased expression of multiple pluripotent genes such as SOX2, Nanog, OCT4, Lin28B, and Notch1 (Blick et al., 2010; Chiou et al., 2010; Kong et al., 2010; Prat et al., 2010; Han et al., 2012).

In veterinary medicine, the same cell-surface markers have been proposed and studied to identify CSCs. Particularly, several studies showed that the CD44⁺/CD24^{-low}/CD133⁺/ALDH1⁺ phenotype can be associated to CSCs from mammary tumors of dogs and cats (Barbieri et al., 2015; Michishita et al., 2011; Michishita et al., 2012; Pang et al., 2012; Michishita et al., 2013). However, CD44 in veterinary species play a controversial role and some authors associated its expression with proliferation rather than a specific CSC population (Blacking et al., 2011).

It is quite unclear whether BCSCs are derived from multipotent mammary stem cells (MaSC), are a unique progenitor population, result from a dedifferentiation of non-stem cells, or arise from some combination of these two processes. The most accepted hypothesis is that BCSCs arise from MaSC and progenitor cells (Crabtree and Miele, 2018). Accumulation of mutations in these progenitor cells may give rise to BCSCs due to the presence of similar phenotypic features in both populations (Visvader and Stingl, 2014; Liu et al., 2014). In any case, "stemness" is a phenotype that can arise through different mechanisms, either by mutation of pre-existing stem cells or by acquisition of a stem-like phenotype by transformed cells, induced by epithelial to mesenchymal transition (EMT), chemotherapy, and targeted therapy.

Understanding the normal cell precursors of CSCs and how these cells are transformed into CSCs is of great importance for elucidating the mechanisms regulating CSC survival, self-renewal, and differentiation.

SIGNALING PATHWAYS IN CANCER STEM CELLS

Multiple signaling pathways have been found to play a role in the regulation of normal mammary stem cells and in CSC and some of these pathways are strictly associated with the EMT process. Particularly, in human medicine, several pathways have been implicated in regulating tumor growth, invasion, and metastasis, such as Wnt, Notch, Hedgehog, and Hippo (Kato, 2017; Piccolo et al., 2014).

Wnt signaling is a complex fundamental process that regulates cellular proliferation, cell fate, cell migration, and stem cell niche integrity. Extracellular Wnt, a family of proteins implicated in many cellular functions such as organ formation, stem cell renewal, and cell survival (Croce and McClay, 2009), can trigger different intra-cellular signal transduction pathways: the Wnt/ β -catenin dependent or canonical pathway and the β -catenin-independent or non-canonical pathway. Two examples of the Wnt/ β -catenin non-canonical pathway include the Planar Cell Polarity pathway (PCP) and the Wnt/ Ca^{2+} pathway (MacDonald et al., 2009). The Wnt/ β -catenin canonical pathway activation is stimulated by the binding of Wnt ligand to the LRP-5/6 receptors and Frizzled receptors. This in turn activates Dishevelled (DVL), causing the recruitment of the Axin, GSK-3 β , CK1, APC complex to the receptor (Wu and Pan, 2010; Bilic et al., 2007; Gordon and Nusse, 2006). The Wnt-Frizzled-Axin-LRP5/6 complex sequesters cytosolic GSK-3 β rendering it incapable of phosphorylating β -catenin. As a result, there is an accumulation of non-phosphorylated β -catenin in the cytoplasm which eventually migrates to the nucleus, where interacts with T-cell specific factor (TCF)/lymphoid enhancer-binding factor (LEF) and co-activators to promote the expression of the Wnt target genes such as c-Myc, cyclin D1, and Cdkn1a (Gordon and Nusse, 2006). In the absence of Wnt ligand the beta-catenin undergoes phosphorylation by GSK-3 β and CK1 and subsequent sequestration in the β -catenin destruction complex. This phosphorylated complex stimulates binding of the E3 ubiquitin ligase β -TrCP to the β -catenin binding site in order to enhance its ubiquitination leading to proteasomal degradation (Spiegelman et al., 2000; Kohn and Moon, 2005). Wnt/ β -catenin pathway deregulation has been found in many types of cancer, such as breast, colorectal, melanoma, prostate, lung, and others (Vermeulen et al., 2010; Khramtsov et al., 2010; Teng et al., 2010). Canonical Wnt pathway activity is involved in the development of benign and malignant breast cancer

(Guo, 2014). As a result of its activation, β -catenin accumulates in the nucleus and/or cytoplasm and can be detected at a higher level by immunohistochemistry or western blotting. Increased β -catenin expression is correlated with poor prognosis in breast cancer patients (Incassati et al., 2010). β -catenin accumulation could be due to several factors: mutation in the gene (CTNNB1), deficiencies in β -catenin destruction complex, overexpression of Wnt ligands, loss of inhibitors and/or decreased activity of regulatory pathways (Minde et al., 2013; Howe and Brown, 2004; Takeito, 2004). HBC metastases have been associated with Wnt involvement and EMT, which are strictly related to each other. Wnt signaling has been implicated as a key player in CSC in mammary tumorigenesis (Crabtree and Miele, 2018). It has been shown that BCSCs with deregulated Wnt pathway are much more tumorigenic than those without (Monteiro et al., 2014) and inhibition of this pathway could potentially suppress breast cancer metastasis development (Jang et al., 2015).

In veterinary medicine, it has been shown that Wnt/ β -catenin pathway is deregulated in canine cutaneous melanotic tumors (Han et al., 2010; Bongiovanni et al., 2015), canine mammary tumors (Yu et al., 2017; Timmermans-Sprang et al., 2015), feline mammary tumors (Zappulli et al., 2012), and in feline squamous cell carcinoma (Giuliano et al., 2016).

The Hippo pathway has been discovered roughly 20 years ago in *Drosophila melanogaster* (Justice et al., 1995; Xu et al., 1995). It is regulated by several upstream signals, such as cell-to-cell contact (Gumbiner and Kim, 2014), extracellular matrix (Dupont et al., 2011), and cell stress (Mohseni et al., 2014) as well as by G-protein-coupled receptors (GPCRs) (Yu et al., 2012) and PI3K (Fan et al., 2013). When Hippo pathway is activated, phosphorylated mammalian sterile 20-like kinase 1/2 (Mst1/2) interacts with Sav1 to form a complex, which phosphorylates the large tumor suppressor 1 and 2 (LATS1/2) and MOB1 that forms another complex with LATS1/2. Activated LATS1/2 phosphorylates transcription coactivators YAP and TAZ, leading to their cytoplasm retention or degradation. Unphosphorylated YAP and TAZ translocate into the nucleus to interact with transcription factors, such as TEAD1-4, Smads, p73 in order to regulate the expression of downstream genes, like CTGF, ANKRD1, Cyr61 (Shi et al., 2015). The Hippo pathway is thought to play a crucial role in controlling organ size in *Drosophila* and mammals by coordination of cell proliferation and survival (Dong et al., 2007). Additionally, the Hippo pathway determines the self-renewal and differentiation of embryonic stem cell (Tamm et al., 2011), mesenchymal stem cell (Hong et al., 2005), induced pluripotent stem cell (Qin et al., 2012), and cancer stem cell (Cordenonsi et al., 2011). The deregulation of this pathway causes different diseases, such as cancer (Chan et al., 2011), cardiovascular diseases (Zhou, 2014), and neurodegenerative diseases (Yao et al., 2014). It is believed that YAP is an oncoprotein that promotes HBC tumorigenesis and progression (Shi et al., 2014) and that TAZ is required for self-renewal and tumor-initiation capacities of breast cancer cells, as measured by the ability of cells to grow as self-regenerating mammospheres as well as to form tumors when cancer cells are injected as limiting dilutions in immunocompromised mice (Cordenonsi et al., 2011). Moreover, TAZ is correlated with resistance to chemotherapy and increased metastatic activity (Bartucci et al., 2015), especially in breast and lung cancer metastasis (Cordenonsi et al., 2011; Lau et al., 2014).

In veterinary medicine, a deregulation of the Hippo pathway has been highlighted in canine (Beffagna et al., 2016; Rico et al., 2018) and feline (Beffagna et al., 2016) mammary tumors.

Recent studies highlighted an integration of YAP/TAZ in the Wnt pathway that explains the extensive overlaps between Hippo and Wnt pathways. Azzolin and collaborators (Azzolin et al., 2014) discovered that YAP and TAZ are active components of the β -catenin destruction complex. Indeed, YAP/TAZ are critical for β -catenin degradation and their depletion leads to the activation of beta-catenin/TCF transcriptional effects, stimulating the expression of downstream genes (Piccolo et al., 2014).

MAMMARY CANCER METASTASIS

HBC is the primary cause of cancer mortality in women (Jemal et al., 2011). The majority of death from HBC are not due to the primary tumor, but are the result of metastasis to distant organs (Weigelt et al., 2005). Currently, detection of HBC metastasis is based on clinical manifestations of the presence of metastatic cancer cells on distant organs, biopsies of affected organs, imaging methods, and circulating tumor markers (Lacroix, 2006; Sun et al., 2011). The mortality rate associated with metastases has been reduced by mammographic screening. However, detecting metastasis at early stage remains extremely difficult (Scully et al., 2012). The metastatic process is characterized by several sequential steps. Cells that are not able to complete all these steps do not give rise to metastasis. The process starts with the local invasion of the host tissue that surrounds the tumor by cells originating from the primary tumor and continues until the tumor cells intravasate into the lymphatic or blood vessels (Hunter et al., 2008; Talmadge & 2010). The tumor cells then travel along the blood stream or the lymphatic vessels and are disseminated to distant organs. Consequently, the tumor cells adhere to capillary beds within the target organ, before extravasating into it. When metastatic tumor cells penetrate the new organ, they proliferate and promote angiogenesis (Hunter et al., 2008). In order to overcome these steps and survive, the tumor cells must simultaneously evade the host's immune response and apoptotic signals (Hunter et al., 2008; Fidler et al., 1978).

The metastatic process starts with the invasion of tumor cells into the surrounding tissue. Tumor cells must alter cell-to-cell adhesion and cell adhesion to the extracellular matrix (ECM). The cadherin family has been reported to play a crucial role in mediating cell-to-cell adhesion and plays an important role in breast cancer metastasis (Li and Feng, 2011). To achieve an invasive phenotype, cancer cells need to migrate from the primary tumor site. Although tumor cells are able to migrate singly, it is thought that they are more prone to migrate coordinately. As a result, after invasion and intravasation, they commonly circulate as emboli in the lymphatic or blood vessels (Fidler, 1970; Fidler, 1973). The EMT is a critical pathway in the invasion and migration of migratory cells. EMT starts with the disintegration of cell-to-cell adhesion molecules by losing epithelial markers, such as E-cadherin or β -catenin, and expressing mesenchymal markers, such as vimentin. The expression of transcriptional repressors of E-cadherin such as zinc finger E-box-binding homebox 1 (ZEB1), zinc finger E-box-binding homebox 2 (ZEB2), twist-related proteins (TWIST), zinc finger proteins (SNAIL and SLUG), involved in signaling pathways including transforming growth factor- β (TGF- β), the Wnt/ β -catenin cascade, and the phosphatidylinositol 3' kinase-serine/threonine kinase (PI3K/AKT) axis linked to the EMT programs, are associated with poor prognosis in HBC (Battle et al., 2000; Comijn et al., 2001; Eger et al.,

2005; Hajra et al., 2002; Yang et al., 2004; Larue and Bellacosa, 2005). Cells which undergo EMT have an elongated fibroblast-like shape and their movement is facilitated by channels produced in the ECM by matrix-degrading enzymes, such as MMPs (Friedl and Wolf, 2008).

Within the blood stream or lymphatic vessels metastatic tumor cells find a different environment from the tissue of origin. They are exposed to mechanic, osmotic, chemical stimuli they are not used to, therefore they must develop specific mechanisms to be able to survive. These cells can travel along these vessel highways to other parts of the body. Many cancer cells die while travelling through the blood and lymph vessels, but some may survive and stick to the vessel wall. Then they move through the vessel wall into another body tissue. These cells may then divide and form a metastatic tumor. Cancer cells tend to spread to certain places in the body depending on the site where primary tumor forms. HBC has been observed to preferentially metastasize to the bone and lungs and less frequently to the liver and brain (Minn et al., 2005). It is postulated that in these organs breast cancer cells find a suitable microenvironment that allow their growth. In the 1980s, Stephen Paget proposed the "seed and soil" theory for metastasis whereby the "seed" (cancer cells) are thought to only grow where they find a suitable "soil" (environment) (Paget, 1989). Indeed, the microenvironment of metastatic tumor cells is critical for tumor cell proliferation. Malignant cells constantly interact with cells of the microenvironment (fibroblasts, immune cells, endothelial cells, and mural cells of the blood and lymph vessels) at both primary and metastatic sites (Fidler et al., 2007; Geiger and Peeper, 2009; Joyce and Pollard, 2009). It is also postulated that tumor cells may secrete substances to prime the "soil" prior to metastasis to establish a "pre-metastatic niche" supporting future metastatic sites (Psaila et al., 2006).

Metastasis remains a frequent cause of cancer-related death in dogs diagnosed with advanced-stage disease or higher-grade tumors (de Araujo et al., 2015; Gupta et al., 2007; Klopfleish and Gruber, 2009; Klopfleish et al., 2011; Sorenmo et al., 2013). In dogs, 50% of the mammary tumors are malignant (Sleeckx et al., 2011; Sorenmo et al., 2003) and most of them eventually metastasize (Millanta et al., 2005). In cats, more than 80% of mammary tumors are malignant and are characterized by rapid progression and metastasis (MacEwen, 1990; Misdorp, 2008; Zappulli et al., 2005). Therefore, similar to HBC, predicting, preventing, and treating metastases represents the most important as well as challenging obstacle to improve outcomes in dogs and cats with clinically aggressive neoplastic subtypes. To do so requires a deep knowledge of the complex biological and molecular changes that occur in those cells that acquire a metastatic phenotype. The process of metastasis, and specifically the interactions between cancer cells and their microenvironment, is not completely understood (Klopfleish and Gruber, 2009).

Mouse models of mammary cancer are fundamental because they provide an opportunity to investigate the mechanisms of metastasis, genetic cancer progression, and the roles of angiogenesis and lymphangiogenesis (Werbeck et al., 2014).

INTERCELLULAR COMMUNICATION THROUGH EXTRACELLULAR VESICLES

Cells can communicate and interact between each other by the exchange of signaling compounds mainly through: 1) simple membrane-crossing diffusion; 2) active transport through membrane ion-channels, pumps, or transporting proteins; 3) the exchange of cell membrane fragments through a process called trogocytosis; and 4) the formation of synapses including immunological and nerve synapses (Nazimek et al., 2018). In addition to that, cells can communicate through auto-, para-, endocrine manner using proteins, lipids, eicosanoids, monoamines (e.g. neurotransmitters), endorphins, and extracellular RNA (mainly miRNA). The majority of these signaling compounds have been associated and found within the content of extracellular vesicles.

Extracellular vesicles (EVs) are membrane-limited vesicles produced by cells under physiological and pathological conditions, including cancer, in which their release is abnormally increased (György et al., 2011).

In human medicine, information regarding human EVs (hEVs) are relatively recent within the literature (Urabe et al., 2017; Noguès et al., 2018; uivo et al., 2017). hEVs are classified based on their release pathway or size. Microvesicles (MVs) or ectosomes range from 100 nanometers (nm) to 1 micrometer (μm) and bud directly from the plasma membrane (Heijnen et al., 1999). Exosomes range from 40 to 120 nm and are formed by the fusion between multivesicular bodies and the plasma membrane (El Andaloussi et al., 2013; Cocucci and Meldolesi, 2015). Apoptotic bodies are also classified within hEVs; they are formed by dying cells and can range from 50 nm to 2 μm (El Andaloussi et al., 2013; Theyry et al., 2001). Oncosomes are larger EVs (1-10 μm), which are produced primarily by malignant cells (Di Vizio et al., 2012; Morello et al., 2013).

hEVs are produced by "donor" cells and they can be taken up by "recipient" cells via endocytosis or membrane fusion (Maas et al., 2017). Through this mechanism, hEVs can therefore transfer information from one cell to other cells as a form of intercellular communication within the same cell population, within the tissue microenvironment, or throughout the body (Abels and Breakefield, 2016). It has been shown that hEVs play a crucial role in many biological processes. In cancer, they are exchanged between tumor cells, promoting proliferation (Al-Nedawi et al., 2008; Skog et al., 2008; Keller et al., 2009), migration, invasion, and metastases (Zaborowski et al., 2015), as well as induction of epithelial-to-mesenchymal transition (EMT) (Aga et al., 2014). Additionally, cancer-derived hEVs modulate the microenvironment to facilitate tumor growth, to promote angiogenesis and tumor cell invasion, and to suppress immune reactions (Di Vizio et al., 2012; Skog et al., 2008; Svensson et al., 2011).

The content of hEVs is variable and includes lipids, proteins, RNAs (mRNA, miRNA, lncRNA, and other RNA species), and DNAs (mtDNA, ssDNA, dsDNA) (Zaborowski et al., 2015; Xu et al., 2016). The loading of the different types of cargo can be specific per vesicle and cell type (Abels and Breakefield, 2016). Extensive research has been performed to study and characterize the content of EVs. As a result, three different databases have been assembled and are now publicly accessible: Exocarta, Vesiclepedia, and EVpedia (Kim et al., 2013; Kalra et al., 2012; Mathivana and Simpson, 2009; Simpson et al., 2012; Mathivanan et al., 2012).

All these databases include the protein, lipid, and nucleic acid content together with the isolation and purification procedures used to generate the data.

Protein content of hEVs is associated with their mechanism of biogenesis (Abels and Breakefield, 2016). For instance, proteins of the endosomal sorting complexes required for transport (ESCRTs), such as Alix and TSG101, are enriched in the vesicle fraction (Zaborowski et al., 2015) as well as proteins responsible for EV formation and release (RAB27A, RAB11B, and ARF6) (Abels and Breakefield, 2016). Yet, hEVs contain different kinds of proteins involved in signal transduction (EGFR), antigen presentation (MHC I and MHC II), as well as tetraspanins (CD63, CD9, and CD81) and other transmembrane proteins (LAMP1 and TfR) (Abels and Breakefield, 2016). Especially CD63, CD9, CD81, TSG101, Alix, and heat-shock chaperones, are commonly found in hEVs, regardless of their cell of origin and hEVs subtype, and are therefore used as hEVs markers (Zaborowski et al., 2015; Abels and Breakefield, 2016). On the other hand, proteins from nucleus, mitochondria, endoplasmic reticulum, and the Golgi complex are mostly absent in EVs (Colombo et al., 2014).

The lipid composition has been extensively studied in various settings (Van Blitterswijk et al., 1982; Carayon et al., 2011; Llorente et al., 2013). Generally, the lipid composition is similar to the cell of origin. Lipids enriched in hEVs include sphingomyelin, cholesterol, ganglioside GM3, disaturated lipids, phosphatidylserine, and ceramide (Llorente et al., 2013). Overall, the membrane composition of both MVs and exosomes contains more phosphatidylserine as compared to the cellular plasma membrane composition, whereas the differences in lipid composition between the different types of vesicles reflect the biogenesis of the different types of hEVs, either originating from the MVBs or the plasma membrane (Abels and Breakefield, 2016).

Within the hEVs, a diverse composition of genetic material is found. DNA, including genomic and mitochondrial DNA is present (Guescini et al., 2010; Balaj et al., 2011; Waldenstrom et al., 2012). However, hEVs are primarily enriched with small RNAs, with many derived from ribosomal 18S and 28S rRNAs and tRNAs. In addition to the commonly known RNA species, such as mRNAs, rRNAs, and miRNAs, tRNA fragments, long and short non-coding RNAs, piwi-interacting RNA, Y RNA, circular RNAs, and vault RNA are present within hEVs (Crescitelli et al., 2013; Cheng et al., 2013; Huang et al., 2013; Ogawa et al., 2013; Xiao et al., 2012; Nolte-Hoen et al., 2012; Li et al., 2013; Li et al., 2015).

The vast majority of the RNA found within hEVs is roughly 200 nucleotides in length with a smaller portion that can reach up to 4 kb (Batagov and Kurochkin, 2013). The release of RNA within the lipid bilayer membrane protects it from RNases present in the extracellular microenvironment that would otherwise degrade it once released. Alternatively, different RNA species can also be associated with ribonucleoproteins (RNPs) or high- and low-density lipoproteins (HDLs and LDLs), which can be associated with the hEVs or included with the hEV fraction according to the isolation method (Arroyo et al., 2011; Vickers et al., 2011; Vickers and Remaley, 2012).

hEVs have been successfully purified from cell culture conditioned medium and body fluids, such as serum, plasma, saliva, urine, breast milk, amniotic fluid, ascites, cerebrospinal fluid, bile, and semen (They et al., 2006; Colombo et al., 2014). Several hEV isolation protocols are present and discussed in the literature. Typically, isolation procedures include differential centrifugation, density-gradient centrifugation, sucrose cushion centrifugation, gel-permeation chromatography, affinity capture, microfluidic devices, synthetic polymer-based precipitation, and membrane filtration (Xu et al., 2016). The most widely used hEV isolation method is based on differential centrifugation. It enables enrichment, but not complete separation, of different hEV fractions. Ultracentrifugation consists of initial low-speed centrifugation steps to remove cell (300 x g, 10 minutes, 4°C) and debris (2,000 x g, 10 minutes, 4°C). In many protocols, this is followed by filtration through 0.2 µm – 0.8 µm filter or a 10,000-20,000 x g centrifugation in order to separate small and large hEV subpopulations. Skipping the filtration steps or the 10,000-20,000 x g centrifugation step results in the isolation of small and large hEV subtypes. Afterwards, a centrifugation at 100,000 x g for 1.5-2 hours using a 70Ti rotor (k factor 44; Beckman Coulter) is performed to pellet hEVs (Zaborowski et al., 2015). The main disadvantage of the differential centrifugation procedure is the co-pelleting of high molecular weight protein complexes such as 26S proteasome, HSPG, fatty acid synthase, lipoproteins, and viral particles (Vickers et al., 2011; Tauro et al., 2012).

Density-gradient centrifugation enables the increased purification of hEVs and the partial separation of different subpopulations (Heijnen et al., 1999; They et al., 2001). This procedure improves the removal of high molecular weight proteins and is useful in the isolation of hEVs from body fluids, that contain high levels of protein aggregates (Runz et al., 2007; Tauro et al., 2012). Sucrose solutions are the most common used for this aim and ioxadinol gradients also appear suitable in the separation of exosomes from viral particles that are likely to co-pellet using ultracentrifugation method (Cantin et al., 2008).

Size-exclusion chromatography (SEC) is a well-established high-yield method for purifying functional hEVs from cell culture supernatants and complex biological fluids (Böing et al., 2014). SEC separates hEVs based on a difference in size. It has been reported that hEVs isolated by chromatographic methods suffer less contamination by non-vesicular proteins and macromolecules structures than after ultracentrifugation (Nordin et al., 2015; Böing et al., 2014; de Menezes-Net et al., 2015).

Although no gold standard isolation method has been established, differential centrifugation is still the most widely used method for hEVs isolation (Zaborowski et al., 2015; Xu et al., 2016). However, in studies where hEV functionality is needed, the ultracentrifugation method is being replaced by other less traumatic procedures, such as SEC (Nordin et al., 2015).

After isolation, all subpopulations of hEVs can be visualized using Transmission Electron Microscopy (TEM) with the additional immunolabelling of hEVs proteins for characterization (Heijnen et al., 1999). Cup-shaped structures once considered characteristic of hEVs result from the chemical fixation step during sample preparation for TEM.

One of the major challenges in hEVs field is how to accurately quantify hEVs. First studies measured total protein content to estimate hEV amount. However, this number is often overestimated because of the presence of high molecular weight proteins that copurify with hEVs. In addition to that, this approach does

not take into account that protein content can be different based on hEV subtypes. Nanoparticle Tracking Analysis (NTA) is based on a light scattering system of particles in suspension and on their Brownian motion to estimate the number and volume distribution of hEVs both in conditioned media and body fluids (Dragovic et al., 2011; Soo et al., 2012). This instrument could underestimate the number of larger particles (those more than 500 nm).

Conventional flow cytometry is not suitable for smaller-size (less than 300 nm) particles (Dragovic et al., 2011). Flow cytometry can be used to count hEVs of more than 500 nm (Orozco and Lewis, 2010), including oncosomes (Di Vizio et al., 2012; Morello et al., 2013). Small hEVs could potentially be analyzed if bound to beads coated with antibodies against surface antigens.

Subsequent labeling by fluorophore-conjugated antibodies enables semi-quantitative evaluation by flow cytometry (They et al., 2006). Another technique used to quantify hEVs is Tunable Resistive Pulse Sensing (TRPS), which is based on the disruption of ionic flow as particles pass through a single nanopore separating two fluidic cells. The rate and magnitude of the disruptions can be used to calculate the concentration and volume of hEVs, respectively (Maas et al., 2014). A comparison of NTA, TRPS, and flow cytometry showed significant differences among the instruments, which suggests that the absolute quantification of hEVs still remains challenging (Maas et al., 2014).

The field of hEVs is rapidly expanding in human medicine and has gained particular attention during the recent years due to their significance in terms of diagnosis, biomarkers, and therapy for many pathological processes (Chen et al., 2013; Jia et al., 2014; Szajnik et al., 2013). To date, this remains a largely unexplored field in veterinary medicine.

AIMS

Human breast cancer (HBC), canine mammary tumors (CMTs), and feline mammary tumors (FMTs) share highly interesting similarities and are heterogeneous entities within which different cell populations can coexist.

The main aim of this PhD project was to investigate the biological and molecular features of the normal and the tumor cell subpopulations of mammary gland, with particular interest for cancer stem cells (CSC). In order to achieve this goal, the study has been split in four phases:

Phase I: isolation and characterization of human, canine, and feline cancer stem cells

In this phase we aimed to isolate cancer stem cells (CSCs) from fresh mammary tissues as well as from well established mammary gland tumor cell lines. Additionally, we wanted to compare the expression of stem-related markers between well-differentiated and CSC-like cells both at protein and mRNA levels.

Phase II: epithelial-to-mesenchymal transition and Wnt/ β -catenin and Hippo pathways

Since CSCs are thought to be involved in the epithelial-to-mesenchymal transition (EMT) process, in this phase we aimed to investigate EMT in mammary gland tumor tissue samples at both protein and mRNA level from all three species. Moreover, it is believed that in CSCs several pathways that orchestrate proliferation, invasion, and metastases are deregulated. Among these, we focused on Wnt/ β -catenin and Hippo pathways investigating them in mammary gland tumor tissue samples at both protein and mRNA level.

Phase III: *in vivo* model of mammary cancer metastases

CSCs are thought to be involved in resistance to chemo/radiotherapy, local relapses, and metastasis development. In this phase we aimed to establish a clinically relevant *in vivo* mouse model of mammary cancer metastasis. Furthermore, we investigated those genetic drivers that are responsible for the migration and colonization of distant organs, with particular attention to the brain.

Phase IV: intercellular communication through extracellular vesicles

To the best of our knowledge, extracellular vesicles (EVs) have never been investigated within the context of veterinary oncology. In this phase we aimed to isolate, identify and characterize EVs produced by canine and feline mammary tumor cell lines and preliminarily test their functional role in tumor aggressiveness.

MATERIALS AND METHODS

Phase I: isolation and characterization of human, canine, and feline cancer stem cells

Isolation of cells from primary tumors

In order to isolate primary cell cultures of both differentiated and undifferentiated (CSC-like) cells, thirteen human breast cancer tissues and 10 healthy human mammary gland tissues adjacent to tumor tissue were collected from Istituto Oncologico Veneto (IOV, Padua, Italy) (thanks to the existing collaboration with Dr. Silvia Michieletto and Dr. Enrico Orvieto).

Similarly, 10 canine mammary gland tumor tissues and 9 healthy/hyperplastic canine mammary gland tissues adjacent to tumor tissue were collected from local veterinary clinics.

Human and canine mammary tissues (roughly 0.5 cm³), from the surgery room, were transported on ice in sterile tubes in 20 ml of DMEM/F12 (Aurogene, Rome, Italy) containing penicillin/streptomycin (200 U/ml; Aurogene, Rome, Italy) to prevent contaminations.

Under a biohazard hood, within 2 hours from surgery, the specimen was transferred onto a 100mm Petri dish and washed with Phosphate Buffer Saline (PBS) to get rid of blood and debris. Tissues were dissected using sterile forceps, razors, and scissors and cut in small pieces (less than 1-2mm).

Slightly different protocols were performed in the attempt of optimization. Not all details are reported here. Briefly, major changes were enzymatic and non-enzymatic treatment, time and temperature of incubation with collagenase/hyaluronidase (see tables 1 and 2 in results section). For some samples minced tissues were enzymatically digested with a 1:1 solution of collagenase/hyaluronidase (Roche Diagnostics GmbH, Mannheim, Germany and Sigma-Aldrich Corp., St. Louis, MO, respectively), as reported in tables 1 and 2, and filtered using a 70 µm cell strainer (Corning, New York, USA) to discard clumps. The single cell suspension was then centrifuged at 1,500 rpm for 5 minutes and washed one in PBS to obtain cell pellet. 500,000 cells were resuspended in RPMI + fetal bovine serum (FBS) + Azide for flow cytometry (see below).

The remaining cells were plated either in a 100mm dish with DMEM/F12 (Aurogene) + 1% penicillin/streptomycin (Aurogene) + Human Epidermal Growth Factor (20 ng/ml; Cell Signaling Technology, Danvers, MA, USA) + Human Fibroblast Growth Factor (20 ng/ml; PeproTech, London, UK) + B27 (1X, Thermo Fisher Scientific, Waltham, MA, USA) to isolate undifferentiated CSC-like cells, or in DMEM/F12 + 1% penicillin/streptomycin + 10% FBS to isolate differentiated epithelial cells. Cells were left into the cell culture incubator for several days.

Immunocytochemistry

To characterize isolated cells from fresh tissues, when they were at 80-90% confluence and after standard trypsinization roughly 20,000 cells were plated on a previously gelatinized coverslip in a 6-well plate. When 70% confluent, the medium was removed, the cells were fixed in 4% paraformaldehyde (PFA), washed once in PBS, permeabilized with 0.5% Triton in PBS for 10 minutes, washed twice in PBS, and incubated with hydrogen peroxidase block for 10 minutes. The cells were then washed twice in PBS and non specific staining

was blocked using 5% bovine serum albumin (BSA) for 30 minutes. After one washing step, the cells were incubated overnight at 4°C with the following antibodies: β -catenin (1:100; #610154, BD Biosciences, Franklin Lakes, NJ, USA), E-cadherin (1:100; #610182, BD Biosciences), calponin (1:200; #M3556, Dako, Agilent Technologies, Santa Clara, CA, USA), p63 (1:200; #SC-8431, Santa Cruz Biotechnology, Dallas, TX, USA), vimentin (1:150; #M0725, Dako), pancytokeratins (1:100; #M3515, Dako), CD44 (1:100; #550538, BD Biosciences). After 3 washes in PBS, cells were incubated with the secondary HRP-conjugated antibody, washed three times in PBS and incubated with the DAB solution for 5 minutes. Cells were then washed three times in PBS. Finally, the coverslip was placed on a slide and visualized under a microscope.

Positivity was evaluated as percentage (0-100%) counting a total of 1000 cells and as intensity (-: negative; +: weak; ++: moderate; +++: strong).

Isolation of CSC-like cells from established cell lines

Additionally, also established cell lines were used to isolate CSC-like cells. Specifically, a canine mammary tumor cell line (CYPp) and a feline mammary tumor cell line (FMCp) (kindly provided by Dr. Raffaella De Maria, University of Turin, Italy) were cultured in Roswell Park Memorial Institute (RPMI 1640) (Aurogene, Rome, Italy) medium containing 1% penicillin/streptomycin and 10% FBS. The triple negative breast cancer MDA-MB-231 (obtained from the American Type Culture Collection (ATCC, Manassas, Virginia) and cultured in high glucose Dulbecco's Modified Eagle Medium (DMEM) (Aurogene, Rome, Italy) containing 1% penicillin/streptomycin and 10% FBS) cell line was used as positive control.

Mammosphere formation from established cell lines

To isolate CSC-like cells, the mammospheres formation assay was performed. In order to form mammospheres, adherent cells (CYPp, FMCp, and MDA-MB-231) were trypsinized according to standard, washed with PBS, and plated at a seeding density equal to 10,000 cells/cm² in an ultra-low attachment T75 flask (Corning) in the following medium: DMEM/F12 (Aurogene) + 1% penicillin/streptomycin (Aurogene) + Human Epidermal Growth Factor (20 ng/ml; Cell Signaling) + Human Fibroblast Growth Factor (20 ng/ml; PeproTech) + B27 (1X, Thermo Fisher Scientific) – N2 (1X, Thermo Fisher Scientific). 3.3 ml of fresh medium were added every 3 days. After 7 days of culture, mammospheres dissociation was performed as following: cells were spun down at 1,500 rpm for 5 minutes, the supernatant was discarded, the cell pellet was resuspended in 400 μ l of accutase (Sigma-Aldrich) and incubated at 37°C for 90 seconds. Then, accutase activity was stopped adding 5 ml of medium, cell suspension was centrifuged at 1,500 rpm for 5 minutes and after counting, 10,000 cells/cm² were seeded in order to start next passage.

To characterize the CSC-like cells contained within the mammospheres, flow cytometry and qPCR were performed at passages 1, 4, and 7, considering 7 days between each passage.

RNA extraction, reverse transcription and real time polymerase chain reaction

Gene expression analysis was performed on established canine and feline cell lines. Specifically, the RNA was extracted from adherent cells at passage 1 and mammospheres at passages 1, 4, and 7 (CYPp and FMCp) using RNeasy Mini Kit (Qiagen, Hilden, Germany) according to manufacturer instructions. 500 ng of

total RNA from each sample was reverse transcribed using RevertAid First Strand cDNA Synthesis Kit (Thermo Fisher Scientific) to obtain first-strand cDNA. The cDNA was then used as a template for quantitative real-time PCR to evaluate expression of CD44, CD133, OCT4, SOX2. ACTB was used as house-keeping gene. Primer sequences are reported in table S1 (supplementary data). cDNA template was amplified in a final volume of 20 μ l, containing 10 μ l of PowerUp SYBR Green Master Mix (2X) (Applied Biosystem, Foster City, CA, USA). The amplification protocol consisted of an initial step of 2 min at 50°C and 2 min at 95°C, followed by 40 cycles of 15 sec at 95°C and 1 min at 60°C. The dissociation curve was performed as following: 15 sec at 95°C, 1 min at 60°C, and 15 sec at 95°C. All experiments were carried out in a Stratagene Mx3000p (Agilent Technologies). For each sample, the Ct (Cycle threshold) was used to determine the relative amount of target gene; each measurement was made in triplicate, and normalized to the reference gene ACTB, in order to calculate the Δ Ct value per each sample. $\Delta\Delta$ Ct was calculated using adherent cells passage 1 as reference sample. $2^{(-\Delta\Delta Ct)}$ values were calculated and expressed as relative fold change.

Flow cytometry

Flow cytometry (FC) was performed on cells isolated from primary tumors. Additionally, FC was performed also on adherent cells and mammospheres at passages 1, 4, and 7 (CYPp, FMCp, and MDA-MB-231 as a control). For the latter analysis, two different cell preparation protocols were tried i) Mechanic dissociation was achieved detaching adherent cells using a cell scraper and dissociating mammospheres using PBS, pipetting up and down several times. ii) Enzymatic dissociation was achieved detaching adherent cells using trypsin EDTA (Aurogene) and dissociating mammospheres using accutase (Sigma-Aldrich). After washing, single cell suspensions were resuspended in RPMI + FBS + Azide for flow cytometry.

Combinations of antibodies against CD45-FITC (1:200; #11-5450, Affymetrix, Santa Clara, CA, USA), CD44-PE (1:100; #553134, BD Biosciences), CD24-APC (1:50; #562349, BD Biosciences), CD117-PE (1:100; #553869, BD Biosciences), CD34-PE (1:500; #559369, BD Biosciences), and CD133(Prominin-1)-APC (1:50; #17-1331, BD Biosciences) were added to the cell suspension at concentrations recommended by the manufacturer and incubated 4°C in dark for 30 minutes. Then, labeled cells were washed in PBS to eliminate unbound antibody, and analyzed on a FACScan (Sysmex Partec, Görlitz, Germany).

Phase II: epithelial-to-mesenchymal transition and Wnt/ β -catenin and Hippo pathways

Tissue collection

Human samples were collected from Istituto Oncologico Veneto (IOV, Padua, Italy), whereas canine and feline samples were collected from local veterinary clinics and preserved in RNALater (Ambion, Austin, TX) within 2 hours after surgery, according to manufacturer's instructions. Specifically, 5 healthy human breast tissues, 5 estrogen receptor-positive human breast cancer tissues, 5 triple-negative human breast cancer tissues, 4 healthy canine mammary gland tissues, 10 canine simple carcinomas, 6 healthy feline mammary gland tissues, and 6 feline simple carcinomas were collected. Before RNA extraction, a small portion per each sample preserved in RNALater was fixed in 4% formaldehyde and included in paraffin.

Four μm tissue sections were stained with hematoxylin and eosin and slides were visualized under the microscope in order to further confirm the presence of healthy tissue in the samples labelled as "healthy" and of tumor tissue in the samples labelled as "tumor".

RNA extraction and real-time polymerase chain reaction

For gene-expression analyses, a small portion of each tissue sample preserved in RNALater was used for RNA extraction using Trizol Reagent (Invitrogen, Carlsbad, CA) following the manufacturer's protocol. The extracted RNA was treated with RNase-free DNase I (New England Biolabs, Ipswich, MA, USA). 500 ng of total RNA from each sample was reverse transcribed using RevertAid First Strand cDNA Synthesis Kit (Thermo Fisher Scientific) to obtain first-strand cDNA. The cDNA was then used as a template for quantitative real-time PCR to evaluate expression of β -catenin (CTNNB1), cyclin D1 (CCND1), YAP, TAZ, CTGF, ANKRD1, SNAIL1, SNAIL2, TWIST1, TWIST2, ZEB1, ZEB2. ACTB was used as house-keeping gene. Primer sequences are reported in table S2 (supplementary data). cDNA template was amplified in a final volume of 20 μl , containing 10 μl of PowerUp SYBR Green Master Mix (2X) (Applied Biosystem). The amplification protocol consisted of an initial step of 2 min at 50°C and 2 min at 95°C, followed by 40 cycles of 15 sec at 95°C and 1 min at 60°C. The dissociation curve was performed as following: 15 sec at 95°C, 1 min at 60°C, and 15 sec at 95°C. All experiments were carried out in a Stratagene Mx3000p (Agilent Technologies). For each sample, the Ct (Cycle threshold) was used to determine the relative amount of target gene; each measurement was made in triplicate, and normalized to the reference gene ACTB, in order to calculate the ΔCt value per each sample.

Protein extraction and Western Blotting

A subset of the above-mentioned tissues was used for protein extraction and Western Blotting. Specifically, proteins were extracted from RNALater-preserved tissues from 2 human healthy breast tissues, 2 human estrogen receptor-positive invasive ductal carcinomas grade III, 2 human triple negative invasive ductal carcinoma grade III, 3 canine healthy mammary gland tissues, 2 canine simple tubular carcinomas grade I, 2 canine simple tubular carcinomas grade II, 2 feline healthy mammary gland tissues, and 3 feline simple tubular carcinomas grade III.

The isolation of soluble and nuclear fractions was carried out according to Maruyama and MacLennan, with slight modifications (Maruyama and MacLennan, 1988). Briefly, tissues (20 μg) were minced with scissor, suspended in a hypotonic solution (10mM Tris-HCl, pH 7.4, 0.5mM MgCl_2 , containing protease inhibitors 100 μM phenylmethylsulfonyl fluoride PMSF, 1 $\mu\text{g}/\text{mL}$ leupeptin) and homogenized on ice with 30 strokes in a precooled glass homogenizer. The homogenates were diluted with an equal volume of a solution of 10mM Tris-HCl, pH 7.5, 0.5M sucrose, 300mM KCl. The suspensions were centrifuged for 10 min at 10,000 g to pellet nuclei and the supernatant containing soluble fractions were collected in a fresh tube. The pellet containing nuclear fractions were resuspended in a lysis buffer containing 20 mM HEPES (4-(2-hydroxyethyl)-1-piperazineethanesulfonic acid) pH 7.5, 1.5 mM MgCl_2 , 0.4 M NaCl, 0,2 mM EDTA, 1% Triton and protease inhibitors 100 μM phenylmethylsulfonyl fluoride PMSF, 1 $\mu\text{g}/\text{mL}$ leupeptin.

Protein concentration of soluble and nuclear fractions was determined by the bicinchoninic-acid method BCA (Thermo Scientific) according to manufacturer's instructions and using bovine serum albumin as standard. Protein fractions were stored at -80°C , until used.

Proteins were resolved by sodium dodecyl sulphate-polyacrylamide gel electrophoresis (SDS-PAGE), using 7.5% or 10% polyacrylamide gels. After electrophoresis, proteins were transferred onto nitrocellulose membrane and probed with the following antibodies:

- rabbit polyclonal antibodies anti WWTR1 (WW domain-containing transcription regulator protein 1) (Sigma Aldrich) recognizing both the YAP and TAZ human proteins (dilution 1:1000);
- mouse monoclonal antibodies anti- β -catenin (BD Transduction Laboratories) (dilution 1:1000);
- rabbit monoclonal antibodies anti non-phospho (active) β -catenin (Cell Signaling) (dilution 1:1000).

Membranes were blocked one hour at room temperature in 10 mM Tris/HCl, pH 7.5, 150 mM NaCl, 0.05% Tween 20 containing 1% bovine serum albumin for anti WWTR1 and anti β -catenin antibodies and in 20 mM Tris/HCl, pH 7.6, 150 mM NaCl, 0.1% Tween 20 containing 5% bovine serum albumin for anti non-phosphorylated (active) β -catenin. Incubation with primary antibodies was carried out at 4°C overnight in the buffers used as blocking solution, without bovine serum albumin. After one-hour incubation at room temperature with the appropriate secondary antibody conjugated with alkaline phosphatase, proteins were detected with the staining solution (5 mg BCIP (5-Bromo-4-chloro-3-indolyl phosphate) and 1 mg NBT (Nitro Blue Tetrazolium) in 30ml of 0.1 M TRIS, 0.1 M NaCl, 5 mM MgCl_2 , pH9.5 buffer).

Immunohistochemistry

The above-mentioned samples as well as human breast tissues selected from the Division of Anatomic Pathology archive of the Padua University Hospital (thanks to the existing collaboration with Dr. Enrico Orvieto) and canine and feline mammary tissues selected from our archive (Anatomic Pathology, Dept. BCA, University of Padua) were used to perform immunohistochemistry (IHC).

Specifically, IHC was performed on the following tissue samples: 5 estrogen receptor-positive human breast cancer, 5 triple-negative human breast cancer, 10 canine simple tubular carcinomas grade I, 10 canine simple tubular carcinoma grade II, 10 feline simple tubular carcinomas grade III. Staining of adjacent healthy/hyperplastic mammary gland tissue was evaluated as well. Sections ($4\ \mu\text{m}$) were processed with an automatic immunostainer (BenchMark XT, Ventana Medical Systems), as previously described (Caliari 2014). Negative controls omitted the primary antibody, whereas adnexa and epidermis, when present, were used as positive controls.

The following antibodies were tested: estrogen receptor alpha (ER) (1:40; NCL-ER-6F11, Novocastra), progesterone receptor (PR) (1:80; #NCL-PGR-312, Novocastra, Leica, Wetzlar, Germany), human epidermal growth factor receptor 2 (HER2) (1:250; #A0485, Dako), cytokeratin(CK) 8/18 (1:30; #NCL-L-5D3, Novocastra), CK5/6 (1:50; #D5/16 B4, Dako), CK14 (1:20; #NCL-LL 002, Novocastra), E-cadherin (1:120; #610182, BD Biosciences), β -catenin (1:100; #610154, BD Biosciences), CD10 (1:200; #NCL-CD10-270, Novocastra), p63 (1:200; #SC-8431, Santa Cruz Biotechnology), CD44 (1:100; #550538, BD Biosciences), vimentin (1:150; #M0725, Dako), WWTR1(YAP/TAZ) (1:100; #HPA007415, Sigma-Aldrich).

A semi-quantitative evaluation of IHC positivity was performed. Specifically, cytoplasmic and nuclear positivity were recorded as percentage of positive cells.

Phase III: *in vivo* model of mammary cancer metastases

The experiments belonging to this phase of the study have been performed at the Department of Neurology of the Massachusetts General Hospital/Harvard Medical School in Boston, MA, where I have been working for 13 months during my period abroad.

Cell lines

Human estrogen receptor-positive (MCF7) and triple-negative (MDA-MB-231) breast cancer cell lines were obtained from the American Type Culture Collection (ATCC, Manassas, Virginia) and cultured in high glucose Dulbecco's Modified Eagle Medium (DMEM) (Gibco, Life Technologies) containing 1% penicillin/streptomycin and 10% FBS.

All cell lines used in the study were stably transduced with packaged lentivirus vectors using a specific service at the MGH Vector Core, Department of Neurology, Boston, MA, USA to express genes of interest. Specifically, cell infection was carried out to express specific genes within the cells of interest. Briefly, for viral spinfection, cells were plated in a 6-well plate and when 60% confluent, the medium was replaced with 1 ml of fresh medium, 1 μ l of Polybrene (10 mg/mL; Sigma-Aldrich) and a volume of lentivirus (MGH Vector Core, Boston, Massachusetts) based on virus titer in order to have a multiplicity of infection (MOI) of 10. The plate was immediately spun at 1,800 rpm at 37°C for 90 minutes and the medium was replaced with fresh medium the day after. In order to have a pure population, cells were selected either by fluorescent-activated cell sorting (FACS) for the fluorophore of interest or by Puromycin treatment (2 μ g/ml).

Caspase3 wild type (CASP3WT) was obtained from Harvard Medical School PlasmID Repository (Boston, MA, USA). Caspase3 mutant (CASP3MT) was obtained from the Addgene Sabatini and Wood Cancer Pathways ORFs Kit (Cambridge, MA, USA).

For lentiviral packaging, a bacterial stab of the CASP3WT plasmid or a glycerol stock of the CASP3MT plasmid was streaked on an LB-agar plate containing 100 μ g/mL ampicillin as a selection marker and incubated for 15 hours at 37°C. A single colony was picked from the plate and grown in 2 mL of LB ampicillin (100 μ g/mL) shaking at 250 rpm at 37°C for 8 hours. The pre-culture was then added to 250 mL of LB ampicillin (100 μ g/mL) shaking at 250 rpm for 12 hours. Plasmid DNA was isolated using ZymoPUREII Maxiprep Kit (cat # 11555B; Zymo Research, Irvine, CA, USA) and submitted for viral packaging to the MGH Vector Core Facility (Boston, MA, USA).

Cancer Pathways Library

The Cancer Pathways Library (CPL) was obtained from Addgene (Cambridge, MA, USA) and packaged into lentivirus vectors by the MGH Vector Core Facility (Boston, MA, USA). The library is a gain-of-function screen to activate 17 different cancer-related signaling pathways (Martz et al., 2014).

Animal studies

All animal experiments were approved by the Massachusetts General Hospital Subcommittee on Research Animal Care following guidelines set forth by the National Institutes of Health Guide for the Care and Use of Laboratory Animals. Female athymic nude mice (6 - 8 weeks) were purchased from Charles River Laboratories (Wilmington, MA, USA).

Mice were injected into the mammary fat pad with 1×10^6 MDA-MB-231 cells expressing Firefly Luciferase (FLuc; for *in vivo* bioluminescence imaging – BLI – of metastases) and mCherry (fluorescent protein) in a 100 μ l mixture composed of Matrigel (50 μ l; BD Matrigel™ 10mg/ml, BD Biosciences) and PBS (50 μ l). Specifically, mice were injected with MDA-MB-231 FLuc-mCherry wild type (WT) (n = 6), MDA-MB-231 FLuc-mCherry overexpressing Her2 (n = 3) (this cell line was already available in our lab), with MDA-MB-231 FLuc-mCherry expressing the CPL (n = 11), and MDA-MB-231 FLuc-mCherry overexpressing CASP3MT (n = 3). Tumor volume was monitored bi-weekly and calculated using the following formula: $[\text{length} \times (\text{width})^2]/2$. Subcutaneous tumors were surgically resected when 500 mm³ of volume. For surgery, mice were anesthetized with a mixture of 100 mg/kg ketamine and 12.5 mg/kg xylazine in 0.9% sterile saline. Post-surgery analgesia was achieved injecting 1 mg/kg buprenorphine every 12 hours. Metastases were weekly monitored using BLI. Briefly, animals were injected with D-luciferin (Santa Cruz Biotechnology) and imaged 10 min post-injection with the Xenogen IVIS imaging system connected to Living Image acquisition and analysis software. Mice were sacrificed when symptoms of distress were evident and main organs (brain, heart, lungs, liver, bone), as well as other metastatic organs, if any, were snap-frozen in liquid nitrogen and stored at -80°C for further analyses.

For brain injection of tumor cells, mice were placed in a stereotaxic frame and intracranially injected into the striatum with 5×10^4 MDA-MB-231 FLuc-mCherry WT (n = 5) or MDA-MB-231 FLuc-mCherry CASP3MT⁺ (n = 5) in 2 μ l using a Micro 4 Microsyringe Pump Controller (World Precision Instruments, Sarasota, FL) attached to a Hamilton syringe with a 30-gauge needle (Hamilton, Reno, NV), at the following coordinates in mm from bregma: +1.0 antero-posterior, +2.0 medio-lateral, -2.5 dorso-ventral. Tumor growth was weekly monitored using BLI as previously described. Regions of interest (ROIs) were measured per each mouse to determine tumor volume.

RNA extraction and Polymerase Chain Reaction

The RNA was extracted from the collected mice tissues using Quick-RNA MiniPrep Kit (Zymo Research, Irvine, CA, USA) following manufacturer's protocol. cDNA was synthesized from 500 ng RNA using 5X All-In-One RT MasterMix (Applied Biological Materials, Richmond, Canada). In order to detect microscopic metastases, a nested PCR for FLuc was carried out using the following primers: FLuc PCR1 Forward: 5' – CCA GGG ATT TCA GTC GAT GT – 3', Reverse: 5' – CGG TAC TTC GTC CAC AAA CA – 3'; FLuc PCR2 Forward: 5' –

TCA AAG AGG CGA ACT GTG TG – 3', Reverse: 5' – GGT GTT GGA GCA AGA TGG AT – 3'. Regarding macroscopic metastases, in order to get the PCR product to be sequenced, a PCR was performed using the following primers: attR1 Forward: 5' – GCT AGC ATC GAT GGA TCA ACA AGT – 3' and WPRE Reverse: 5' – CAT AGC GTA AAA GGA GCA ACA. Concerning microscopic metastases, in order to get the PCR product to be sequenced, a nested PCR was carried out using the following primers: PCR1 – PGK Forward: 5' – CAT TCT GCA AGC CTC CGG A – 3', WPRE Reverse; PCR2 – attR1 Forward, WPRE Reverse.

DNA sequencing

cDNA from macroscopically and microscopically metastatic organs was amplified by PCR as described above. PCR product was purified using Monarch PCR & DNA Cleanup Kit (New England Biolabs, Ipswich, MA, USA) following manufacturer's protocol. Samples were then submitted to MGH DNA Core (Boston, MA, USA) for Sanger sequencing using WPRE Reverse primer.

Proliferation assay

In order to assess proliferation rate, Gaussia Luciferase (GLuc)-expressing cells (MDA-MB-231 and MCF7) were plated on a 24-well plate at a concentration of 5,000 cells/well or 10,000 cells/well in 2ml of DMEM supplemented with 10% FBS. 60 μ l of medium was collected 1.5h, 24h, 48h, 72h, 96h, 120h after seeding and stored in -20°C. 15 μ l of stored medium was plated in triplicates into a white 96-well luminometer plate. GLuc activity was then measured by an MLX Microtiter plate luminometer (Dynex Technologies, Chantilly, VA, USA) with automated injection of 50 μ l coelentraine (CTZ; 8 ng mg⁻¹; NanoLight, Pinetop, AZ).

Wound healing assay

A wound healing assay was performed to assess migration. Cells were seeded in a 6-well plate. When 100% confluent, two scratches per well were performed using a p100 tip. The wells were then washed once with PBS to remove any cellular debris and to smooth the scratch edges. Using an inverted microscope, images were taken 1h, 12h, and 18h after for MDA-MB-231, and 1h, 12h, 18h, 22h, and 48h after for MCF7. ImageJ was used to calculate the distance (expressed in pixels) between the scratch edges at each time point. Specifically, 3 reference points were made per each scratch and 10 values were calculated per each picture. Migration was measured comparing the distance calculated 1h after the scratch to the distance calculated in the other time points.

Transwell migration assay

To assess migration, a transwell migration assay was carried out using 24-well Transwell migration chamber (Corning, Corning, NY) with 8- μ m-pore-size polyethylene membranes. 5 x 10⁴ cells were placed in the upper chamber of the insert with 100 μ l DMEM + 0.5% FBS. The lower chamber was filled with 400 μ l DMEM + 10% FBS. Cells were allowed to migrate towards the lower chamber for 7 hours at 37°C. The medium containing floating cells from the lower chamber was then transferred into a new well. 500 μ l of trypsin-EDTA were added to the lower chamber to detach cells attached to the bottom side of the chamber. After 10 min incubation at 37°C, trypsin activity was stopped with FBS and the medium was moved to the well where

floating cells-containing medium was previously moved. 500 μ l of CellTiter Glo (Promega, Madison, WI) were added to each well. The plate was covered with aluminium foil, shaken for 10 min, and then incubated for 10 min at room temperature. 75 μ l of medium was moved to a white 96-well luminometer plate in triplicate (3 wells per condition). The plate was read by an MLX Microtiter plate luminometer (Dynex Technologies, Chantilly, VA, USA).

Phase IV: intercellular communication through extracellular vesicles

The majority of the experiments belonging to this phase have been performed at the Department of Neurology of the Massachusetts General Hospital/Harvard Medical School in Boston, MA, where I have been working for 13 months during my period abroad.

Cell lines

Established primary human glioblastoma cells (GBM8, kindly provided by A. Krichevsky, Harvard Medical School, Boston, MA) were cultured in 0.22 μ m-filtered Neurobasal® medium (Gibco™ Invitrogen Corporation, San Diego, CA) supplemented with Glutamax (Gibco™ Invitrogen Corporation, San Diego, CA) (3mM), N2 (Gibco™ Invitrogen Corporation, San Diego, CA) (0.5mL/100mL), B27 (Gibco™ Invitrogen Corporation, San Diego, CA) (2mL/100mL), EGF (R&D system) (20ng/mL), FGF (PEPROTECH) (20ng/mL), and penicillin-streptomycin (10 IU ml⁻¹ and 10 μ g ml⁻¹, respectively, Sigma-Aldrich, St Louis, MO, USA).

Primary Human Brain Microvascular Endothelial Cells (HBMVEC) from Cell Systems (Catalogue #ACBRI-376, Kirkland, WA, USA) were cultured in EGM-2 MV (Lonza, Basel, Switzerland). Cells were maintained at 37°C in a humidified atmosphere with 5% CO₂.

Growth medium from plates where no cells were seeded (unconditioned medium – UCM) was included in all the experiments and used as a negative control.

A canine mammary tumor cell line (CYPP) and a feline mammary tumor cell line (FMCp) (kindly provided by Dr. Raffaella De Maria, University of Turin, Italy) were cultured in Roswell Park Memorial Institute (RPMI 1640) (Aurogene, Rome, Italy) containing 1% penicillin/streptomycin and 10% FBS. Additionally, as a positive control for EV characterization, human breast cancer MCF7 cell line has been used.

Extracellular vesicle purification

Extracellular vesicles were purified for two main experiments. The first included the analysis of endothelial cell proliferation and tube formation (tubule formation assay) under the influence of glioblastoma (GBM) cells-derived EVs. The second experiment included the identification of EVs from feline and canine mammary tumor cells.

For EVs purification, GBM8 single cells were seeded at 10,000 cells/cm² in four 150mm dishes and cultured as neurospheres for 8 days, adding fresh medium every 3 days. GBM8 neurospheres were then transferred on basal medium (EBM-2 Basal Medium, Lonza, Basel, Switzerland) for 48 hours before extracellular vesicle (EV) isolation.

The conditioned basal medium (100mL) from approximately 20 millions GBM8 cells was harvested after 48 hrs. The EVs were isolated by differential centrifugation. Briefly, conditioned and unconditioned media were centrifuged at $300 \times g$ for 10 min at 4°C to remove any cells/cell debris. The supernatant was transferred to a clean 50 mL tube and further centrifuged at $2,000 \times g$ for 10 minutes at 4°C to remove additional cell debris. The supernatant was then transferred to a clean ultracentrifuge tube (Beckman Coulter, Brea, CA, USA) and ultracentrifuged at $100,000 \times g$ for 90 min at 4°C (70.Ti Beckam rotor) to obtain EV-enriched pellet. The ultracentrifuged conditioned and unconditioned supernatants were removed and preserved at 4°C and the EV pellets and the UCM pellets were resuspended in $200\mu\text{L}$ of sterile double-filtered (df) ($0.22\mu\text{m}$) PBS. EV pellets were measured for their nanoparticles content using Nanosight instrument technology (Nanosight NTA 2.2 software) (3x60sec videos/sample, detection threshold: 6). For comparison, EVs were identically purified and measured from filtered Neurobasal® supplemented medium (100mL) identically harvested after 48h of neurospheres growth from approximately 20 millions GBM8 cells.

Similarly, for the EV analyses from human, canine, and feline cells, 1×10^6 ($6.5 \times 10^3/\text{cm}^2$) CYPp, FMCp, and MCF7 cells per plate were seeded into two 15-cm culture plates in 25 ml of growth medium. After 24 hours, the medium was replaced by the same medium prepared with 5% EV-depleted FBS for 48 hours prior to EV isolation. EV-depleted FBS was prepared by overnight (16 hours) ultracentrifugation at $100,000 \times g$ at 4°C . The pellet was then discarded and the supernatant (EV-depleted FBS) was sterile filtered using a $0.22 \mu\text{m}$ filter (Millipore, Billerica, MA, USA). For each experiment, 50 ml of conditioned medium from each cell line were used to isolate EVs. Additionally, 50 ml of UCM were used as negative control from both DMEM and RPMI. Total cell count prior to EVs isolation was assessed using a hemocytometer. The media were first centrifuged at $300 \times g$ for 10 minutes at 4°C to remove any cells/cell debris. The supernatant was then transferred to a clean 50 ml Falcon tube and centrifuged at $2,000 \times g$ for 10 minutes at 4°C to remove additional debris. The supernatant was then transferred to a clean ultracentrifuge tube (Beckman Coulter, Brea, CA, USA) and ultracentrifuged at $100,000 \times g$ for 90 minutes at 4°C to obtain EVs-enriched pellet. The supernatant was removed and the pellet was resuspended for further analyses (see below).

HBMVEC in vitro angiogenesis assay

In order to study the role that GBM-derived EVs play on endothelial cells and therefore to investigate whether EVs stimulate and are involved in angiogenesis, HBMVECs (500,000/well) were cultured on Matrigel™-coated (BD Matrigel™ 10mg/mL, BD Biosciences, Franklin Lakes, NJ, USA) wells in a 6-well plate in i) endothelial basal medium (EBM-2); ii) EBM-2 supplemented with a cocktail of angiogenic factors (EGM-2 SingleQuot Kit Suppl. & Growth Factors, Lonza); iii) EBM-2 with $200 \mu\text{l}$ GBM8-derived EV pellet (10×10^4 EVs/cell); iv) EBM-2 with $200 \mu\text{l}$ GBM8-derived supernatant; v) EBM-2 with $200 \mu\text{l}$ UCM-derived pellet; and vi) EBM-2 with $200 \mu\text{l}$ UCM-derived supernatant. Pellets and supernatants were measured for particles content by Nanosight instrument technology (Nanosight NTA 2.2 software) (3x60sec videos/sample, detection threshold: 6). After 16 hours of exposure, 3 random pictures at 4X and 25 random pictures at 10X per well were taken. Angiogenesis was analyzed with the ImageJ software (NIH). Specifically, the tubules length (10X), the number

of tubules (10X), the number of branching points (10X), and the number of meshes (4X) were assessed. Experiments were conducted in triplicates.

Total RNA extraction from HBMVECs

For HBMVECs transcriptome analyses after GBM8-derived EVs exposure, after 16 hours of exposure, the medium was gently removed, centrifuged at 2,000 x g for 15 minutes at 4°C to collect floating cells, and dry pellets preserved at 4°C. Equilibrated (37°C) Dispase (BD Biosciences, Franklin Lakes, NJ, USA) was added (0.2 mL per cm²) to Matrigel™ and incubated at 37°C for 1.5 h. After pipetting to carefully suspend the cells, 3.6 ml EDTA (5mM sterile, pH=8) was used to stop Dispase activity and cells were pelleted twice by centrifugation (2,000 x g for 15 minutes at 4°C). Cell pellets from medium and Matrigel™ were collected for each sample and washed in 600 µl sterile dfPBS (2,000 x g for 15 minutes at 4°C) and finally resuspended in 100 µl sterile dfPBS for RNA extraction. Total RNA was purified using Exiqon miRCURY RNA Isolation Kit-Cell & Plant (Exiqon, Denmark), according to the manufacturer's protocol.

Transmission Electron Microscopy (TEM)

TEM was performed to visualize and measure EVs derived from canine and feline cells. HBC cells were included always as positive control.

TEM was performed at the Department of Biology of the University of Padua, Italy. After ultracentrifugation, the EV-enriched pellet and a presumptive UCM pellet were resuspended in 100 µl of double 0.22 µm filtered (df) PBS for 30 minutes on ice.

Twenty microliters of each sample were adsorbed for 2 minutes to 300 mesh carbon-coated copper grids that were made hydrophilic by a 15-second exposure to a glow discharge. Excess liquid was removed with filterpaper (Whatman, Maidstone, UK) and the samples were stained with 1% uranyl acetate for 2 minutes. After removing the excess uranyl acetate with filter paper the grids were examined with a Tecnai G² (FEI) transmission electron microscope operating at 100 kV. Images were captured with a Veleta (Olympus Soft Imaging System) digital camera.

Immunogold staining

Immunogold staining was applied to identify at TEM the EVs derived from canine and feline cells. HBC cells were included always as positive control.

Resuspended samples (twenty microliters) were adsorbed for 2 minutes to 300 mesh carbon-coated. For labelling, a first blocking step was performed with 0.5% BSA in PBS 1X for 30 minutes. The samples were successively incubated with mouse anti-CD63 (1:50; BD Bioscience, clone H5c6) or mouse anti-Alix (1:50; Santa Cruz, sc-53538) for 30 minutes followed by secondary anti-mouse 10 nm protein A-gold conjugates (Sigma-Aldrich) for 30 minutes. After the staining with 1% uranyl acetate, they were observed using a Tecnai G² (FEI) transmission electron microscope operating at 100 kV. Images were captured with a Veleta (Olympus Soft Imaging System) digital camera.

Protein extraction and Western Blotting analysis

Western Blotting was performed to identify the protein content from the EVs derived from canine and feline cells. HBC cells were included always as positive control.

Cell proteins were isolated from MCF7, CYPp, and FMCp at 90% confluence on a 15-cm plate using 2 ml of M-PER Mammalian Protein Extraction Reagent (Thermo Fisher #78501) according to manufacturer's protocol. Proteins from the EVs-enriched pellets and a presumptive UCM pellet (from RPMI) were extracted resuspending the pellets after ultracentrifugation in 70 μ l M-PER Mammalian Protein Extraction Reagent (Thermo Fisher #78501).

Cells and EV-derived protein concentrations were calculated using Pierce BCA Protein Assay Kit (Thermo Scientific #23225) according to manufacturer's protocol.

Twenty μ g of proteins from cells/EVs were denatured at 95°C for 5 minutes. Proteins were then resolved by NuPAGE 4-12% Bis-Tris gel (Invitrogen, Thermo Fisher, Rockford, IL, USA) and transferred to nitrocellulose membrane (Whatman_GE Healthcare Life Science, Maidstone, UK). Nonspecific binding sites were blocked for 1 h in 5% nonfat dry milk in TBS-T (TBS containing 0.05% Tween-20) at room temperature. Blots were then incubated at 4°C overnight with primary antibodies against Alix (1:200; Santa Cruz sc-53538), TSG101 (1:500; Abcam ab83), and GAPDH (1:1000; Merck CB1001). This step, after 3 washes in TBS-T, was followed by the membranes incubation in a peroxidase-conjugate secondary antibody (1:5000; GE Healthcare Life Sciences, Maidstone, UK) for 1 h at room temperature. All antibodies were diluted in TBS-T containing 3% nonfat dry milk. After washing in TBS-T, the reactive bands were visualized with a chemiluminescence detection kit (SuperSignal West Pico Chemiluminescent Substrate, Thermo Fisher, Rockford, IL, USA) followed by exposure of the membrane to autoradiography film (Denville Scientific, NJ, USA).

Nanoparticle Tracking Analysis

In order to visualize, quantify, and measure EVs derived from GBM8, MCF7, CYPp, and FMCp cells, Nanoparticle Tracking Analysis (NTA) was performed at the Department of Neurology of the Massachusetts General Hospital/Harvard Medical School, Boston, MA, USA. EVs were purified by ultracentrifugation and quantified using the NanoSight LM10 (Malvern, Framingham, MA). EVs and a presumptive UCM pellet were resuspended in 100 μ l of dfPBS. The samples were incubated on ice for 30 minutes and then transferred to a new tube. For NTA measurement, samples were diluted 1:100, 1:500, and 1:1000 in dfPBS. Five movies of 30 seconds were recorded for each sample and each dilution and analyzed using the 2.2 NTA software (Malvern, UK) with the following settings: screen gain 6.0 and camera level 10. For EVs quantification, only the values within the instrument optimal working range (1×10^8 – 25×10^8) were considered. Particles number measured in the presumptive UCM pellet was subtracted to particles number measured in EV-enriched pellet to calculate the total number of EVs produced by the cells. In order to have the specific UCM-derived particles both DMEM and RPMI were analyzed. Since it is known that different media might contain different amount of particles due to their different composition in terms of proteins and salts, also Endothelial Basal Medium (EBM; Lonza, Allendale, NJ, USA) and Neurobasal Medium (NB; Gibco, Thermo Fisher Scientific, Waltham, MA, USA) were included as UCM for comparison.

EV uptake analysis

To assess EV uptake by recipient cells (CYPp), the system developed by Lai and collaborators was applied (Lai et al., 2015). For EV donor, CYPp cells were infected with lentiviruses to stably express palmtTomato reporter (CYPp-palmtTomato). For EV recipient cells, CYPp cells were infected with lentiviruses to stably express GFP reporter (CYPp-GFP). Briefly, for viral spinfection, cells were plated in a 6-well plate and when 60% confluent, the medium was replaced with 1 ml of fresh medium, 1 μ l of Polybrene (10 mg/ml; Sigma-Aldrich, St. Louis, MO, USA) and a volume of lentivirus (MGH Vector Core, Boston, MA, USA) based on virus titer in order to have a multiplicity of infection (MOI) of 10. The plate was immediately spun at 1,800 rpm at 37°C for 90 minutes and the medium was replaced with fresh medium the day after. After 48 hours cells were harvested and FACS-sorted in order to have a pure palmtTomato- or GFP-positive population for the next experiment. 50,000 CYPp-palmtTomato cells were seeded on top of the 1- μ m pore cell culture Transwell insert (Corning, New York, USA) in a glass-bottom 12-well plate in 500 μ l of growth medium. 30,000 CYPp-GFP cells were seeded in the bottom chamber in 1 ml of medium. Images of CYPp-GFP cells were acquired 4 hours and 4 days after seeding using confocal microscopy (Zeiss LSM 710). Confocal Z-stack images were captured using a 63X objective.

Statistical analysis

Statistical analysis was performed using either Prism version 5.0 (GraphPad Software, San Diego, CA, USA) or R statistical software.

To verify mean differences among groups, the Student's t test in case of two samples and the one-way ANOVA in case of more than two samples groups were used when values were normally distributed. Mann-Whitney test in case of two samples and Kruskal-Wallis test in case of more than two samples were used when values were not normally distributed. The Spearman's rank correlation analysis was used to analyze associations between variables. Level of significance was fixed as $p < 0.05$.

RESULTS

Phase I: isolation and characterization of human, canine, and feline cancer stem cells

Isolation of cells from primary tumors

The clinico-pathological features of the 13 human and 10 canine primary mammary tumor (CMT) samples are summarized in table 1 and table 2, respectively.

ID	Age (years)	Diagnosis	ER (%)	PR (%)	Her2 (%)	Ki67 (%)	Subtype	Isolation protocol
HBC1	44	IDC III	90	90	1+	20	luminal B	C/H 3h 37°C and 70um filtered
HBC2	66	IDC II	100	20	1+	40	luminal B	C/H 3h 37°C and 70um filtered
HBC3	69	IDC II	70	90	0	25	luminal B	C/H 3h 37°C and 70um filtered
HBC4	77	IDC II	100	100	1+	25	luminal B	C/H 3h 37°C and 70um filtered
HBC5	60	IDC II	NA	NA	NA	NA	NA	C/H 5.5h 37°C and 70um filtered
HBC5	60	IDC II	NA	NA	NA	NA	NA	C/H ON 4°C and 70um filtered
HBC6	54	ISC I	99	90	0	15	luminal B	no enzymatic treatment
HBC7	62	ILC I	90	3	1+	<5	luminal A	no enzymatic treatment
HBC8	73	IDC II	90	90	0	12	luminal A	no enzymatic treatment
HBC9	65	ILC I	90	5	0	2	luminal A	no enzymatic treatment
HBC10	55	IDC II	90	55	1+	25	luminal B	no enzymatic treatment
HBC11	52	ILC II	90	50	1+	18	luminal B	no enzymatic treatment
HBC12	59	IDC II	NA	NA	NA	NA	NA	no enzymatic treatment
HBC13	44	IDC II	50	0	0	50	luminal B	no enzymatic treatment

Table 1. Clinico-pathological features and isolation protocol details of human breast cancer (HBC) samples. ER, estrogen receptor; PR, progesterone receptor; IDC, invasive ductal carcinoma; ISC, invasive solid carcinoma; ILC, invasive lobular carcinoma; NA, not available; C/H, collagenase/hyaluronidase; ON, overnight.

ID	Age (years)	Diagnosis	Isolation protocol
CMT1	NA	SAD	no enzymatic treatment
CMT2	8	CC II	no enzymatic treatment
CMT3	5	SAD	no enzymatic treatment
CMT5	7	MC I	no enzymatic treatment
CMT6	10	SAD	no enzymatic treatment
CMT8	14	SPC II	no enzymatic treatment
CMT9	13	STC I	no enzymatic treatment
CMT10	15	SoC III	no enzymatic treatment
CMT11	11	CoC met	no enzymatic treatment
CMT12	11	SPC II	no enzymatic treatment

Table 2. Clinico-pathological features and isolation protocol details of canine mammary tumor (CMT) samples. SAD, simple adenoma; CC, complex carcinoma; MC, mixed carcinoma; SPC, simple papillary carcinoma; STC, simple tubular carcinoma; SoC, solid carcinoma; CoC, comedonic carcinoma.

At time of surgery, the mean age of women was 60 (\pm 9.8) and of dogs was 9.55 (\pm 3.3). Histological diagnoses of human breast cancer (HBC) samples included 9 invasive ductal carcinomas (8 grade II, 1 grade III), 3 invasive lobular carcinomas (2 grade I, 1 grade II), and 1 invasive solid carcinoma (grade I). Histological diagnoses of canine mammary tumors included 3 simple adenomas, 1 complex carcinoma (grade II), 1 mixed carcinoma (grade I), 5 simple carcinomas (2 papillary carcinomas grade II, 1 tubular carcinoma grade I, 1 comedonic carcinoma with vascular/lymphatic invasion, 1 solid carcinoma grade III). As routine diagnostic procedure for HBC, immunohistochemical analysis of 11 out of 13 tissues was present. Three tumors were

classified as luminal A (ER⁺ and/or PR⁺, Her2⁻, and Ki-67<14%) 8 tumors were classified as luminal B (either ER⁺ and/or PR⁺, Her2⁺ or ER⁺ and/or PR⁺, Her2⁻, and Ki-67>14%).

In 10 out of 13 HBC patients and in 9 out of 10 CMT subjects, the adjacent healthy/hyperplastic mammary gland tissue was collected as well.

We evaluated whether it was possible to isolate and grow *in vitro* putative cancer stem cells (CSC) from the collected mammary tumors. Based on the protocol developed by Dontu and collaborators (Dontu et al., 2003), we used optimized culturing medium containing 20 ng/ml EGF and 20 ng/ml bFGF as a stem-permissive medium, which is supposed to promote the growth of undifferentiated cells with self-renewal capacity (CSC-like). In addition, B27 was added to the medium, as previously described (Wang et al., 2014).

After collection of samples directly from the operating room, cells were cultured for several days adding fresh medium every 3 days. Unfortunately, none of the samples showed the presence of floating spheres (mammospheres) as expected. Instead, many samples showed the presence of spindle-shape cells attached to the flask/dish.

Additionally, we evaluated whether it was possible to isolate and grow *in vitro* well-differentiated cells from the collected mammary tumors culturing the cells with a 10% FBS medium. After collection, during the first days of culture, some of the samples showed the presence of both epithelial-like cells and spindle-like cells attached to the flask/dish. Cells were grown for several days, passing them when confluent. After several days or after a few passages, spindle-like cells grew faster than epithelial-like cells such that the latter were completely replaced by cells with an elongated morphology.

In order to characterize cells from primary tumors, flow cytometry against CD45, CD44, CD24, CD117, CD34, and CD133 was performed on the day of sample collection on 3 human breast cancer (HBC3, HBC4, HBC5), 1 healthy tissue adjacent to one of the previous tumor samples (HBC5), and 1 canine mammary tumor sample (CMT9).

Specifically, after collection in the surgery room, 2 HBC samples (HBC3, HBC4) were minced with sterile forceps, scissors, and razors and enzymatically digested with collagenase/hyaluronidase for 3 hours at 37°C. Afterwards, samples were filtered to discard clumps. The single cell suspension was then split and roughly 500,000 cells were prepared for flow cytometry, whereas the rest was transferred onto a petri dish and placed into the incubator. Flow cytometry showed the presence of many cellular debris. Results are summarized in table 3. Briefly, all the samples showed a heterogeneous phenotype, presumably due to the presence of several cell types. A double staining for CD44 and CD24 was performed and we showed that the majority of the cells were CD44⁺/CD24⁻ (63.96% - 71.57% for HBC samples and 91.33% for CMT sample). The other markers (CD45, CD34, CD117, CD133) showed a variable positivity.

ID	Diagnosis	CD44 ⁻ CD24 ⁻	CD44 ⁺ CD24 ⁻	CD44 ⁺ CD24 ⁺	CD44 ⁻ CD24 ⁺	CD45 ⁺	CD34 ⁺	CD117 ⁺	CD133 ⁺
HBC3	IDC II	9.15%	63.96%	4.98%	21.91%	67.97%	46.31%	61.87%	30.86%
HBC4	IDC II	11.70%	71.57%	6.29%	10.44%	31.97%	29.78%	34.21%	11.17%
HBC5H_5.5h	healthy	7.51%	77.64%	0.96%	13.90%	36.00%	31.23%	33.57%	10.52%
HBC5T_5.5h	IDC II	23.28%	36.29%	3.82%	36.62%	87.93%	60.87%	68.43%	38.76%
HBC5H_ON	healthy	6.99%	45.65%	6.81%	40.56%	94.91%	82.44%	85.60%	49.91%
HBC5T_ON	IDC II	7.10%	17.61%	1.43%	73.86%	97.57%	84.26%	86.68%	77.70%
CMT9	STC I	0.70%	91.33%	2.47%	5.50%	85.46%	38.72%	50.59%	13.33%

Table 3. Flow cytometry results on human breast cancer (HBC) and canine mammary tumor (CMT) samples for CD44, CD24, CD45, CD34, CD117, CD133. IDC, invasive ductal carcinoma; STC, simple tubular carcinoma.

Cells plated in a cell culture dish were left into the incubator for several days in a medium composed of DMEM/F12 + 10% FBS, adding fresh medium every 3 days. During the first days of culture, the samples showed the presence of both epithelial-like cells and spindle-like cells attached to the flask/dish. Cells were grown for several days, passing them when confluent. After several days or after a few passages, spindle-like cells grew faster than epithelial-like cells such that the latter were completely replaced by cells with an elongated morphology. The growth of these cells was highly slow. Afterwards, we tried to slightly modify the isolation procedure increasing the incubation time with collagenase and hyaluronidase to see whether the number of single cells after the enzymatic treatment increased as well.

Samples from patient HBC5 (adjacent healthy tissue – HBC5H – and tumor tissue – HBC5T –) was split into two different conditions: a portion of the sample was enzymatically digested with hyaluronidase and collagenase for 5.5 hours at 37°C (HBC5-5.5h) and another portion was digested overnight (14 hours) at 4°C (HBC5-ON). After digestion, cells were filtered and a portion of the sample was placed in a cell culture Petri dish, whereas a second portion was prepared for flow cytometry. Flow cytometry displayed that many cellular debris were present in all the samples. Overnight-incubated samples showed slightly more cellular debris than 5.5h-incubated samples. Results are summarized in table 3. Briefly, most of the samples were predominantly positive for CD45. Regarding CD44/CD24 positivity, the majority of the cells were either CD44⁺/CD24⁻ or CD44⁺/CD24⁺. Samples incubated overnight showed a higher percentage of CD45⁺, CD34⁺, CD117⁺, and CD133⁺ when compared to samples incubated for 5.5 hours.

Cells plated in a cell culture dish were left into the incubator for several days in a medium composed of DMEM/F12 + 10% FBS, adding fresh medium every 3 days. A few fibroblast-like cells attached to the dish but their growth was extremely slow. Cells were grown for several days, passing them when confluent. After several days or after a few passages, spindle-like cells grew faster than epithelial-like cells such that the latter were completely replaced by cells with an elongated morphology. The growth of these cells was highly slow.

As said, according to flow cytometry, many cellular debris were present. For this reason, we decided to avoid the enzymatic digestion for one of the canine mammary tumor samples (CMT9). Therefore, this sample was minced with sterile forceps, scissors, and razors, and placed in a Petri dish with a medium composed of DMEM/F12 + 10% FBS. After a few days of culture, we saw many spindle-like cells growing in the dish. After 15 days of culture spindle-like cells were split into a new petri dish and after 7 days, cells were trypsinized and a portion was placed in a new flask, whereas another portion was prepared for flow cytometry. Results are summarized in table 3. Cells did not show as many cellular debris as present in enzymatically digested samples (HBC3, HBC4, HBC5). When it comes to CD44/CD24 positivity, the vast majority of the cells (91.33%) were CD44⁺/CD24⁻. Moreover, cells were predominantly CD45⁺. The other markers (CD34, CD117, CD133) showed a variable positivity.

Spindle-like cells isolated from sample CMT9 grew quickly and therefore, in order to check their immunophenotype, we decided to perform an immunocytochemistry against the following antibodies: β -catenin, E-cadherin, calponin, vimentin, p63, pancytokeratins, and CD44.

Cells were negative for β -catenin, p63, CD44; 5% of the cells were moderately positive for panCK; 10% of the cells were moderately positive for E-cadherin; all the cells were strongly positive for calponin and vimentin.

The isolated human and canine cell lines that showed an active growth were stocked in liquid nitrogen for further analyses.

Mammosphere formation from cell lines

Due to the fact that isolation of CSC-like cells from primary tumors was not as expected, we decided to isolate them from well-established cell lines (CYPp and FMCP), using a human mammary cancer cell line (MDA-MB-231) as a positive control. Serum-free culture has been proven to be an efficient way to enrich CSCs (Wang et al., 2014). In the literature, different media were tried for mammosphere (MS) culture. Based on the study of Wang and collaborators (Wang et al., 2014) and on our experience with glioblastoma stem cell culture (see below), the following medium composition was used: DMEM/F12 (1:1) supplemented with bFGF, EGF, B27, N2. Both the canine mammary tumor cell line CYPp and the feline mammary tumor cell line FMCP were able to form MS under mammosphere culture condition for 7 days (figure 1). After 7 days in culture, MS reached the size of roughly 80 μm and were therefore dissociated and seeded again in order to make a new passage.

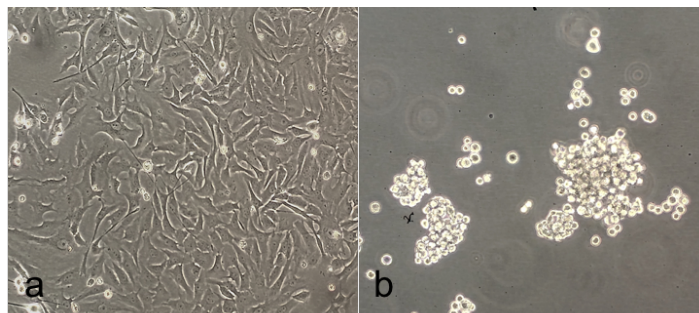


Figure 1. Representative images of CYPp adherent (a) and mammospheres (b).

RNA extraction, reverse transcription and real time polymerase chain reaction

In order to compare the mRNA expression of CD44, CD133, SOX2, and OCT4 between adherent cells (AD) and MS at different passages, we isolated RNA from AD at passage 1, MS at passage 1, MS at passage 4, and MS at passage 7. Then, after reverse transcription, a quantitative real-time PCR was performed to achieve this goal. The $\Delta\Delta\text{Ct}$ method was used to calculate the expression of stem cell markers. As shown in figure 2, the expression of CD44, CD133, and SOX2 in CYPp is higher in MS when compared to AD. Moreover, the expression of these markers, especially of CD133 and SOX2 increases over passages (MSp1 < MSp4 < MSp7). In CYPp the expression of OCT4 instead does not show any difference in MS compared to AD.

As shown in figure 3, the expression of CD44, CD133, SOX2, and OCT4 in FMCP is higher in MS than AD. Specifically, CD44 expression increases over passages (MSp1 < MSp4 < MSp7). CD133 and OCT4 expression slightly increases over passages (MSp1 < MSp4 < MSp7). SOX2 expression increases in MSp1, then it decreases in MSp4 and decrease again in MSp7. Overall, SOX2 expression in MS is higher than in the AD.

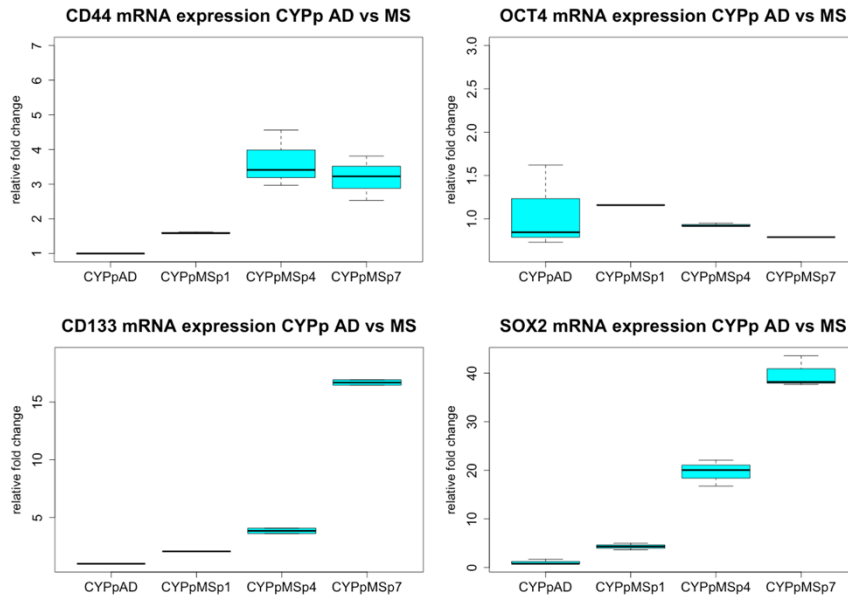


Figure 2. Gene expression of CD44, CD133, OCT4, SOX2 in CYPpAD, CYPpMSp1, CYPpMSp4, and CYPpMSp7.

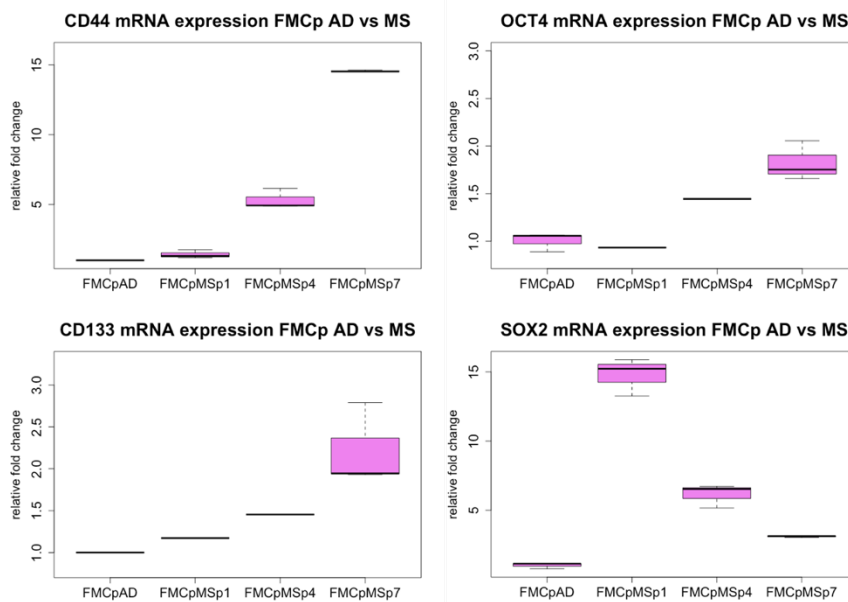


Figure 3. Gene expression of CD44, CD133, OCT4, SOX2 in FMCpAD, FMCpMSp1, FMCpMSp4, and FMCpMSp7.

Flow cytometry

Similar to gene expression, we wanted to study the expression of the following surface markers by flow cytometry: CD45, CD44, CD24, CD117, CD34, CD133. Specifically, we compared their expression in adherent cells at passage 1, 4, and 7 with their expression in MS at passage 1, 4, and 7. We performed flow cytometry on TNBC MDA-MB-231 cell line as well, as a positive control (data not shown). To prepare the cells for flow cytometry, adherent cells are typically detached from the flask using trypsin and MS are dissociated using accutase. It is known that trypsin might affect and therefore modify the expression of membrane markers by cleavage of protein domains, as it happens for CD44 (Quan et al., 2013). For this reason, we wanted to

avoid the use of enzymatic treatment (trypsin/accutase). Therefore, we initially compared enzymatic treatment with mechanic treatment. With the latter, AD were detached from the cell culture dish using a cell scraper and MS were dissociated pipetting up and down several time with PBS. In addition to a slightly worse morphology, AD showed 20% of propidium iodide-positive events when mechanically harvested, whereas almost none propidium iodide-positive events were present when enzymatically harvested. MS did not show any difference between mechanic (PBS) and enzymatic (accutase) treatment in terms of morphology and viability (data not shown). Since performing flow cytometry analyses on a population that shows 20% of propidium iodide-positive events, therefore dead cells, is not ideal and might create subsequent biases, we decided to carry on the experiment considering only the enzymatic treatment.

Both cell lines CYPp and FMCp were negative for CD45 and CD34.

Figure 4 and figure 5 show the expression of CD44, CD24, CD133 in CYPp in terms of percentage and mean fluorescent intensity (MFI). In summary, the expression of CD44⁺/CD24⁻ cells is almost 100% in all the samples. The CD44⁺/CD24⁺ population slightly increases in MS if compared to AD. MFI of CD44 is higher in MS than AD. Regarding CD133 expression, no differences between MS and AD were detected.

Figure 6 and figure 7 show the expression of CD44, CD24, CD133 in FMCp in terms of percentage and mean fluorescent intensity (MFI). In summary, the expression of CD44⁺/CD24⁻ cells is almost 100% in all the samples but MSp7, which showed a higher percentage of CD44⁺/CD24⁺ population if compared to the other samples. MFI of CD44 is higher in MS p1 and p7 when compared to AD p1 and p7, respectively. Interestingly, CD133 expression increases in MS compared to AD.

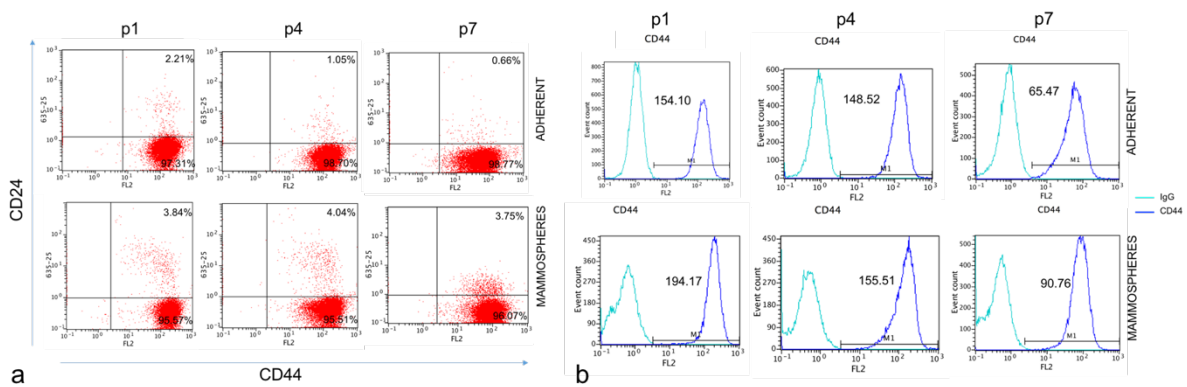


Figure 4. Flow cytometry for CD44 and CD24 on CYPp adherent and mammospheres at different passages (p1, p4, p7). Positivity is expressed as percentage (a) and mean fluorescence intensity (MFI) (b).

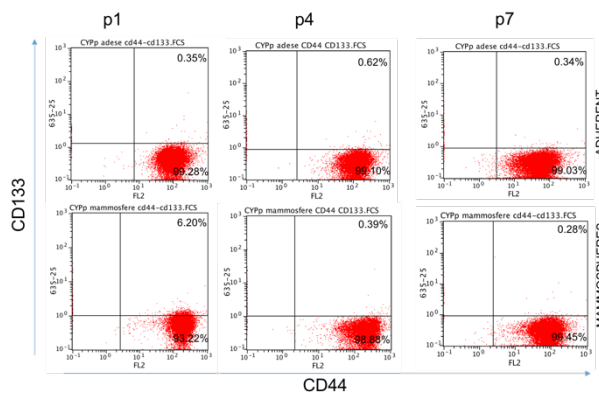


Figure 5. Flow cytometry for CD44 and CD133 on CYPp adherent and mammospheres at different passages (p1, p4, p7). Positivity is expressed as percentage.

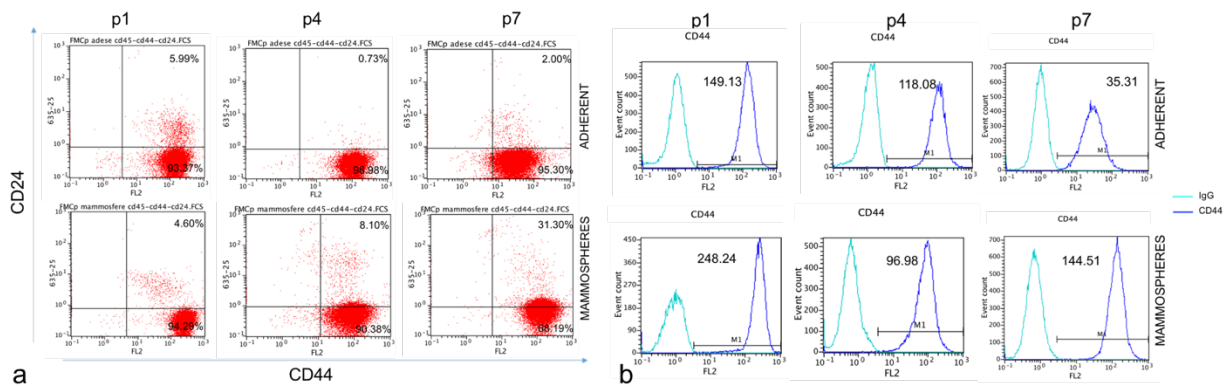


Figure 6. Flow cytometry for CD44 and CD24 on FMCP adherent and mammospheres at different passages (p1, p4, p7). Positivity is expressed as percentage (a) and mean fluorescence intensity (MFI) (b).

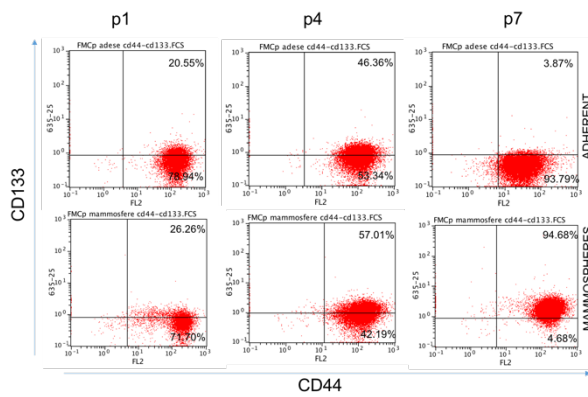


Figure 7. Flow cytometry for CD44 and CD133 on FMCP adherent and mammospheres at different passages (p1, p4, p7). Positivity is expressed as percentage.

Phase II: epithelial-to-mesenchymal transition and Wnt/ β -catenin and Hippo pathways

Gene expression

For gene expression analysis we collected 5 healthy human mammary gland tissues, 10 human breast cancer tissues (5 estrogen receptor-positive (ER+) and 5 triple-negative (TNBC)), 4 healthy canine mammary gland tissues, 10 canine mammary tumor tissues (5 simple tubular carcinomas (STC) grade I, 5 STC grade II), 6 feline healthy mammary gland tissues, and 6 feline STC grade III. Figures 8, 9, 10 show gene expression analysis in HBCs, CMTs, and FMTs, respectively.

Briefly, in human breast cancer YAP expression is higher in healthy tissues than in TNBC ($p < 0.05$) and than in ER+ ($p < 0.05$); CCND1 expression is higher in ER+ than in healthy tissues ($p < 0.05$) and than in TNBC ($p < 0.05$); SNAIL2 expression is lower in TNBC than in healthy tissues ($p < 0.05$); TWIST1 and TWIST2 expression is higher in healthy tissues than TNBC ($p < 0.05$ and $p < 0.01$, respectively) and than in ER+ ($p < 0.05$); ZEB1 expression is higher in healthy tissues than TNBC ($p < 0.05$) and ER+ ($p < 0.05$); ZEB1A expression is lower in TNBC than in healthy tissues ($p < 0.05$).

Regarding canine mammary tumors, CCND1 expression in STC grade II is higher than in healthy tissues ($p < 0.05$).

In feline mammary tumors, TWIST2 and ZEB1 expression is lower in STC III than in healthy tissues ($p < 0.05$).

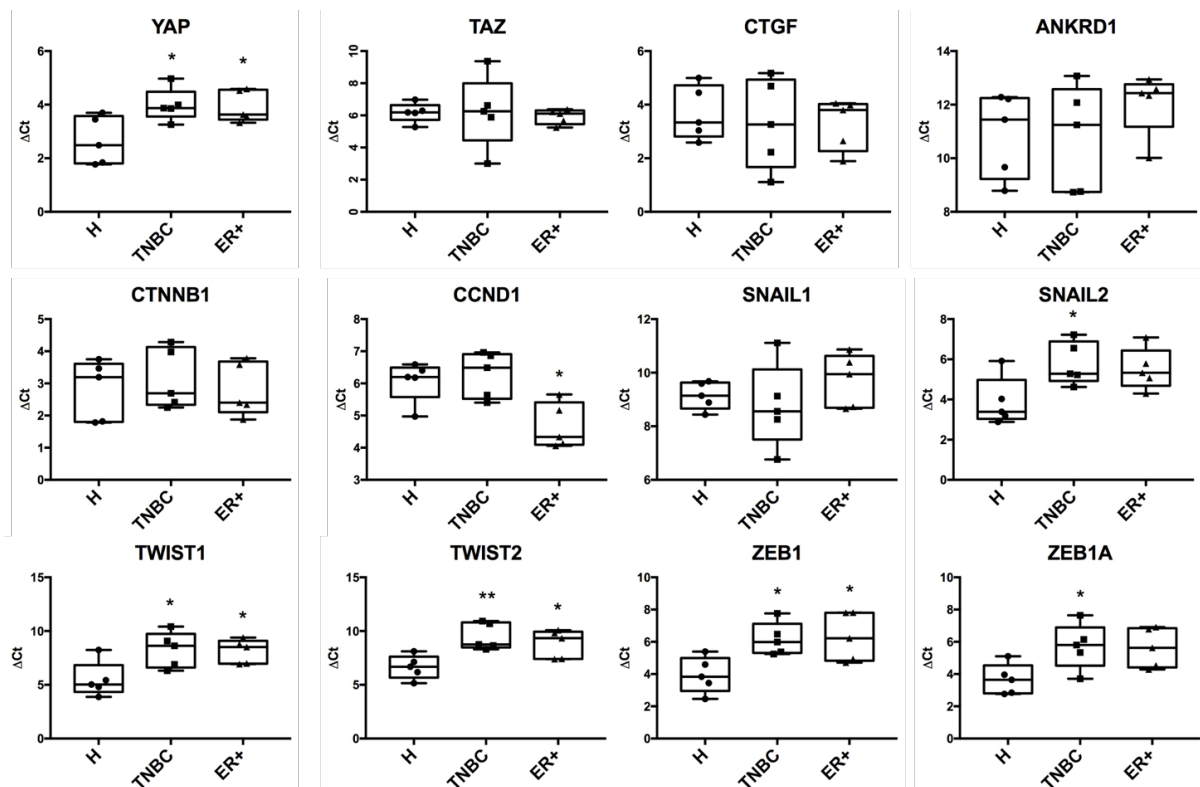


Figure 8. Gene expression in human breast cancer tissues. H, healthy mammary gland; TNBC, triple negative breast cancer; ER+, estrogen receptor-positive. * $p < 0.05$, ** $p < 0.01$.

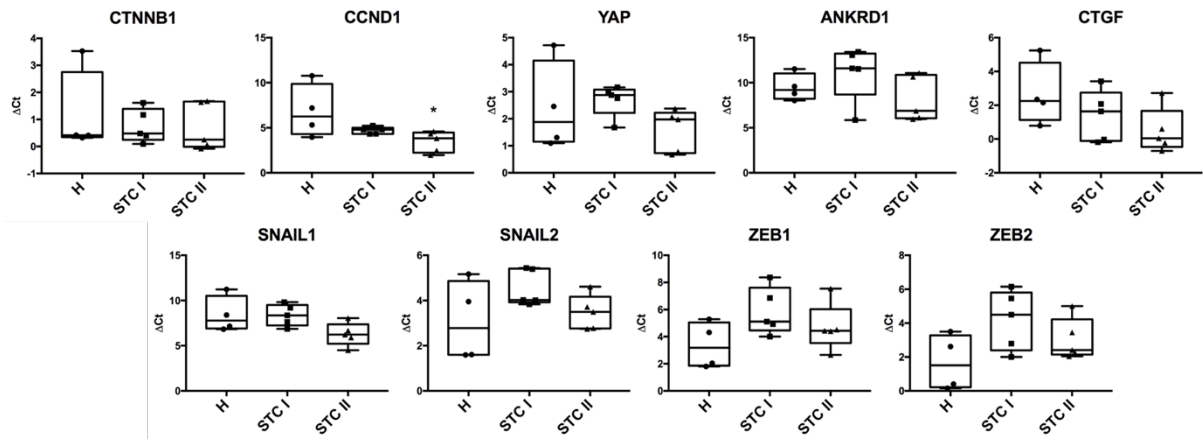


Figure 9. Gene expression in canine mammary tumors. H, healthy/hyperplastic mammary gland; STC I, simple tubular carcinoma grade I; STC II, simple tubular carcinoma grade II. * $p < 0.05$.

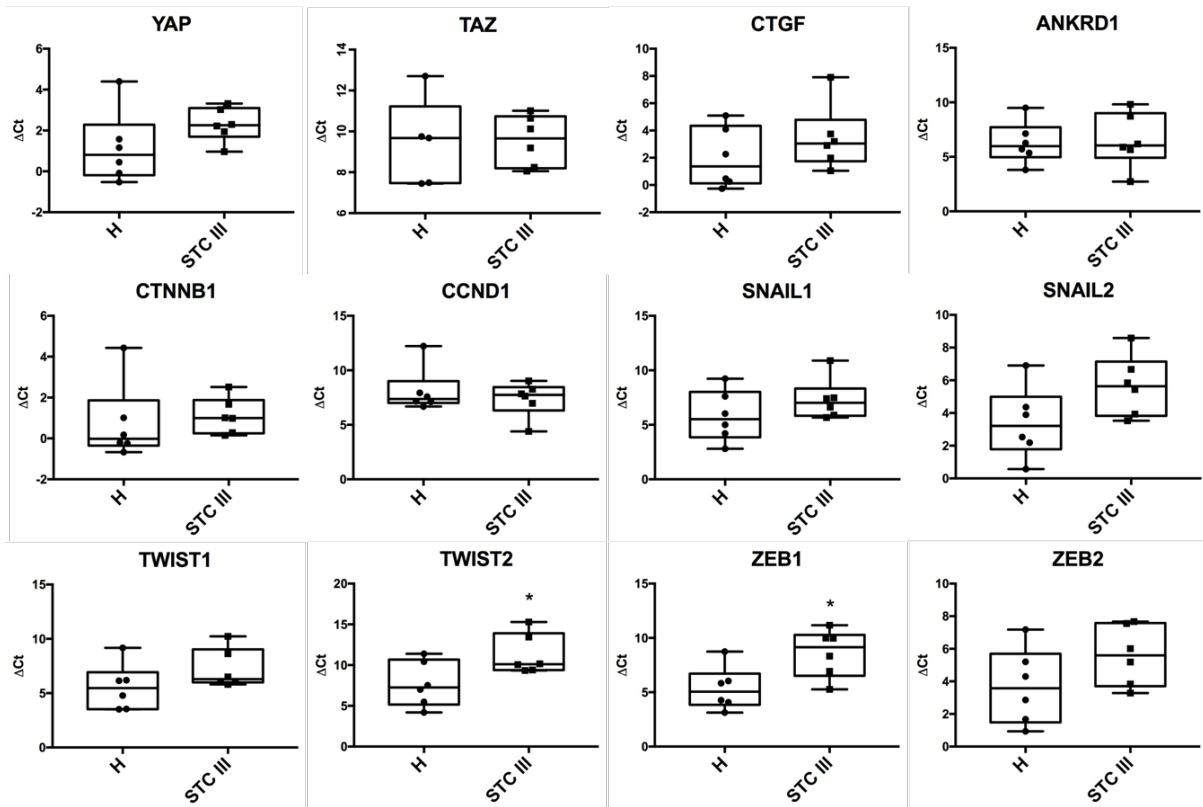


Figure 10. Gene expression in feline mammary tumors. H, healthy mammary gland; STC III, simple tubular carcinoma grade III. * $p < 0.05$.

Western blotting

Immunoblotting experiments with the antibodies anti-WWTR1, anti- β -catenin, and anti-non phosphorylated β -catenin (active form) showed bands of the expected sizes at 70 kDa (YAP), 55 kDa (TAZ), 95 kDa (β -catenin), and 95 kDa (non phosphorylated β -catenin), confirming the specificity of the antibodies against human, canine, and feline proteins as previously described (Beffagna et al., 2015). Figure 11 shows the presence of YAP, TAZ, and β -catenin in both soluble (cytoplasmic) and nuclear fractions in human, canine, and feline samples. Non-phosphorylated β -catenin is not evident in the soluble fraction, whereas is present in the nuclear fraction, as expected.

Human samples showed a higher expression of YAP and TAZ in both soluble and nuclear fractions in tumor than in healthy samples. The expression of β -catenin in the soluble fraction was higher in tumor than in healthy tissues. In the nuclear fraction, the expression of β -catenin was higher in samples 4 (ER+) and 6 (TNBC) than in samples 1 (healthy), 2 (healthy), 3 (ER+), and 5 (TNBC). In the soluble fraction the expression of non phosphorylated β -catenin was extremely low in all the samples, whereas in the nuclear fraction, tumor samples, especially samples 4 and 6, showed a higher expression than healthy tissues.

Canine samples showed a higher expression of YAP and TAZ in both soluble and nuclear fractions in tumor tissues when compared to healthy tissues. β -catenin in the soluble fraction showed a clearly higher expression in samples 5 and 6 than in samples 1, 2, 3, 4, and 7. β -catenin in the nuclear fraction showed a higher expression in tumor samples than in samples 2 and 3 (healthy tissues). Sample 1 showed a similar expression to tumor tissues. In the soluble fraction the expression of non phosphorylated β -catenin was nearly absent in all the samples, whereas in the nuclear fraction, the expression was higher in tumors than in healthy tissues.

Feline samples showed a higher expression of YAP in the soluble fraction in sample 5 (STC grade III) than in samples 1, 2, 3, and 4, whereas in the nuclear fraction the expression was higher in tumors than in healthy tissues. TAZ was higher in both soluble and nuclear fractions in tumors than in healthy tissues. The expression of beta-catenin in both soluble and nuclear fraction was higher in tumors than in healthy tissues. In the soluble fraction the expression of non phosphorylated β -catenin was nearly absent in all the samples, whereas in the nuclear fraction, the expression was higher in tumor than in healthy tissues.

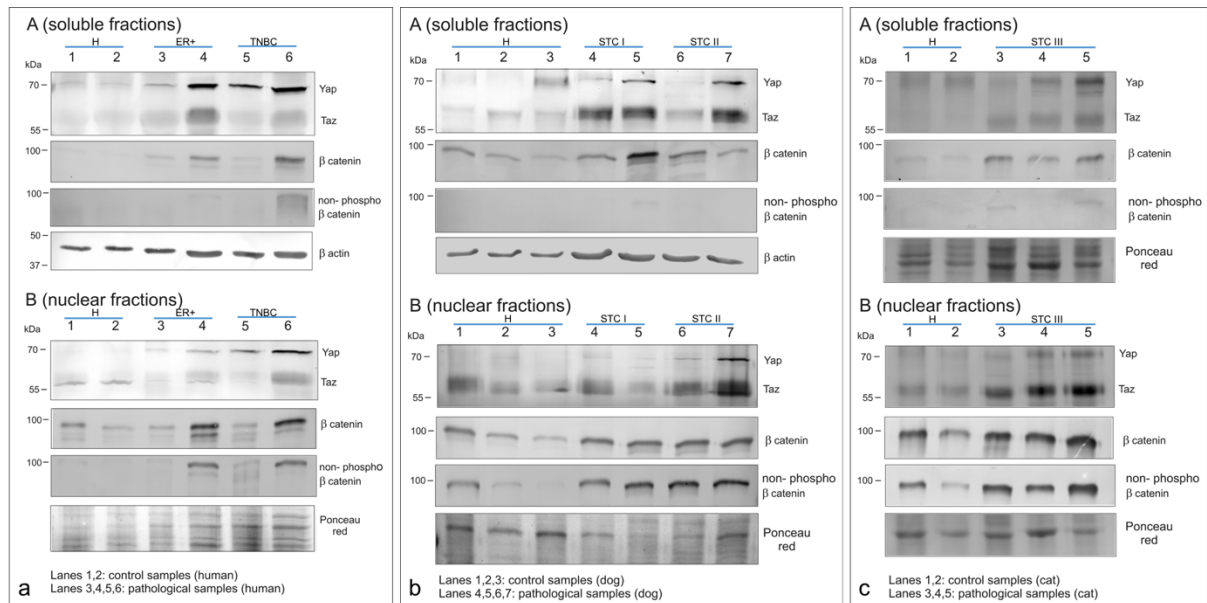


Figure 11. Western Blot for YAP, TAZ, β -catenin, non-phosphorylated β -catenin in soluble (A) and nuclear (B) fractions in human breast cancer (a), canine mammary tumor (b), and feline mammary tumor (c). H, healthy mammary gland; ER+, estrogen receptor-positive breast cancer; TNBC, triple negative breast cancer; STC I, simple tubular carcinoma grade I; STC II, simple tubular carcinoma grade II; STC III, simple tubular carcinoma grade III.

Immunohistochemistry

Selected samples were simple carcinomas, therefore composed of a single epithelial/luminal cell population. Hence, the expression of the studied markers in tumors was evaluated in the epithelial/luminal component. Staining was also observed in healthy/hyperplastic adjacent mammary tissue.

CD44 and Her2 staining was membranous; CK8/18, CK5, CK14, and vimentin staining was cytoplasmic; E-cadherin and β -catenin staining was present in either or both membrane (E-cad M, β -cat M) and cytoplasm (E-cad C, β -cat C) and it was separately evaluated; TAZ, Ki-67, ER, and PR staining was nuclear. Cutaneous adnexa and epidermis were used as positive internal controls.

As expected, epithelial/luminal cells of healthy/hyperplastic mammary gland tissue were diffusely positive for CK8/18, E-cad M, β -cat M, ER, PR and occasionally positive for CK5, CK14, and CD44. Basal/myoepithelial cells of healthy/hyperplastic mammary gland tissue were positive for CK5, CK14, CD44, TAZ, and vimentin.

Results of human, canine, and feline mammary tumors are summarized in table 4 and are graphically represented in figures 12, 13, and 14.

Regarding HBC, ER⁺ tumors had a high expression (roughly 100%) of CK8/18, whereas they were negative for basal cytokeratins CK5 and CK14. In TNBC, the expression of CK8/18, although fairly heterogeneous, was lower than in ER⁺ ($p < 0.0001$) and the expression of CK5 was higher than in ER⁺ ($p < 0.05$). In ER⁺ tumors the expression of E-cadherin and β -catenin was predominantly membranous, whereas in TNBC was predominantly cytoplasmic. Overall, the expression of these proteins was quite heterogeneous across the samples. However, a negative correlation between E-cad M and E-cad C was found in ER⁺ ($r = -1$, $p < 0.0001$) and in TNBC ($r = -0.9$, $p < 0.001$). Also, a negative correlation between β -cat M and β -cat C was detected in ER⁺ ($r = -0.888$, $p < 0.05$). TAZ expression, although heterogeneous in TNBC, was higher in TNBC than ER⁺ ($p < 0.01$).

All CMTs were positive (>1%) for ER, therefore classified as ER⁺. ER expression was lower in STC II than STC I (p<0.01). The expression of E-cad and β-cat was quite heterogeneous across the samples. However, like in HBC, a negative correlation between E-cad M and E-cad C and between β-cat M and β-cat C was found in STC I (r=-0.988, p<0.0001 and r=-0.918, p<0.0001, respectively) and STC II (r=-0.959, p<0.0001 and r=-0.7, p<0.05, respectively).

All FMTs were negative for ER, PR, and Her2, therefore classified as triple negative. Overall, the expression of CD44 was low (4.71 ± 5.36) and the expression of vimentin and Ki-67 was fairly high (68.92 ± 34.28 and 49.64 ± 13.88, respectively). TAZ, E-cad, and β-cat expression was quite heterogeneous. As found in HBC and CMT, a negative correlation between E-cad M and E-cad C and between β-cat M and β-cat C was found (r=-0.984, p<0.0001 and r=-0.909, p<0.001, respectively).

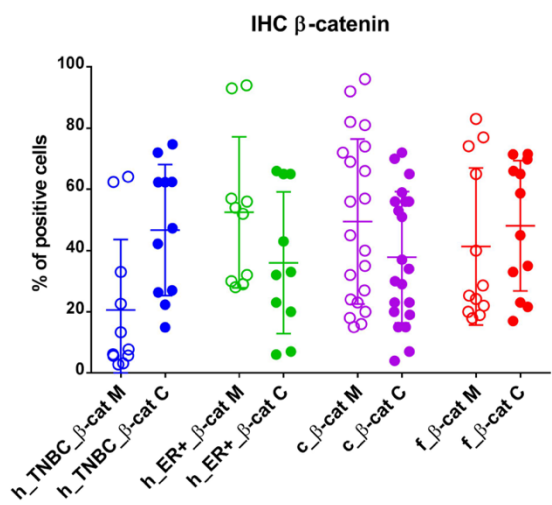


Figure 12. Immunohistochemistry results for membranous (β-cat M) and cytoplasmic (β-cat C) β-catenin in human (h), canine (c), and feline (f) mammary cancer.

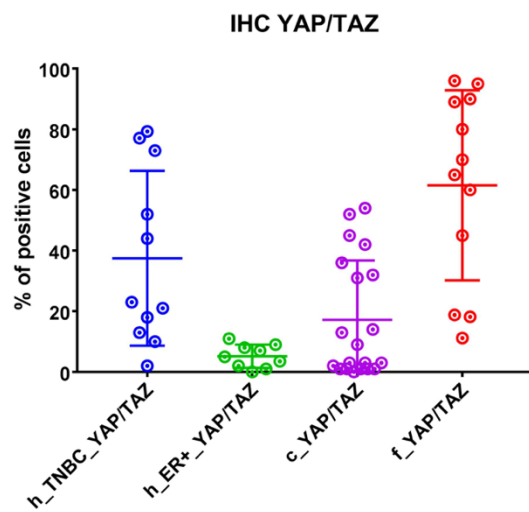


Figure 13. Immunohistochemistry results for YAP/TAZ in human (h), canine (c), and feline (f) mammary cancer.

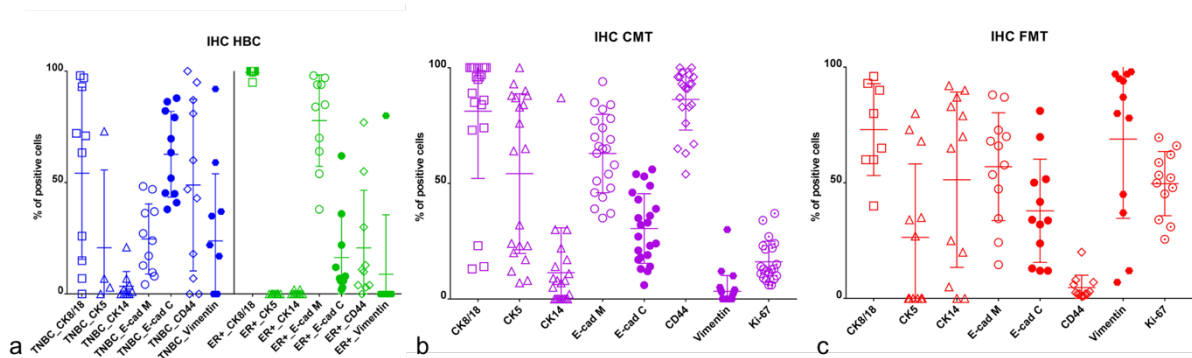


Figure 14. Immunohistochemistry results for immunophenotypic markers in human (a), canine (b), and feline (c) mammary cancer. TNBC, triple negative breast cancer; ER+, estrogen receptor-positive breast cancer.

IHC (mean ± sd)	HBC ER+	HBC TNBC		CMT STC I	CMT STC II	FMT STC III
<i>ER</i>	>1%	negative		30.36 ± 17.39**	13.10 ± 16.39**	negative
<i>PR</i>	NA	negative		NA	NA	negative
<i>Her2</i>	NA	negative		negative	negative	negative
<i>CK8/18</i>	99.50 ± 1.58****	52.95 ± 36.91****		91.70 ± 10.42	70.80 ± 37.96	73.00 ± 19.85
<i>CK5/6</i>	negative*	14.18 ± 26.24*		54.89 ± 32.85	53.64 ± 37.49	26.42 ± 31.75
<i>CK14</i>	0.40 ± 0.84	3.18 ± 6.32		9.64 ± 11.73	13.09 ± 25.42	51.33 ± 37.92
<i>CD44</i>	20.70 ± 25.82	48.91 ± 38.57		85.73 ± 14.54	86.82 ± 12.43	4.71 ± 5.36
<i>E-cad M</i>	77.80 ± 20.53****	24.70 ± 15.70****		58.91 ± 18.76	66.91 ± 14.76	56.97 ± 23.29
<i>E-cad C</i>	16.40 ± 19.08***	62.74 ± 19.25***		35.09 ± 15.65	25.82 ± 13.60	37.91 ± 22.29
<i>β-cat M</i>	52.50 ± 24.67*	20.59 ± 23.01*		43.73 ± 25.75	54.45 ± 27.13	41.33 ± 25.65
<i>β-cat C</i>	36.00 ± 23.15	46.70 ± 21.42		44.82 ± 21.86	30.09 ± 18.10	48.08 ± 21.30
<i>TAZ</i>	5.35 ± 3.65**	37.49 ± 28.82**		4.18 ± 9.32	2.46 ± 3.11	61.52 ± 31.35
<i>Vimentin</i>	8.89 ± 26.67	23.82 ± 30.12		23.60 ± 23.30	10.00 ± 12.74	68.92 ± 34.28
<i>Ki-67</i>	NA	NA		14.04 ± 6.96	18.40 ± 10.44	49.64 ± 13.88

Table 4. Immunohistochemistry results in human (HBC), canine (CMT), feline (FMT) mammary cancer represented as average ± standard deviation (sd) of percentage of positive cells and comparisons between groups of the same species for the same marker. ER, estrogen receptor; PR, progesterone receptor; E-cad, E-cadherin; β-cat, β-catenin; M, membrane; C, cytoplasm; TNBC, triple negative breast cancer; STC I, simple tubular carcinoma grade I; STC II, simple tubular carcinoma grade II; STC III, simple tubular carcinoma grade III. * p < 0.05; ** p < 0.01; *** p < 0.001; **** p < 0.0001.

Phase III: *in vivo* model of mammary cancer metastases

Animal model of breast cancer metastases

In order to study metastases from breast cancer, mice were injected into the mammary fat pad with the triple negative breast cancer cell line MDA-MB-231. Tumors were surgically removed when 500 mm³ of volume and metastases were monitored using *in vivo* bioluminescence. Mice were sacrificed when symptoms of distress were evident.

Injected cells stably expressed the fluorescent protein mCherry and the enzyme Firefly Luciferase (FLuc), that catalyzes the reaction with a substrate (D-luciferin) allowing the visualization of tumor cells within the mice using *in vivo* bioluminescence.

To develop a clinically relevant mouse model for breast cancer metastases, with particular attention to brain metastases, we initially injected 20 mice as following: 6 mice were injected with MDA-MB-231 FLuc-mCherry wild type (WT); 3 mice were injected with MDA-MB-231 FLuc-mCherry that overexpressed Her2 (Her2⁺); 11 mice were injected with MDA-MB-231 FLuc-mCherry that expressed the Cancer Pathways Library (CPL). The CPL is a gain-of-function screen to activate 17 different cancer-related signaling pathways that are implicated in cancer cell proliferation, survival, differentiation, and apoptosis (Martz et al., 2014). For each pathway, a group of one to three mutant complementary DNAs (cDNAs) were identified representing crucial molecule in each pathway that, when overexpressed, activated or inactivated the pathway. Pathway-activating mutants were used for those pathways that typically have tumor promoting roles, whereas pathway-inhibiting mutants were used for those pathways that have tumor-suppressive roles. MDA-MB-231 were stably transduced with 39 different mutant cDNAs such that we generated a heterogeneous cell population where each cell contained only a single viral integration. In other words, in each cell only one gene of the library was expressed.

Subcutaneous tumor volume was weekly measured using a caliper. The fastest tumor growth was achieved by CPL cells, followed by Her2⁺ and by WT (data not shown). Between 30 and 45 days after injection, all the mice underwent surgery to remove the subcutaneous primary tumor. Two WT mice and one CPL mouse died after surgery. After surgery, metastases were weekly monitored using *in vivo* bioluminescence. Between 13 and 17 weeks after injection all the mice were sacrificed because of symptoms of distress. After euthanasia, a necropsy was performed on the animals and main organs (brain, heart, lungs, liver, and bone) as well as other metastatic organs, if any, were collected for further analyses. As seen using *in vivo* bioluminescence (figure 15), necropsy confirmed that 2 WT mice (33%), 3 Her2⁺ mice (100%), and 7 CPL mice (63%) developed macroscopic metastases in various organs: subcutaneous tissue, lungs, bone, heart, liver, and abdominal cavity.

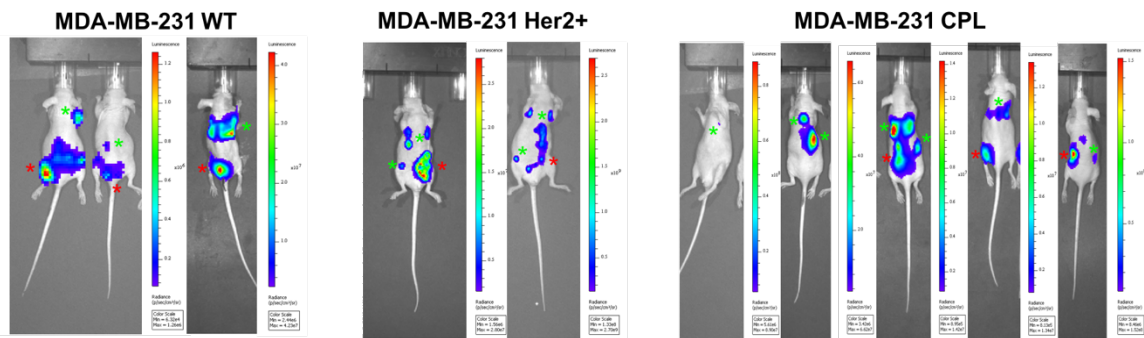


Figure 15. *In vivo* bioluminescence of a subset of mice. Green stars: metastases. Red stars: subcutaneous relapses on site of injection. WT, wild type; CPL, Cancer Pathways Library

In order to look for microscopic metastases, RNA was isolated from the collected organs and after reverse transcription, a PCR for FLuc was performed. In some cases, a regular PCR was not able to detect the presence of microscopic metastases. Therefore, to increase specificity and sensitivity, a nested PCR for FLuc was carried on. Nested PCR involves the use of two primer sets and two successive PCR reactions. The first set of primers are designated to anneal to sequence upstream from the second set of primers and are used in an initial PCR reaction. Amplicons resulting from the first PCR reaction are used as template for a second set of primers and a second amplification step. Sensitivity and specificity of DNA amplification may be significantly enhanced with this technique (Carr et al., 2010). This approach revealed the presence of micrometastases in one more WT mice and two more CPL mice. As a result, considering macroscopic and microscopic metastases 3 out of 6 WT mice (50%), 3 out of 3 Her2+ mice (100%), and 9 out of 11 CPL mice (82%) developed metastases in lungs, abdomen, heart, liver, bone, brain, and subcutaneous tissue. Among those mice that showed the presence of either macroscopic or microscopic metastases, brain metastases were present in 1 WT mouse, 1 Her2 mouse, and 5 CPL mice.

To study genetic drivers of breast cancer tropism to metastatic organs, with specific regard to the brain, we used a gain-of-function Cancer Pathways Library. MDA-MB-231 were stably transduced with the CPL, as previously described. After *in vitro* selection, cells were injected into the mammary fat pad of mice. Each injected cell had a viral vector which contained the sequence of the mutant cDNA and a promoter which ensured its expression. After surgery, RNA has been isolated from the primary tumor to verify whether all the clones were able to proliferate *in vivo*. Since each gene/mutant cDNA of the library had a different length, amplifying the region of the vector where the gene/mutant cDNA was inserted, we detected multiple bands by PCR, suggesting that multiple clones proliferated after injection and gave rise to a heterogeneous tumor (data not shown).

We used those samples that showed either macroscopic or microscopic metastases (by FLuc amplification) to amplify the sequence that contained the mutant cDNA either by PCR or nested PCR. After purification, the amplification product was sent for Sanger DNA Sequencing. Table 5 summarizes the DNA sequencing results obtained from metastatic organs. Briefly, the most represented gene in the metastatic organs was mutant caspase 3 (CASP3MT). CASP3MT was present in all the brain metastases. One brain metastasis, beside CASP3MT, showed an amplification of HRAS as well. HRAS was also present in other metastatic organs (lungs,

bone, heart, muscle). Sequencing results showed the involvement of other genes in the metastatic process, such as estrogen receptor (ER) (heart and liver), RHEB (heart and lungs), RalA (liver and abdominal mass), and JNK2 (heart).

Mouse	Metastatic organ	DNA sequencing result	Mouse	Metastatic organ	DNA sequencing result
CPL_R	brain	CASP3 (apoptosis)	C1CPL_L	muscle	HRAS (Ras-MAPK)
CPL_R	abdominal mass	CASP3 (apoptosis)	C1CPL_N	heart	JNK2WT (MAPK9) (JNK)
CPL_R	SC neck mass	CASP3 (apoptosis)	C1CPL_R	heart	RHEB (PI3K-mTOR pathway)
CPL_L	lungs	CASP3 (apoptosis)	C1CPL_R	lungs	RHEB (PI3K-mTOR pathway)
C1CPL_B	brain	CASP3 (apoptosis)	C1CPL_RR	brain	CASP3 (apoptosis)
C1CPL_B	lungs	HRAS (Ras-MAPK)	C1CPL_RR	liver	RalA (Ral pathway)
C1CPL_B	heart	ER (estrogen receptor)	C2CPL_B	brain	CASP3 (apoptosis)
C1CPL_B	liver	ER (estrogen receptor)	C2CPL_L	brain	CASP3 (apoptosis)
C1CPL_L	bone	HRAS (Ras-MAPK)	C2CPL_L	brain	HRAS (Ras-MAPK)
C1CPL_L	heart	HRAS (Ras-MAPK)	C2CPL_L	abdominal mass	RalA (Ral pathway)

Table 5. Sanger DNA sequencing results of metastatic cells.

Since we demonstrated that CASP3MT was the most relevant gene involved in the metastatic process, especially in the colonization of the brain, 3 mice were injected into the mammary fat pad with MDA-MB-231 FLuc-mCherry that overexpressed CASP3MT to see whether these cells were more aggressive and more prone to metastasize to the brain. *In vivo* CASP3MT cells grew faster than CPL and WT (data not shown). Between 29 and 32 days after injection, the mice underwent surgery for primary tumor resection. One CASP3MT animal died while waking up after surgery. One out of two CASP3MT mice developed a local relapse 30 days after surgery. Roughly 15 weeks after injection, the animals were euthanized and main organs (brain, lungs, liver, heart) were collected. Neither *in vivo* bioluminescence nor necropsy showed the presence of macroscopic metastases. However, nested PCR for FLuc showed that one animal had microscopic metastases in the brain, lungs, and liver. The other mouse had microscopic metastases in the lungs. Therefore, both animals developed metastases in the lungs and one animal developed metastases in the brain and in the liver as well.

Moreover, we perform an intracranial injection of MDA-MB-231 FLuc-mCherry CASP3MT (n = 5 mice) and MDA-MB-231 FLuc-mCherry WT (n = 5 mice) as a control, to see if and how these cells grow when directly injected into the brain. The two groups did not show any difference in tumor growth (data not shown).

Migration and proliferation assays

Three complementary approaches including wound healing assay, transwell migration assay, and proliferation assay were used to evaluate the effects of CASP3MT overexpression on cell migration and proliferation. Initially, we performed these experiments using MDA-MB-231 cell line, therefore the same cell line used in the *in vivo* study. We compared cells overexpressing CASP3MT with proper control. Wound healing assay (figure 16) showed after 12 and 18 hours a faster migration of CASP3MT cells than control. The difference after 12 hours was statistically significant (p<0.05). A higher migration (p<0.05) of CASP3MT cells was confirmed by the transwell migration experiment (figure 17). The proliferation assay (figure 18) showed that CASP3MT proliferated less than control after 24h (p<0.01), 48h (p<0.01), 72h (p<0.05), 96h (p<0.01), and 120h (p<0.05).

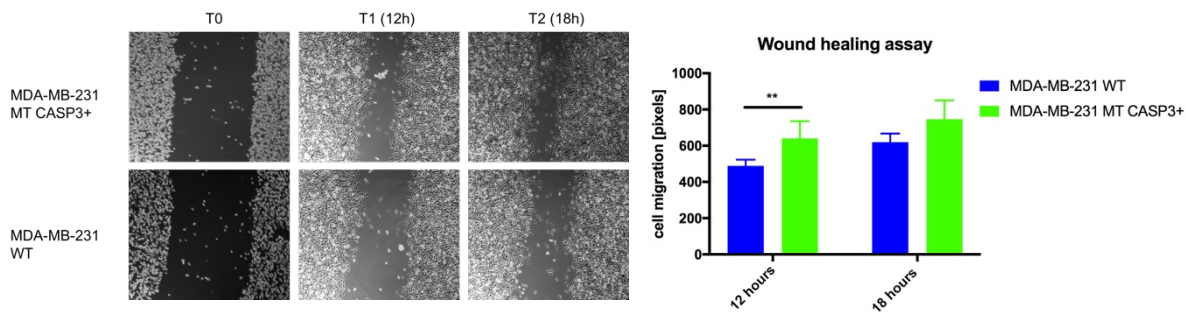


Figure 16. Wound healing assay (scratch assay) of MDA-MB-231 wild type (WT) vs MDA-MB-231 overexpressing mutant CASP3 (MT CASP3+). ** $p < 0.01$

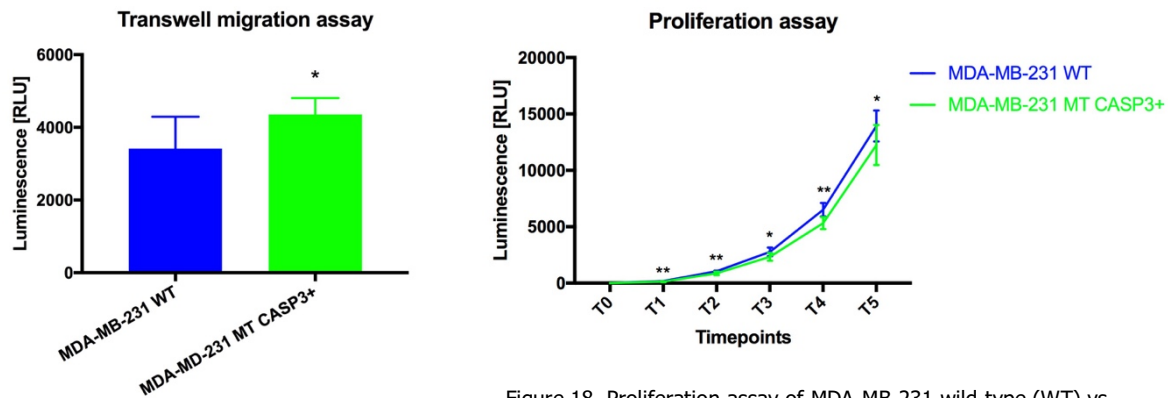


Figure 17. Transwell migration assay of MDA-MB-231 wild type (WT) vs MDA-MB-231 overexpressing mutant CASP3 (MT CASP3+). * $p < 0.05$

Figure 18. Proliferation assay of MDA-MB-231 wild-type (WT) vs MDA-MB-231 overexpressing mutant CASP3 (MT CASP3+). * $p < 0.05$; ** $p < 0.01$

The same experiments were performed on the human breast cancer cell line MCF7, which is known to be caspase-3-deficient (Jänicke, 2009), comparing the following cell lines: MCF7 WT, MCF7 overexpressing CASP3WT, and MCF7 overexpressing CASP3MT. Wound healing assay (figure 19) showed that after 12, 24, and 48 hours MCF7 WT cells migrated faster than CASP3WT ($p < 0.0001$) and CASP3MT cells (not significant). Additionally, CASP3MT cells migrated faster than CASP3WT after 24 hours ($p < 0.1$) and 48 hours ($p < 0.05$). However, transwell migration assay (figure 20) showed that the number of MCF7 CASP3MT cells that migrated into the lower compartment was significantly higher when compared to MCF7 WT ($p < 0.0001$). Similarly, the number of MCF7 CASP3WT cells that migrated into the lower compartment was significantly higher when compared to MCF7 WT ($p < 0.0001$).

Proliferation assay (figure 21) showed a higher proliferation of MCF7 CASP3MT cells than MCF7 CASP3WT and MCF7 WT ($p < 0.05$).

We also tested, by qPCR, the expression of CASP3 in breast cancer patient tissues. Specifically, CASP3 mRNA expression was calculated in 5 healthy mammary gland tissues, 5 estrogen receptor positive breast cancer, and 5 triple negative breast cancer. No differences in CASP3 expression was seen among the samples (data not shown).

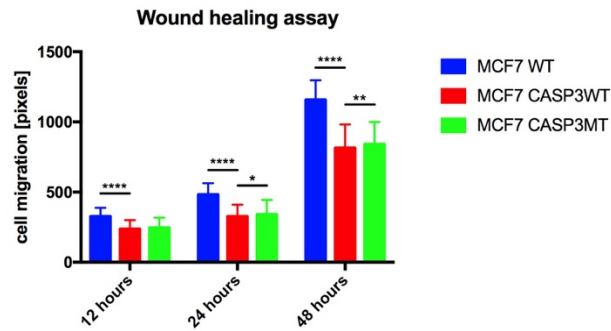


Figure 19. Wound healing assay (scratch assay) of MCF7 wild type (WT) vs MCF7 overexpressing WT CASP3 (CASP3WT) vs MCF7 overexpressing mutant CASP3 (CASP3MT). * $p < 0.05$; ** $p < 0.01$; **** $p < 0.0001$

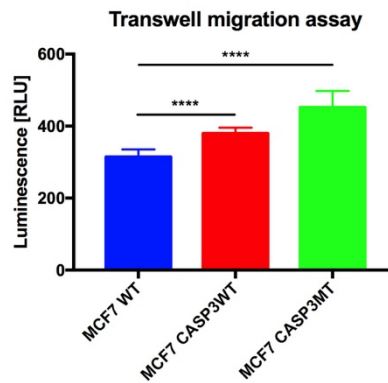


Figure 20. Transwell migration assay of MCF7 wild type (WT) vs MCF7 overexpressing WT CASP3 (CASP3WT) vs MCF7 overexpressing mutant CASP3 (CASP3MT). **** $p < 0.0001$

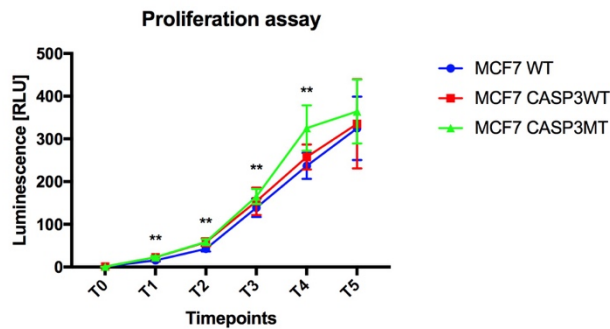


Figure 21. Proliferation assay of MCF7 wild type (WT) vs MCF7 overexpressing WT CASP3 (CASP3WT) vs MCF7 overexpressing mutant CASP3 (CASP3MT). Statistics at T1 and T2 refers to MCF7WT vs MCF7 CASP3WT and MCF7WT vs MCF7 CASP3MT; statistics at T3 refers to MCF7WT vs MCF7 CASP3MT; statistics at T4 refers to MCF7WT vs MCF7 CASP3MT and MCF7 CASP3WT vs MCF7 CASP3MT. ** $p < 0.01$

Phase IV: intercellular communication through extracellular vesicles

HBMVEC in vitro angiogenesis assay

In order to investigate the role that EVs produced by tumor cells play to promote cancer progression, we used a primary glioblastoma-derived cancer stem cell line present in the laboratory at the Department of Neurology of the Massachusetts General Hospital, where I have been working under the supervision of Prof. Xandra O. Breakefield. Specifically, to study how tumor cells stimulate angiogenesis through EV communication, we performed an experiment evaluating the effect of glioblastoma multiforme (GBM)-derived EVs on recipient endothelial cells. Endothelial cells under different conditions (EBM; growth factors; GBM8 EVs; GBM8 supernatant; UCM pellet; UCM supernatant) were cultured on Matrigel. After 16 hours of exposure, angiogenesis was phenotypically evaluated measuring the tubule length, the number of tubules, the number of branching points, and the number of meshes. As shown in figure 22, the highest values for the parameters measured were achieved by the endothelial cells treated with growth factors, followed by endothelial cells treated with GBM8 EVs. Cells treated with GBM8 supernatant showed the third highest values and the other three conditions (EBM, UCM pellet, UCM supernatant) showed the lowest values.

After angiogenesis evaluation, the RNA from endothelial cells was extracted to perform RNA sequencing. These analyses are still ongoing and the results will not be included here.

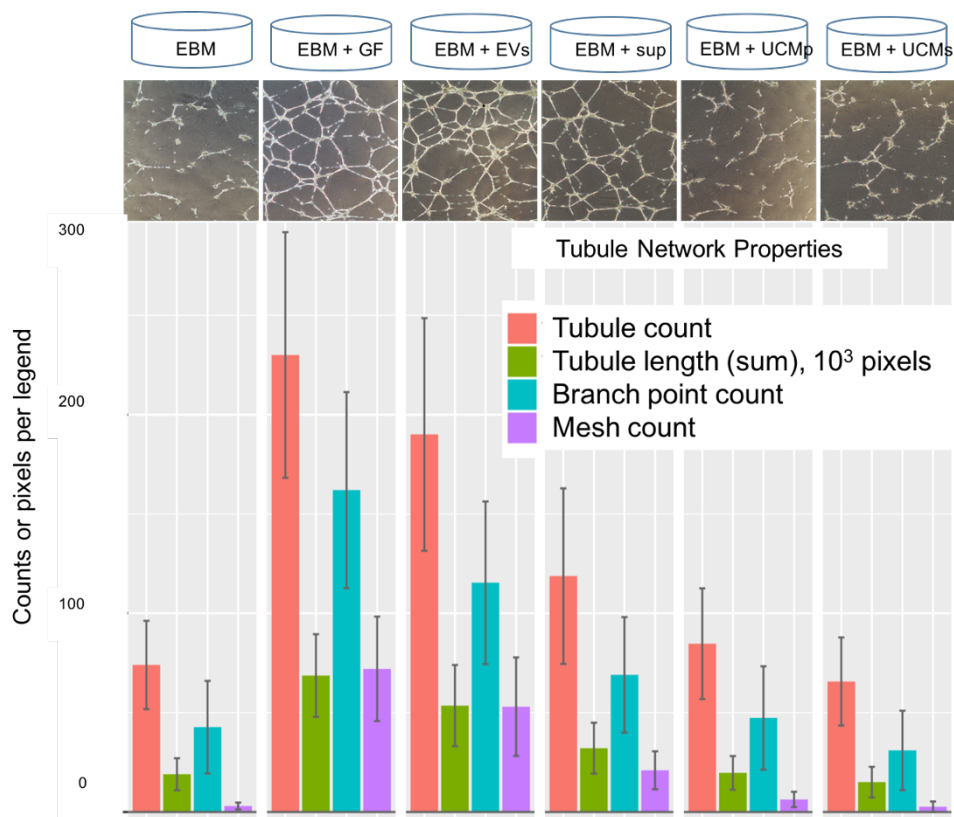


Figure 22. Photomicrographs (4X, top figure) and phenotypic evaluation of Human Brain Microvascular Endothelial Cells tubule formation. EBM, endothelial basal medium; GF, growth factors; EVs, extracellular vesicles; sup, supernatant; UCMp, unconditioned medium pellet; UCMs, unconditioned medium supernatant.

Canine and feline extracellular vesicle characterization

Canine and feline mammary tumor cell lines (CYPp and FMCp, respectively) have been used to isolate and characterize EVs from these species. Human breast cancer MCF7 cell line has been used as a positive control.

After ultracentrifugation, a macroscopically visible pellet (1-2mm) (data not shown) was detectable at the bottom of the tubes from the three cell line samples (MCF7, CYPp, and FMCp). No visible pellet was present at the bottom of the tube from UCM. This sample (UCM presumptive pellet) was included in all further analysis as a negative control, considering that high molecular weight proteins and particles might be present at the bottom even when the pellet is not macroscopically visible.

EV-enriched pellets from CYPp, FMCp, and MCF7 cell lines, after ultracentrifugation were analyzed by TEM. Additionally, the UCM presumptive pellets were also analyzed to check whether or not particles were present in the growth medium *per se*. No membrane-bound particles were present in the UCM presumptive pellets (figure 23a). TEM confirmed the presence of membrane-bound vesicles from all three cell lines (figure 23b). By TEM, vesicles apparently ranged from 50 to 400 nm, being therefore compatible with exosomes and microvesicles.

In order to better identify and characterize these membrane-bound vesicles, immunogold labelling for CD63 and Alix was performed on CYPp-, FMCp-, and MCF7-derived EVs, as well as on UCM presumptive pellet. The membrane-bound vesicles from all three species showed a membrane-associated positivity to both proteins Alix (figure 23c) and CD63 (figure 23d). UCM presumptive pellet did not show any positivity.

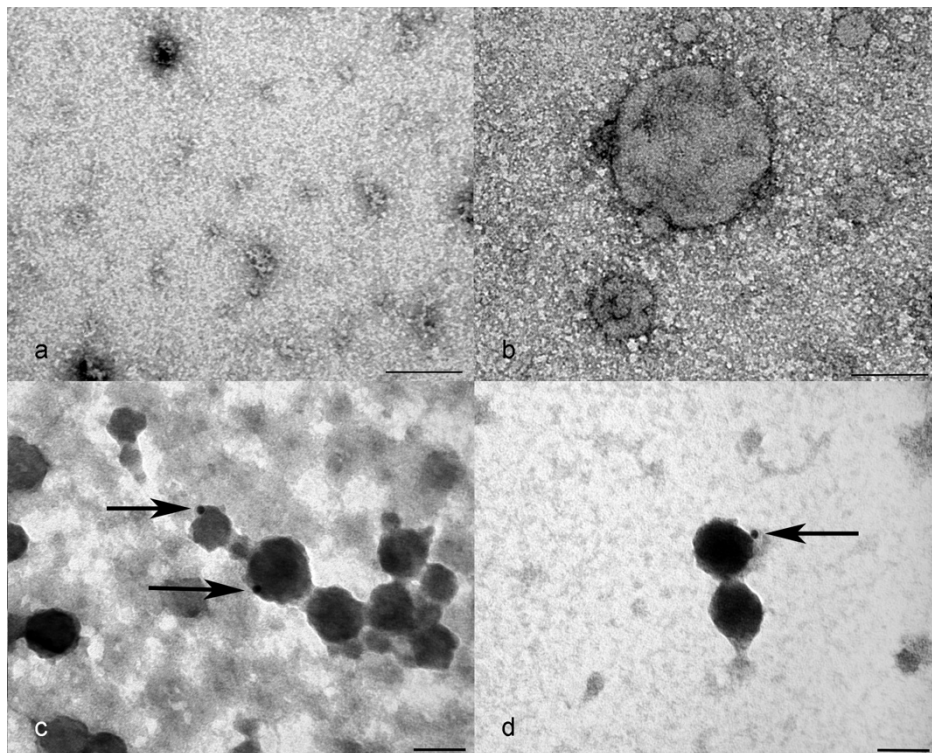


Figure 23. Transmission Electron Microscopy. (a) Unconditioned medium presumptive pellet after ultracentrifugation: absence of membrane bound structures. Scale bar: 200 nm. (b) Extracellular vesicle (EV)-enriched pellet after ultracentrifugation: presence of membrane-bound structures of 50 to 400 nm. Scale bar: 200 nm. (c) EVs are positive to anti-Alix antibody staining at immunogold (arrows). Scale bar: 100 nm. (d) EVs are positive to anti-CD63 antibody staining at immunogold (arrow). Scale bar: 100 nm.

Western Blot analysis was performed on proteins isolated from CYPp, FMCp, and MCF7 cells as positive controls and from proteins extracted from the EV-enriched pellets obtained from the medium of the same cell lines and from the UCM presumptive pellet. A band of the expected size was detected both for Alix and TSG101 from the three cell lines and from the putative EVs proteins derived from them (figure 24). The UCM pellet did not show any band, indicating the absence of cells/EVs-derived Alix and TSG101. Moreover, the putative EVs-derived proteins showed an enrichment of Alix when compared to the cells (figure 24).

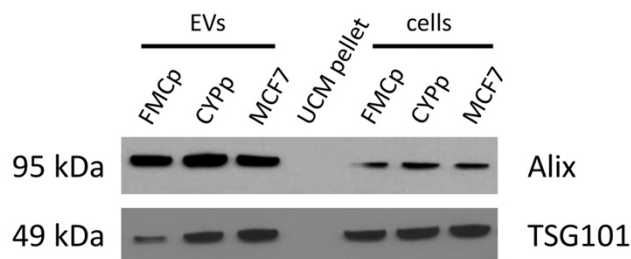


Figure 24. Western Blot analysis of protein lysate from extracellular vesicle (EV)-enriched pellets, unconditioned (UCM) presumptive pellet and cells. FMCp, feline mammary tumor cell line; CYPp, canine mammary tumor cell line; MCF7, human breast cancer cell line.

EV number and size distributions were determined by Nanoparticle Tracking Analysis (NTA).

1×10^6 cells were seeded per 15-cm plate and 72 hours later, EVs were isolated from approximately 2×10^7 CYPp cells, 2.4×10^7 FMCp cells, and 2.3×10^6 MCF7 cells.

The 1:1000 dilution showed NTA values that were outside the optimal working range of the instrument ($1 \times 10^8 - 25 \times 10^8$) for all samples, therefore this dilution was not considered. The number of particles in each sample (both 1:100 and 1:500 dilutions) was normalized to the number of particles measured in the UCM presumptive pellet. The average of particles in RPMI UCM presumptive pellet was $1.38 \times 10^{10} (\pm 3.6 \times 10^9)$, whereas in DMEM UCM presumptive pellet was $3.3 \times 10^{10} (\pm 2.3 \times 10^9)$ (figure 25). EBM contained a lower average of 2.5×10^9 particles ($\pm 1.4 \times 10^8$), whereas in NB the average of particles was $1.8 \times 10^{10} (\pm 1.5 \times 10^9)$ (data not shown). The average of particles in cell-derived EV-enriched pellet was $6.6 \times 10^{10} (\pm 1.7 \times 10^{10})$ for CYPp, $5.7 \times 10^{10} (\pm 1.5 \times 10^{10})$ for FMCp, and $3.8 \times 10^{10} (\pm 3.8 \times 10^9)$ for MCF7 (figure 25). The average yield of EVs measured was $2.56 \times 10^2/\text{cell} (\pm 72.61)$ for CYPp cells, $1.67 \times 10^2/\text{cell} (\pm 51.07)$ for FMCp cells, and $2.52 \times 10^2/\text{cell} (\pm 96.73)$ for MCF7 cells (figure 25). The size distribution ranged approximately from 80 nm to 600 nm when it comes to EVs samples (figure 25), whereas from 100 nm to 350 nm for UCM pellet (data not shown).

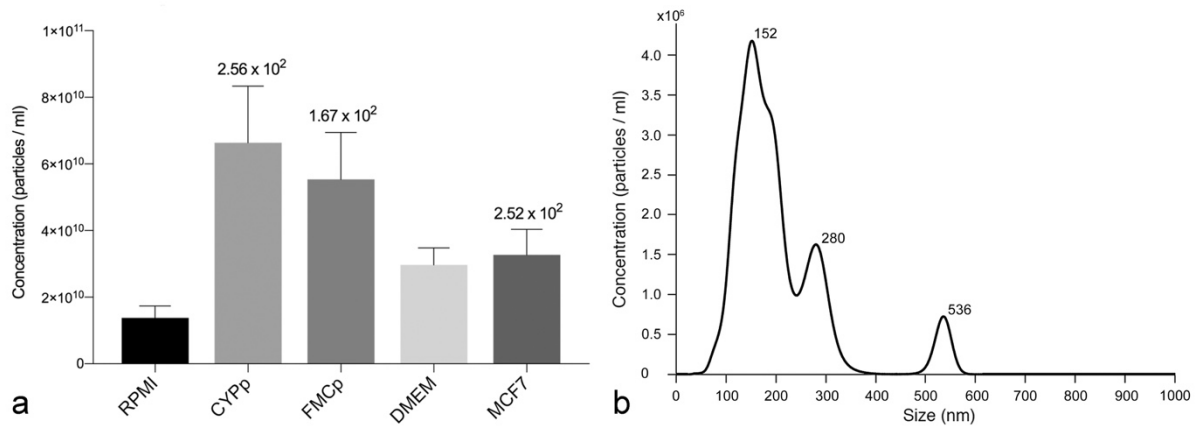


Figure 25. Nanoparticle Tracking Analysis. (a) Concentration (particles/mL) of particles in Unconditioned medium presumptive pellets (RPMI and DMEM) and on cell-derived extracellular vesicles (EVs). On top of the histograms, the average number of EVs/cell is reported. (b) Size distribution (nm) of particles in a representative sample. CYPp, canine mammary tumor cell line; FMCp, feline mammary tumor cell line; MCF7, human breast cancer cell line.

In order to verify whether EVs were produced by donor cells and taken up by recipient cells, CYPp-palmtDTomato cells were seeded on top of the $1 \mu\text{m}$ pore size Transwell, whereas CYPp-GFP cells were plated in the bottom chamber.

Confocal microscopy of CYPp-GFP cells was performed after approximately 4 days of culture. The analysis allowed the identification of palmtDTomato-positive membrane bound particles of roughly 200 nm in diameter (consistent with EVs) within the bottom seeded CYPp-GFP cells (figure 26), indicating recipient cell (CYPp-GFP) uptake of donor cells (CYPp-palmtDTomato)-derived EVs.

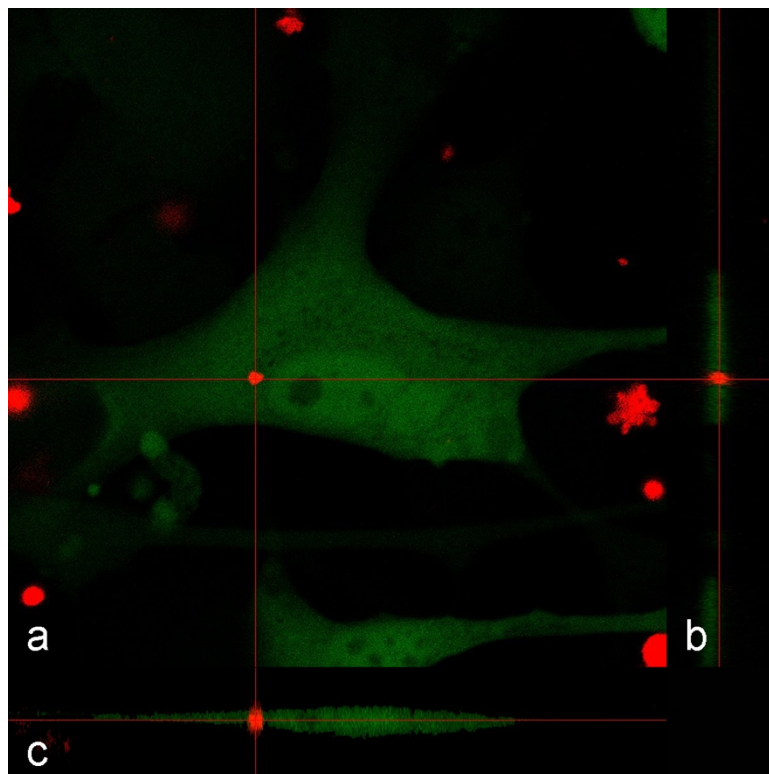


Figure 26. Confocal microscopy of extracellular vesicle (EV) uptake. Presence of a palmtDTomato-positive canine mammary tumor cell line (CYPp)-derived EV into a GFP-positive CYPp cell. Orthogonal views (a) XY, (b) YZ, (c) XZ.

DISCUSSION

It is well known that solid tumors, including mammary cancer, are characterized by a functional cell hierarchy and are made of different cell subpopulations, comprising differentiated cells and stem-like cells, called cancer stem cells (CSCs), capable of initiating tumors and driving cell heterogeneity (Park et al., 2010).

The hypothesis that a tumor originates from a small subset of cells with stem cell characteristics has been extensively demonstrated by different studies in different types of tumors, such as breast, brain, and other solid tumors (Al-Hajj et al., 2003; Singh et al., 2003; Fang et al., 2005; Tirino et al., 2011; Liu et al., 2013a; Liu et al., 2013b). This hypothesis is supported by several studies, in which xenotransplantation experiments demonstrate that only human breast cancer stem cells (hbCSCs) are able to generate tumors in immunocompromised mice (Tirino et al., 2013; Al-Hajj et al., 2003; Singh et al., 2003; Fang et al., 2005; Tirino et al., 2011; Liu et al., 2013a; Liu et al., 2013b). However, beside tumorigenicity assays in immunocompromised mice, phenotypic and functional characterization of CSCs is still under discussion and several open questions are still unanswered (Thomasson, 2009; Clevers, 2011; Bakhshinyan et al., 2018).

In this study we aimed to investigate the biological and molecular features of tumor cell subpopulations of mammary gland, with particular interest for CSCs.

We started (**phase I**) collecting primary tumors from human patients as well as from dogs directly from the operating room. Only a small portion of the fresh tissue is obtainable from these tumors for the isolation of cell subpopulations. Mammary cancer is the most common neoplasia in women and female dogs, therefore it has been fairly easy to get access to these samples. Instead, although the third most common tumor in cats (Zappulli et al., 2005), mammary cancer is a bit less common in this species compared to humans and dogs and considering that the isolation procedure needs to be performed as fast as possible after surgery, we were not able to collect feline samples for this purpose. Thirteen human and 10 canine mammary tumor samples have been collected. Beside a histological classification, a molecular classification subdivides breast cancer in 4 main subtypes (luminal A, luminal B, Her2 overexpressing, and triple negative breast cancer) according to the expression of estrogen receptor, progesterone receptor, and Her2 (Provenzano et al., 2018). In addition to these 3 markers, Ki-67 is routinely assessed for the prognostic classification of breast cancer. On the other hand, in veterinary medicine, mammary cancer is classified on the basis of morphological/histopathological features (Goldschmidt et al., 2011; Misdorp et al., 1999) and, despite some preliminary studies (Peña et al., 2014; Gama et al., 2008; Sassi et al., 2010; Soares et al., 2016; Brunetti et al., 2013), immunohistochemistry is not routinely performed to further classify these tumors.

In the literature, many studies collected primary mammary tumors from women, dogs, and cats in order to isolate different cell subpopulations, with particular attention to CSCs (Wang et al., 2014; Barbieri et al., 2015; Barbieri et al., 2012). It has been postulated that CSCs are associated to the EMT process and are responsible for resistance to therapy, relapse, and metastasis development (Geng et al., 2014). Several experimental approaches have been used to obtain *in vitro* cultures enriched in CSC-like cells from human (Stingl, 2009), canine (Cocola et al., 2009), and feline (Barbieri et al., 2012) mammary gland tumors:

CD44⁺/CD24^{-/low} fluorescence- or magnetic-activated cell sorting (FACS and MACS, respectively) (Ponti et al., 2005), Hoechst-dye effluxing side population by FACS analysis (Clarke et al., 2003), and *in vitro* cultures in serum-free growth factor-enriched medium (stem cell permissive) as non-adherent spherical clusters, named mammospheres (MS) (Barbieri et al., 2012).

In our study, we aimed to isolate CSC-like cells from primary tumors using serum-free medium as well as differentiated cells using medium containing FBS. Based on the literature, we tried several protocols with slight modifications to isolate these two populations.

As mentioned, many studies isolated MS from primary tumors plating them with serum-free medium (Dontu et al., 2003; Ponti et al., 2005; Wang et al., 2014). Some of these studies specified the use of ultralow attachment plates to isolate MS (Dontu et al., 2003). Similarly, Cocola and collaborators successfully isolated MS from canine primary mammary tumors using serum-free stem cell permissive medium (Cocola et al., 2009). However, they did not place isolated cells directly in serum-free medium, as other authors (Dontu et al., 2003; Ponti et al., 2005; Wang et al., 2014), but they initially cultured the cells in a serum-containing medium and then transferred to a serum-free medium in ultralow attachment plates (Cocola et al., 2009). Differently, Barbieri and collaborators isolated canine CSCs from primary tumors plating them in serum-free medium right after enzymatic digestion (Barbieri et al., 2015). The same authors isolated feline CSCs using a similar protocol (Barbieri et al., 2012). These authors used modifications of the protocol and sometimes they did not specify all the details. Following what is described in the literature, we tried several protocols, either with or without enzymatic digestion, using different medium composition. Nevertheless, unfortunately, we were not able to isolate CSCs from the human and canine primary tumors collected. One possible explanation could be that the success strictly depends upon the starting material. It is known that in a solid tumor, CSCs constitute only a small percentage (1-3%) of the total tumor mass (Bao et al., 2013; Chang, 2016) and this could contribute to make the isolation procedure quite challenging. We believe that if the primary tumor from which the CSCs are isolated is well differentiated, is much more difficult to isolate them, whereas starting from less differentiated tumors becomes probably easier. Additionally, there are many technical details, such as the use of ultralow attachment plates as well as a specific seeding density, that presumably play a crucial role in the isolation of CSCs.

Another approach used to isolate different cell subpopulations from primary tumors is based on surface marker expression. From the mammary gland, luminal/epithelial cells are typically isolated using the following markers: cytokeratin (CK) 8, CK18, CK19, epithelial membrane antigen (EMA), epithelial surface antigen (ESA), and mucin 1 (MUC-1). Whereas myoepithelial cells are isolated using CD10, Thy1, calponin (CALP), smooth muscle actin (SMA), and p63.

As previously mentioned, many studies isolated differentiated cells dissociating them from primary tumors and cultivating them in medium containing 10% FBS (Ponti et al., 2005; Cocola et al., 2009; Barbieri et al., 2015). In our study, we used the same approach to isolate differentiated cells as well, with particular interest to epithelial cells. Flow cytometry was performed on three human samples right after collection, after enzymatic dissociation. Results are highly suggestive of the presence of a heterogeneous cell population variably positive to CD45, CD34, CD117, CD133, CD44, CD24. CD45, also known as leukocyte common antigen, is a receptor-linked protein tyrosine phosphatase that is expressed on all leukocytes (Altin and Sloan, 1997).

CD34 is a glycoprotein expressed on the surface of bone marrow-derived progenitors of hematopoietic and endothelial cells (Yang et al., 2011; AbuSamra et al., 2017). The presence of a CD45⁺ and of a CD34⁺ population could be due to the presence of leukocytes coming from the original tissue. However, it has been shown that normal mammary stroma harbors huge numbers of CD34⁺ fibrocytes (Catteau et al., 2013). CD117 is a transmembrane tyrosine-kinase receptor which is expressed on hematopoietic progenitor cells as well as on many types of cancer cells, including breast carcinoma (Luo et al., 2018). CD44 and CD24 have been widely associated to a CSC-like phenotype. Specifically, CSCs have been isolated from mammary cancer using CD44⁺/CD24^{-/low} phenotype (Camerlingo et al., 2013). The normal/neoplastic mammary gland is composed of several cell subpopulations: epithelial/luminal cells, myoepithelial/basal cells, fibroblasts, endothelial cells, perhaps some leukocytes. Therefore, the variable positivity to these markers in our collected samples is not surprising. Without the use of specific antibodies that would select specific cell populations, all the cell subtypes present within the tissue are isolated. Morphologically, after a few days of culture, we could see that both cuboidal/epithelioid-like cells as well as spindle/fibroblast-like cells were present in the flask, and this suggests the presence of more than one population within the flask, as reported by other authors (Nishikata et al., 2013). Within the literature it is not always well specified if using serum-containing medium multiple populations are isolated. It looks like when isolating cells from the tumor bulk without specific antibodies that would select specific subpopulations, after several passages the clones that have the highest proliferation rate grow faster and therefore there is a natural selection of the most aggressive cell types, which are presumably cancer cells. In our study, the growth of the majority of the primary cell lines isolated was slow, therefore we decided to freeze and store them for further studies to avoid senescence. Very few isolated primary cell lines showed a fast growth and in these culture, after either several days or roughly 4 to 6 passages, spindle-like cells grew faster than epithelial-like cells such that the latter were completely replaced by cells with an elongated morphology, as reported by other authors (Nishikata et al., 2013). In order to better characterize these cells, we performed immunocytochemistry for beta-catenin, E-cadherin, calponin, vimentin, p63, pancytokeratins, and CD44 on one cell line isolated from a canine mammary tumor. All the cells were strongly positive for calponin (CALP) and vimentin. CALP is a protein expressed on cells that have contractile filaments, such as myofibroblasts and myoepithelial cells (de las Mulas et al., 2004). Vimentin is a type III intermediate filament protein that is expressed in mesenchymal cells (Gama et al., 2003). In the mammary gland, fibroblasts, myofibroblasts, and myoepithelial cells express vimentin. Therefore, cells positive for CALP and vimentin could be either myofibroblasts or myoepithelial cells. However, since these cells were negative for p63, which is a myoepithelial cell marker, we believe that the phenotype found is suggestive of myofibroblasts. Fibroblast contamination is common in primary cell cultures. To avoid fibroblast contamination and overgrowth in culture cells, some authors eliminated fibroblasts using an immunomagnetic separation with anti-fibroblast microbeads (Florio et al., 2008; Barbieri et al., 2012). Nevertheless, in other studies they did not worry about a possible fibroblast contamination and therefore no elimination of fibroblasts was performed (Barbieri et al., 2012; Nishikata et al., 2013). In summary, trying different protocols we were able to isolate adherent/well differentiated cells that have been frozen for further studies.

According to our flow cytometry results on a few cell lines, we believe that these cell lines are probably composed of a heterogeneous cell population and further culture passages will probably help to switch to a

homogeneous cell population that needs then to be immunophenotypically characterized. We were not able to isolate CSCs directly from primary mammary tumors, which is presumably due to the high difficulty and the lack of a precise standardization of the procedure. It is possible that in order to obtain CSCs, primary tumor cells need to be placed in serum-containing medium to stabilize the culture and then passing them to a serum-free medium, as other authors reported (Cocola et al., 2009).

Lastly, canine primary cultures were isolated from fresh tissues without knowing the histological diagnosis of the tumors. The nature (benign vs malignant) and the morphological phenotype could certainly affect the yield and the type of cells isolated in primary cultures and should be further investigated.

For these reasons, we decided to isolate CSC-like cells from well-established canine and feline cell lines (CYPP and FMCp, respectively). These cell lines were isolated by other authors from aggressive primary mammary tumors of a dog and a cat that developed metastases as well (Uyama et al., 2005; Uyama et al., 2006). Serum-free culture has been proven to be an efficient way to enrich CSCs (Wang et al., 2014). Many studies that isolate hCSCs from well-established cell lines are present within the literature (Wang et al., 2014; Lombardo et al., 2015; Fu et al., 2016). In human medicine, several studies investigated the phenotype associated to CSCs and different markers have been identified. The first report identifying and isolating tumorigenic CSCs from non-tumorigenic cancer cells used the combined analysis of expression of two cell surface markers: CD44⁺/CD24^{-/low} (Al-Hajj et al., 2003; Bauerschmitz et al., 2008; Abraham et al., 2005).

Using *in vitro* and *in vivo* experimental systems, Ginestier and collaborators (Ginestier et al., 2007) demonstrated that normal and cancer human mammary epithelial cells with increase aldehyde dehydrogenase activity (ALDH) show stem/progenitor cell properties. Interestingly, ALDH1 breast CSC marker can further divide the CD44⁺/CD24^{-/low} population into fractions that are highly tumorigenic: ALDH1⁺/CD44⁺/CD24^{-/low} cells were able to generate tumors from only 20 cells, whereas ALDH1⁻/CD44⁺/CD24^{-/low} were not tumorigenic using the same cell density (Ginestier et al., 2007; Croker et al., 2009). Based on this, there is evidence to support the idea that the use of CD44 and CD24 cell surface markers in combination with the ALDH1 activity is the most accurate method to identify and isolate CSC-like cells within breast cancer cell populations (Ricardo et al., 2011). Additionally, CD133, c-kit, CD49f, and CD29 have been identified as CSC markers (Bao et al., 2013).

In veterinary medicine, similar to human medicine, CD44, CD24, ALDH1, and CD133 have been proposed as CSC markers by several authors (Barbieri et al., 2012; Barbieri et al., 2015; Michisita et al., 2011; Michisita et al., 2012; Pang et al., 2012; Michisita et al., 2013). However, CD44 seems to play a controversial role because in canine culture cells it has been associated by some authors with proliferation rather than with a specific cancer stem cell population (Blacking et al., 2011).

In our study, we aimed to investigate the protein expression of CD44, CD24, CD133, CD45, and CD34 comparing adherent cells and mammospheres at different passages. We also wanted to compare an enzymatic versus a mechanic procedure to prepare the cells for flow cytometry to see whether or not the expression of the cell surface markers analyzed was affected by the method by which cells were detached from the flask. In the literature, it is described that different techniques in cell preparation can affect marker expression and might lead to the controversial results that have been described (Quan et al., 2013).

With the mechanic treatment, AD were detached from the cell culture dish using a cell scraper and MS were dissociated pipetting up and down several times with PBS. With the enzymatic treatment, AD were detached from the cell culture flask using trypsin and MS were dissociated using accutase. When AD were mechanically detached, flow cytometry showed that cells had a worse morphology when compared to those enzymatically harvested, and roughly 20% of them were dead. Mechanic treatment is more aggressive than enzymatic treatment, especially cell morphology could be severely altered, and this can explain the high number of dead/damaged cells. MS morphology did not show differences between mechanic and enzymatic treatment. Working with 20% of dead cells within the population would have generated a bias in all the subsequent analyses. For this reason, we decided to enzymatically harvest the cells for all the analyses, similar to what other authors performed (Wang et al., 2014; Fu et al., 2016).

In addition to the protein analysis, we investigated the gene expression of CD44, CD133, SOX2, and OCT4 to compare the results of protein and gene expression when it comes to CD44 and CD133. Gene expression of CD24 has not been investigated because the gene has not been sequenced in the canine and feline species yet. We tried to amplify CD24 sequence using human primers designed for human CD24 gene, but we were not able to get any amplification. Therefore, its gene expression could not be evaluated.

When it comes to protein expression, CD44 did not show any difference between MS and AD in terms of percentage in both species. This is due to the fact that AD are already almost 100% positive, therefore any potential difference could be seen only in terms of staining intensity, calculated as mean fluorescence intensity (MFI). We found that CD44 MFI was higher in MS than AD.

Now, this could be due to either a real increase of CD44 expression in MS or to a "false" lower expression of CD44 in AD caused by the trypsin, used to harvest the cells. Quan and collaborators demonstrated that enzymatic digestion could generate artificial results of CSCs detection and isolation via flow cytometer based on cell-surface antigen markers. Their results indicate that accutase reagent reserves the antigenicity of CD44 and CD24 surface antigen better than trypsin (Quan et al., 2013).

In order to better elucidate whether the increased expression of CD44, measured as MFI, in MS was real, we looked at CD44 gene expression by qPCR and we found a higher expression of CD44 in MS than AD in both species, more pronounced in feline MS. Although trypsin could certainly play a role in CD44 expression, as reported (Quan et al., 2013), our gene expression results suggest that the higher protein expression, measured as MFI, of CD44 in MS is real. Additionally, CD44 gene expression increases in MS throughout the passages, more evident in FMCp, where its expression is higher in MS passage 7, than MS passage 4, than MS passage 1, than AD. This result suggests that over time, MS acquire CSC-like properties. In human medicine, to the best of our knowledge, nobody has never investigated the expression of this protein in different subsequent passages. Wang and collaborators investigated the expression of CD44 and CD24 in adherent cells as well as mammospheres on day 7, 14, 21 of primary cell lines, MCF7, and MDA-MB-231. However, they did not pass the cells, but they rather performed flow cytometry 7, 14, 21 days after plating the cells. They found an increase of CD44 expression over time in primary mammospheres and MCF7 mammospheres, but not in MDA-MB-231, probably due to the already high stem cell proportion in this aggressive TNBC cell line (Wang et al., 2014). CYPp and FMCp are highly aggressive because they have been isolated from a primary mammary

tumor that gave rise to metastasis in the same animal (Uyama et al., 2005; Uyama et al., 2006). Their phenotype as adherent cells (CD44^{high}/CD24^{low}) is similar to MDA-MB-231, therefore they might be characterized by an already high stem cell proportion, as speculated by Wang and collaborators for MDA-MB-231 (Wang et al., 2014). However, from our results, it is evident that looking at the percentage of CD44 expression might lead to incomplete conclusions. Therefore, when performing these studies, the intensity of the protein expression, measured as MFI, as well as the gene expression give more complete information than looking at the percentage alone.

Due to its controversial role, in addition to CD44, other markers should be considered. For this reason, we also investigated the expression of CD133 in MS and AD both at protein and mRNA levels. By flow cytometry, CD133 did not show any difference between MS and AD in CYPp, whereas in FMCp its expression was higher in MS than AD. Specifically, MS became almost 100% CD133⁺ at passage 7. Interestingly, at the mRNA level, CD133 was higher in MS if compared to AD in both species, and this difference was more pronounced in CYPp. Based on these results, we noticed a discrepancy between protein and gene expression of CD133 in CYPp.

The antibody used was the 13A4 clone which is the most common used antibody in veterinary medicine, especially in dogs (Fujimoto et al., 2013; Moulay et al., 2013; Michishita et al., 2014; Liu et al., 2015; Blacking et al. 2011). All these studies showed that the expression of CD133 is never clearly different from the isotype control, reasonably doubting the specificity of the antibody. According to the datasheet (eBioscience, distributed by Thermo Fisher Scientific, cat# 14-1331-80) it has been reported to work in dogs, although nobody has never performed a Western Blot with canine proteins. Interestingly, Thamm and collaborators investigated different CD133 antibody clones in several species and they found that monoclonal antibodies 13A4 and AC133 do not recognize the canine ortholog of stem cell antigen prominin-1 (CD133) (Thamm et al., 2016). This could explain why in our setting no differences were found between MS and AD in CYPp by flow cytometry, but CD133 gene expression was higher in MS when compared to AD. A Western Blot on canine protein lysates would clarify whether or not this clone recognizes canine CD133 epitope. Based on these results, we believed that CD133 is a useful marker in both species. However, flow cytometry alone could give misleading results when working with canine cell lines, therefore a gene expression evaluation should always be considered.

In addition to these well-studied CSC markers, we investigated the expression of two genes which is thought to be increased in CSCs: SOX2 and OCT4 (Yu et al., 2016; Stewart et al., 2017; Zhang et al., 2018). We found that SOX2 expression was remarkably higher in CYPp MS than AD and higher in FMCp MS passage 1 than AD, and lower in FMCp MS passage 4 and 7 when compared to MS passage 1. Although SOX2 expression decreases in MS at higher passages, overall its expression in MS is still higher than AD. OCT4 expression in CYPp MS is not different from AD, whereas in FMCp MS is higher than in AD, especially at passage 7. This results suggest and confirm that MS have a CSC-like phenotype when compared to AD. It is important to remind that these primers have been designed based on predicted sequences of SOX2 and OCT4 genes. Therefore, these results will be more reliable when these genes will be fully sequenced.

In summary, CD44 could not be used alone as CSC marker because it might be related to aggressiveness rather than a specific CSC-like phenotype. CD133 is confirmed to be a reliable CSC marker, although the cross-reactivity with the canine antigen needs to be clarified. Beside protein expression, it would be better to evaluate the gene expression in order to avoid alterations of the results due to technical issues.

In the **phase II** of this study, we focused on two of the main pathways that are thought to be deregulated in CSCs: Wnt/ β -catenin and Hippo pathways (Geng et al., 2014; Piccolo et al., 2014). Additionally, since CSCs are involved in the EMT process, we looked at gene expression as well as protein expression of several EMT-related molecules.

The Wnt family is a group of proteins implicated in several cellular functions, such as organ formation, stem cell renewal, and cell survival (Croce & McClay, 2009). Accumulating evidence indicates that the Wnt/ β -catenin pathway contributes to the neoplastic process, of which β -catenin is one of the key downstream effectors (Nelson & Nusse, 2004). An inappropriate activation of this pathway leads to the development of human cancer, including breast cancer (Hwang et al., 2013).

More than half of breast cancers have activation of Wnt and that is associated with lower overall survival (Khramtsov et al., 2010). High levels of Wnt receptor and co-receptor expression, as well as aberrant activation of β -catenin, have been detected in breast cancer tissues. Downregulation of the Wnt/ β -catenin pathway can inhibit the EMT and reduce spontaneous invasion of breast cancer cells (Wu et al., 2012; Ahmad et al., 2012). Several studies have reported increased cytoplasmic and nuclear β -catenin in primary breast cancers, especially basal-like breast cancers, and correlated with poor prognosis and survival (Lin et al., 2000; Prasad et al., 2007; Khramtsov et al., 2010).

In our study, we did not find any difference in terms of gene expression of β -catenin (CTNNB1) between healthy and neoplastic tissues in the three species. CyclinD1 (CCND1), one of the downstream genes regulated by the Wnt/ β -catenin pathway, is higher in ER⁺, but not in TNBC, when compared to healthy human tissues. Similarly, CCND1 is higher in CMT grade II when compared to STC I and healthy tissues. These results are quite different from what other authors found in human breast, ovarian, colorectal, and squamous cell carcinomas (Chen et al., 2005; Cheng et al., 2011; Cheng et al., 2012; Huang et al., 2012). Cheng and collaborators found a higher gene expression of CTNNB1 and CCND1 in breast cancer tissues when compared to the adjacent noncancerous cells (Cheng et al., 2012). However, they did not distinguish between ER⁺ tumors and TNBC. Also, they measured gene expression on laser capture microdissected tissues, therefore they eliminated non-mammary tissue, that could significantly lead to unexpected results, considering the high abundance of non-mammary tissue that is present in the normal mammary gland. In veterinary medicine, Han and collaborators found a higher expression of CTNNB1 in canine oral melanoma tissues when compared to normal melanocytes (Han et al., 2012). Moreover, Yu and collaborators found a higher expression of CTNNB1 in canine mammary gland tumors compared to healthy tissues. However, their samples are not only simple carcinomas, like in our study, but also other tumor subtypes, therefore the two studies are difficult to compare (Yu et al., 2017). CTNNB1 and CCND1 gene expression have never been investigated in FMTs.

In all the three species, a higher expression of β -catenin in tumor than healthy tissues was found by Western Blot in both cytoplasm and nucleus. An activation of Wnt/ β -catenin pathway in HBC has been found also by other authors (Khramtsov et al., 2010). Interestingly, a higher expression of non-phosphorylated β -catenin (active form) was found in tumor than in healthy tissues within the nuclear fraction. These results suggest an activation of the Wnt/ β -catenin pathway in tumor tissues, which is not regulated at the gene expression level, but at the protein level. In other words, our data indicate a post-transcriptional regulation of β -catenin accumulation into the cytoplasm. Indeed, higher amount of the protein within the cytoplasm and of the non-phosphorylated protein within the nucleus indicate the translocation of β -catenin from the membrane to the cytoplasm, where it is not phosphorylated and therefore can migrate into the nucleus activating the expression of downstream genes (oncogenic function). As already said, one example of the downstream genes is CCND1, which we found to be increased in human ER⁺ tumors and canine STC II tumors, although the gene expression of CTNNB1 is similar between healthy and tumor tissues. To the best of our knowledge, in veterinary medicine, nobody has never investigated the protein expression by Western Blot of β -catenin and phosphorylated β -catenin in cytoplasmic and nuclear fractions.

By IHC, the expression of β -catenin in the three species was highly heterogeneous. In human ER⁺ tumors the expression is predominantly membranous, whereas in TNBC is predominantly cytoplasmic, indicating an activation of the Wnt/ β -catenin pathway in the latter. Additionally, a negative correlation between β -cat M and β -cat C has been found in all the species, suggesting an activation of the pathway in those samples with a lower membranous expression, as confirmed by other authors in HBC (Geyer et al., 2011), CMT (Restucci et al., 2007), and FMT (Zappulli et al., 2012).

The Hippo pathway has been found to regulate organ size and maintain tissue stability by controlling cell proliferation and apoptosis (Fu et al., 2018). Its deregulation results in tissue overgrowth and tumorigenesis in humans (Hong and Guan, 2012; Jeong et al., 2013; Piccolo et al., 2013; Vermeulen, 2013; Han et al., 2014; Liang et al., 2014; Sanchez and Aplin, 2014). YAP and TAZ transcriptional coactivators are the key effectors of this pathway, and both proteins are overexpressed in a wide spectrum of cancers (Johnson & Halder, 2014; Pan, 2010; Steinhard et al., 2008; Harvey et al., 2013). Bartucci and collaborators suggest that YAP/TAZ plays a key role in the aggressive behavior of HBCs and may represent a major determinant of fatal clinical outcome in advanced HBC patients (Bartucci et al., 2015). Very little is known about the potential involvement of the Hippo pathway in canine and feline mammary tumors. In a preliminary study performed on CMTs and FMTs we found by IHC that YAP/TAZ expression is higher in carcinomas grade III compared to grade I in both species, suggesting a potential role in disease progression (Beffagna et al., 2016). More recently, Guillemette and collaborators investigated the expression and function of YAP/TAZ in six CMT cell lines (Guillemette et al., 2017). They found that pharmacologic inhibition of YAP-mediated transcriptional co-activation induces apoptosis in CMT cells, and attenuates key behavior of malignant cells including migration, invasion and anchorage-independent growth. Rico and collaborators evaluated the expression of YAP and TAZ proteins in normal canine mammary gland, hyperplasia, and in benign and malignant CMT across all stages of disease progression (Rico et al., 2018). They found that by IHC the expression of TAZ was increased in lobular hyperplasia in both the cytoplasm and nucleus when compared to normal tissues. Moreover, by IHC nuclear

YAP and TAZ expression was significantly increased in malignant vs benign tumors, whereas cytoplasmic levels of both proteins were comparable in both groups. Immunoblots showed that TAZ increased in malignant tumors relative to normal mammary gland, suggesting a correlation between increased TAZ expression and the acquisition of a malignant phenotype. Conversely, YAP expression did not vary between normal and neoplastic tissues (Rico et al., 2018).

In our study, we analyzed the gene expression of YAP, CTGF and ANKRD1, as well as the protein expression of YAP/TAZ in a subset of normal and tumor tissues of human, canine, and feline mammary gland. The gene expression of TAZ has been analyzed in human and feline mammary gland.

In humans and cats, the gene expression of TAZ is not different between normal and tumor tissues and between different tumor subgroups. In dogs and cats, the gene expression of YAP is not different between normal and tumor tissues and between different tumor subgroups. Surprisingly, the gene expression of YAP in human healthy mammary gland is higher than in tumor tissues (ER⁺ and TNBC).

Conversely, in the three species, the protein expression of YAP and TAZ analyzed by WB is overall higher in tumors than in healthy tissues in both cytoplasm and nucleus, which reflects what we previously found by IHC (Beffagna et al., 2016). This discrepancy between gene and protein expression data could be due to a regulation of YAP/TAZ expression at a post-transcriptional level, rather than at the gene expression level, as proposed by other authors (Zhu et al., 2015). In other words, the higher presence of the proteins is not due to a higher gene expression but to an accumulation of the unphosphorylated proteins presumably caused by a deregulation of the Hippo pathway. The expression of Hippo pathway downstream genes CTGF and ANKRD1 is not different between normal and tumor tissues in all the three species. This could be due to the high variability among different samples that we found in our study as well as to the low number of cases that do not allow to have a statistical power. In CMTs it looks like there is a trend in the expression of CTGF that increases in STC II than in STC I and than in healthy tissues. However, these differences are not statistically significant probably because only 5 cases per group have been analyzed. Another possible explanation is that healthy tissues are not only composed of the mammary gland *per se*, but also of other tissues, such as connective tissue, adipose tissue, as well as blood and lymph vessels. Indeed, some authors showed that YAP/TAZ expression in adipose tissue could be deregulated by several conditions, such as obesity (Tharp et al., 2018). In addition to that, different patients could have a slightly different composition of the healthy mammary gland; for instance, the amount of adipose tissue, rather than the connective tissue, could be higher in a patient than in another one, therefore when analyzing the expression of these genes in healthy tissues, it is not surprising to find such a high variability within groups.

Also, it is important to specify that healthy mammary gland tissues have been collected from the same patients the tumor tissues have been collected from, therefore, what has been considered "healthy mammary gland" could have been stimulated by the same microenvironment changes the tumor tissues have been stimulated by (Bezdenzhnykh et al., 2014).

A high variability among samples in gene expression has been often found in tumor tissues as well.

This reflects the tremendous cellular heterogeneity by which mammary cancer is characterized (Polyak, 2007). In our study, we found a remarkable heterogeneity in YAP/TAZ expression by IHC across all the samples, especially in TNBC, CMTs, and FMTs. Human ER⁺ showed a more homogeneous distribution.

Nevertheless, TNBC showed a higher expression of YAP/TAZ when compared to ER⁺ tumors, as found by other authors (Diaz-Martin et al., 2015), confirming that in TNBC, which are highly aggressive, the Hippo pathway is deregulated. Also, although it is somehow meaningless and difficult to interpret interspecies differences, FMTs showed a higher expression of YAP/TAZ than CMTs. Though this result is presumably due to the fact that all the FMTs analyzed in this study were STC grade III, whereas CMTs were grade I and II, it is well known that FMTs have a higher aggressive behavior than CMTs (Zappulli et al., 2015; Sleenckx et al., 2011).

In conclusion, all these data suggest a Hippo pathway deregulation in HBCs, CMTs, and FMTs. The higher level of YAP/TAZ in highly aggressive tumors (TNBCs and FMTs) suggests a highly tumorigenic role of these proteins, as we previously found (Beffagna et al., 2016).

EMT is an evolutionally conserved morphogenetic program during which epithelial cells undergo a series of changes allowing them to acquire a mesenchymal phenotype (Thiery, 2002). During EMT, epithelial cells lose the expression of tight junction molecules such as E-cadherin and acquire mesenchymal properties such as migration, invasiveness, and elevated resistance to apoptosis. Transcription factors like ZEB, SNAIL, TWIST regulate this process and are activated by a variety of signaling pathways, including TGF- β , Notch, and Wnt/ β -catenin (Lamouille et al., 2014; Liu et al., 2008; Nieto, 2002; Yang et al., 2004). It has been postulated that EMT process contributes to the pathogenesis of cancer metastasis (Thiery et al., 2009). In breast cancer, an EMT signature is enriched in basal-like and claudin-low subtypes compared to luminal A/B subtypes (Prat et al., 2010). Since tumor progression is correlated with acquisition of mesenchymal features, this may be an explanation for why basal and claudin-low breast cancers are more aggressive (May et al., 2011). It has been shown that downregulation of activators of EMT, such as TWIST, SNAIL, and ZEB in human or mouse breast cancer cells, greatly inhibits metastasis induced by mammary fat pad or tail vein injection (Guo et al., 2012; Roy et al., 2014; Tran et al., 2014; Yang et al., 2004; Zhang et al., 2013). On the other hand, activating EMT in human breast cancer cells can enhance metastatic dissemination (Tran et al., 2014).

In our study, we aimed to investigate the gene expression of SNAIL, TWIST, and ZEB in human, canine, and feline healthy as well as tumor tissues.

SNAIL is a classical regulator of EMT that represses E-cadherin transcription in both mouse and epithelial cell lines (Peinado et al., 2007). In HBC, it has been associated with tumor recurrence and metastases (Come et al., 2006) and poor patient prognosis (Moody et al., 2005). In our samples, differently from other authors' findings (Geradts et al., 2011), in TNBC the expression of SNAIL2 was significantly lower than in healthy tissues. In CMTs, SNAIL1 and SNAIL2 did not show any statistically significant difference between healthy and tumor tissue. Im and collaborators showed a higher protein expression of SNAIL in carcinomas when compared to adenomas and to normal tissue. However, no significant differences were found between normal and tumor tissues in terms of mRNA expression, confirming our results (Im et al., 2012). They speculated that there could be a post-transcriptional regulation of its expression (Zidar et al., 2008). However, it looks like there is a trend such that STC II have a higher expression of SNAIL1 when compared to healthy tissues and STC I, suggesting that EMT process is associated to the aggressiveness of these tumors.

It is believed that TWIST plays an essential role in cancer metastasis. In our samples, the gene expression of TWIST1 and TWIST2 was lower in tumor than in healthy tissues, differently from what other authors found (Tan et al., 2017).

ZEB1 has been implicated in breast carcinogenesis (Eger et al., 2005) because it enhances tumor cell migration and invasion (Aigner et al., 2007). In our samples, ZEB1 expression is lower in tumor than in healthy tissues, as previously reported by other authors (Montserrat et al., 2011).

Overall, it looks like these transcriptional factors are downregulated in tumors compared to healthy tissues, with the exception of SNAIL1 in CMTs. These results are quite surprising. However, the RNA isolated from healthy tissues come from the whole mammary gland, therefore from all the different cell subpopulations that compose the organ. Especially in the healthy mammary gland, among these populations, connective tissue as well as adipose tissue are present and the latter can be quite abundant. Although these transcription factors are barely detectable in normal mesenchymal cells of adult tissues (Isenmann et al., 2009), adipose tissue variably expresses these genes and especially the expression of TWIST in adipocytes could be high and is influenced by body weight status and weight loss (Pettersson et al., 2011). As a result, the mRNA levels of these genes in healthy samples could be dramatically influenced by the presence of non-mammary gland tissues, such as fat.

Another possible explanation could be that in this setting we isolated the RNA from the primary tumor tissues, therefore the RNA reflects the expression of these genes in the primary tumor tissue bulk. It is possible that cells undergoing EMT might be a small number when compared to the whole tumor bulk, which is well known to be characterized by a remarkable intra-tumor heterogeneity (Hong et al., 2018). Moreover, some authors believe that the analysis of these genes, especially SNAIL, in tissues is hindered by the fact that their expression is tightly controlled at the post-transcriptional level and usually cannot be correctly estimated by RNA analyses (Come et al., 2006; Diaz and de Herreros, 2016; Diaz et al., 2014; Škovierová et al., 2018). In order to overcome these issues, it would be interesting in the future to investigate the protein expression by WB or IHC or to use Laser Capture Microdissection to specifically isolate the cell subpopulation of interest. This approach would remove non-desired tissues, such as connective or adipose tissues.

Over the last 20 years, the investigation of cell differentiation markers has been used in both human and veterinary medicine primarily to improve our knowledge of the histogenesis of mammary tumors (Sorenmo et al., 2011). In the normal human, canine, and feline mammary gland 2 cell subpopulations are present: luminal epithelial cells, positive for CK7, CK8, CK18, CK19 and basal/myoepithelial cells, variably positive for CK5, CK6, CK14, CK17, SMA, calponin, vimentin, and p63 (Rasotto et al., 2014). Some authors hypothesized that there is a close relationship between the basal/myoepithelial compartment and the stem-progenitor cells of the mammary gland (Deugnier et al., 2002; Polyak and Hu, 2005).

In HBC, the evaluation of cell differentiation proteins is frequently performed in association with other markers such as ER, PR, Her2, and Ki-67. These IHC results form the basis for a diagnostic algorithm of tumor subtypes, identified using gene expression profile studies. These IHC panels subdivide breast cancer into: 1) luminal tumors, expressing ER and/or PR receptors as well as luminal cytokeratins (CK7, CK8, CK18, CK19); 2) basal-like tumors, negative for hormonal receptors and Her2 and expressing basal markers (CK5, CK6,

CK14, CK17, SMA, calponin, vimentin, and p63), and 3) Her2 positive tumors, overexpressing the Her2 receptor (Nielsen et al., 2004; Rakha et al., 2008; Reis-Filho and Tutt, 2008).

In the present study, we assessed the expression of several phenotypic markers, such as ER, PR, Her2, CK8/18, CK5/6, CK14, E-cadherin, CD44, vimentin, Ki-67 in a subset of HBCs, CMTs, and FMTs.

In human ER⁺ breast cancer samples, the expression of luminal CK8/18 was nearly 100% in all the samples, whereas the expression of basal CK5 and CK14 was negative, confirming the strong association between ER⁺ tumors and high expression of luminal CK (CK8/18) as well as null expression of basal CK (CK5, CK14). In TNBC, the expression of CK8/18 was highly heterogeneous, whereas the expression of CK5 and CK14 was low in the majority of the samples. This result, in concordance with another study (Hashmi et al., 2018), supports the idea that the terms "basal-like cancer" and "triple negative breast cancer" are not interchangeable. Indeed, only a small percentage of TNBC are basal-like (Krishnamurthy et al., 2012). Triple negative is a HBC phenotype, which can include basal-like cancers, claudin-low cancer, normal breast-like tumors and BRCA1-deficient tumors (Krishnamurthy et al., 2012). CMTs were positive for ER, whereas FMTs were negative for ER, PR, Her2. Despite only a few samples were analyzed these data suggest, as already done in the literature (Abdelmegeed et al., 2018; Caliari et al., 2014), a more similar behavior of CMTs and ER⁺ HBC and of FMTs and TNBCs. In CMTs and FMTs the expression of CK8/18, CK5, CK14 was highly heterogeneous, confirming the high inter-tumor heterogeneity that characterizes these tumors (Abdelmegeed et al., 2018; Adegá et al., 2016). Basal cytokeratin 14 expression was higher in FMTs than in CMTs, confirming that FMTs are more "basal-like" when compared to CMTs (Caliari et al., 2014).

E-cadherin is a cellular adhesion molecule and its disruption may contribute to enhanced migration and proliferation of tumor cells, leading to invasion and metastasis (Dong et al., 2012) and it also plays a crucial role during EMT process (Scheel et al., 2012). In humans and experimental animal models, loss of E-cadherin expression was reported to cause cell migration or metastasis of tumor cells in breast cancer (Kowalski et al., 2003), as well as in other cancers (Chunthapong et al., 2004; Khoursheed et al., 2003). Tan and collaborators found a lower expression of E-cadherin in HBC tissues compared to adjacent healthy tissue (Tan et al., 2017). In our samples, E-cadherin expression has been evaluated in the membrane and in the cytoplasm separately. Overall, the expression of E-cadherin is highly heterogeneous across all the samples of the three species, confirming once more the high inter-tumor heterogeneity of mammary cancer in the three species. In human ER⁺ tumors, E-cadherin expression was predominantly membranous, whereas in TNBC was predominantly cytoplasmic, suggesting that the location of its expression is associated with aggressiveness such that less aggressive tumors express the protein in the membrane, whereas highly aggressive tumors express E-cadherin in the cytoplasm (Krishnamurthy et al., 2012; Liu et al., 2017). In CMTs, E-cadherin expression was predominantly membranous, similar to human ER⁺ tumors, confirming their strong similarities. In all the species, a negative correlation was found between the membranous and the cytoplasmic expression of the protein. Altogether these results suggest that probably is not only the loss of E-cadherin that correlates with an aggressive behavior, but also the protein translocation from the membrane to the cytoplasm, as described in colorectal cancer (Jiang and Hiscox, 1997).

Together with E-cadherin, another molecule that is well studied in tumor metastasis is CD44. As previously said, CD44 is a marker of stem cells and CSCs, but CD44 is a cell surface transmembrane glycoprotein which also plays a role in tumor cell differentiation, invasion, and metastasis (Sneath and Mangham, 1998). Although a few studies in HBC have shown that protein overexpression of CD44 is associated with poor prognosis and metastasis (Qiao et al., 2018), others have shown that downregulation of its expression correlated with adverse outcome (Sneath and Mangham, 1998; Schneider et al., 1999). For this reason, the role of CD44 in the behavior and prognosis of HBC is controversial (Schneider et al., 1999; Lyzak et al., 1997).

In our study, we investigated CD44 expression also by IHC and the expression was highly heterogeneous in TNBCs and overall lower in ER⁺ tumors than in TNBC, even if no statistical significance was found maybe due to the low number of samples. Increasing the number of cases would probably strengthen this interesting relationship.

CD44 is highly expressed (roughly 85%) in CMTs regardless of the tumor grading as well as in the healthy/hyperplastic mammary gland. Damasceno and collaborators found that in CMTs, CD44 is moderately expressed in benign epithelial cells, in carcinomas and mixed tumors, and in carcinosarcomas. Curiously, CD44 expression in invasive carcinomatous cells was lower than in *in situ* areas (Damasceno et al., 2016). Paltian and collaborators found that in benign and malignant canine mammary tumors CD44 is expressed by epithelial cells but with an intensity that was not significantly different compared to control tissue (Paltian et al., 2009). They also postulated that the expression pattern of CD44 in bitches may be influenced by endogenous stimuli (e.g. sexual hormones), which have an influence on CD44 expression in humans (Regidor et al., 1996; Hebbard et al., 2000; Herrlich et al., 2000). Moreover, they found no significant up-regulation of CD44 expression amongst simple carcinomas and metastatic cells compared with the adjacent normal mammary tissue, indicating that CD44 does not play an important role in this aggressive mammary tumor (Paltian et al., 2009). As confirmed by these studies, it looks like CD44 expression in normal mammary gland is already high, therefore it could not be used as a useful marker of aggressiveness in this species.

In FMTs, the expression of CD44 was overall low (roughly 5%). Sarli and collaborators evaluated the intramammary/intratumor and extramammary/extratumor expression of CD44 in feline normal mammary tissues, benign, and malignant tumors in relationship to lymphangiogenesis (Sarli et al., 2007) and found that CD44 is significantly more expressed in intramammary/intratumor areas than extramammary/extratumor areas in benign and malignant tumors. Additionally, no statistically significant differences in CD44 expression between normal mammary gland, benign tumors, and malignant tumors were found. To the best of our knowledge, no other studies on CD44 expression in FMT tissues are present within the literature. These data, together with our data, suggest that in this species CD44 could not be used as a useful marker of malignancy.

Another protein that is well-studied and plays a central role in the EMT process, therefore in tumor invasion and metastasis is vimentin. Vimentin is one of the major intermediate filament proteins and is ubiquitously expressed in normal mesenchymal cells (Green et al., 2005). Recent studies have reported that vimentin knockdown causes a decrease in genes linked to breast cancer metastasis, such as the receptor tyrosine kinase Axl (Gjerdrum et al., 2010). In this study, we also evaluated the expression of vimentin in

HBCs, CMTs, and FMTs. We found a higher expression of vimentin in TNBCs than ER+, although not significant presumably due to the low number of cases. This result suggests that vimentin expression is associated with the triple negative subtype, aggressive behavior, and a poor prognosis of HBC, as previously reported (Yamashita et al., 2013; Hemalatha et al., 2013; Rismanchi et al., 2014; Tanaka et al., 2016). In CMTs, vimentin expression is fairly low (roughly 15%), confirming a low aggressiveness of mammary tumors in dogs, which is in concordance to what other authors recently found (Raposo-Ferreira et al., 2018). Whereas in FMTs, the expression of vimentin, although heterogeneous, was quite high (roughly 70%), suggesting the already mentioned high aggressiveness of mammary tumors in this species (Zappulli et al., 2015) as well as their similarities with TNBC (Caliari et al., 2014).

Taken together, all the IHC data seem to support the already proposed similarities between FMTs (grade III) and TNBC as well as between CMTs (grade I and II) and ER⁺ HBC. The two species are widely discussed as potential spontaneous models of specific HBC subtypes (Abdelmegeed et al., 2018; Wiese et al., 2013; Caliari et al., 2014).

It is well known that CSCs, characterized by a deregulation of several pathways, as described above, are thought to be responsible for cancer metastasis and that EMT is a key process during early stages of metastasis development (Hong et al., 2018; Velasco-Velazquez et al., 2011; Ye et al., 2017). For these reasons, in the **phase III** of this study we focused on mammary cancer metastases. Metastasis to distant organs is the major cause of morbidity and mortality in cancer patients (Nathoo et al., 2005; Palmieri et al., 2007). Metastasis is a complex biological phenomenon resulting from the successful completion of several steps of molecular and cellular processes, including detaching from the primary tumor, invading the surrounding tissue, entering the circulation (intravasation), surviving into the circulation, exiting from the circulation (extravasation), colonizing a distant organ, and eventually outgrowing to symptomatic metastatic tumor (Fidler, 2003). According to the specific subtype, HBC has been observed to preferentially metastasize to the bone and lungs and less frequently to other organs such as the liver and brain (Minn et al., 2005). Brain metastasis is the most common central nervous system (CNS) malignant disease (Zhang and Dihua, 2016) and an increasing number of human patients manifests brain metastasis in the clinic, for which the only treatment options remain palliative care (Kong et al., 2015). Understanding the genetic changes and molecular mechanisms by which cancer cells acquire their metastatic ability is one of the most challenging issues in cancer research. The general mechanism of mammary cancer metastases is poorly understood partly due to the lack of robust clinically relevant *in vivo* metastatic models. Therefore, proper *in vivo* animal models are indispensable for scientific investigation of breast cancer metastasis (Daphu et al., 2013). From the 1970's and onwards, several HBC brain metastasis models have been developed (Daphu et al., 2013). After intravenous or intracardial injection in nude mice, brain metastases were observed at various take rates (Yano et al., 2000; Fidler et al., 2002; Schackert and Fidler, 1988) where one of the most widely used cell line is the TNBC cell line MDA-MB-231. Ideally, tumor cell inoculation and metastatic spread should mimic progress of clinical disease, but these inoculation methods do not fully reflect disseminated disease in humans. Injecting tumor cells into the bloodstream of animals, either by tail, heart or carotid injection, is not likely to reflect the changes seen in primary tumors prior to the metastatic process (Daphu et al., 2013). In our study, we aimed to develop

a clinically relevant mouse model of HBC metastasis, with particular attention to brain metastases to then similarly develop a metastatic mouse model also with canine and feline cell lines.

As previously said, all the experiments of this phase have been performed at the Department of Neurology of the Massachusetts General Hospital during my period abroad, under the supervision of Prof. Christian Badr.

To initially establish the model, we decided to use the MDA-MB-231 cell line. Before injection, we stably transduced MDA-MB-231 with the fluorescent protein mCherry and the enzyme Firefly Luciferase (FLuc), which catalyzes a light-emitting reaction when the substrate D-luciferin is present. If injected cells express FLuc, they can be visualized using *in vivo* bioluminescence after the intraperitoneal administration of D-luciferin.

TNBC MDA-MB-231 cells have been injected orthotopically in the mammary fat pad of three groups of mice. The first group has been injected with the wild type. The second group has been injected with cells overexpressing Her2. Her2⁺ breast tumors are highly metastatic and two to four times more likely to metastasize to the CNS than Her2⁻ tumors (Niikura et al., 2014). We wanted to investigate whether this protein confers to the cells the ability to colonize the brain more than what the wild type does. The third group has been injected with cells infected with the Cancer Pathways Library (CPL), which is made of 39 different mutant cDNAs involved in several cancer-related pathways, as already described (Martz et al., 2014).

It is well known that solid tumors are composed of a heterogeneous cell population (Park et al., 2010). Only a few clones have the potential to invade the tissue surrounding the tumor, enter the circulation, survive into the circulation, extravasate, and then eventually to grow into a distant organ (Valastyan and Weinberg, 2011). But which are the features of those cells able to go through the whole metastatic process? Is metastatic dissemination a stochastic event or is precisely regulated by a specific gene signature? In other words, does specific gene deregulation correlate with specific organ dissemination? These are still questions that need to be answered. Using the CPL cell line, we wanted to resemble the heterogeneity of HBC, composed of different clones. *In vivo*, CPL cells grew faster than wild type and than Her2, suggesting that this library conferred to the cells a higher aggressiveness, as expected considering that in these cells several cancer-related pathways have been deregulated (Martz et al., 2014).

A few weeks after injection, when the tumor reached 500 mm³ of volume, it has been surgically removed in order to prolong the survival of the mice to mimic the real situation happening in women and therefore also to allow the microscopic metastases, if any, to expand into macroscopic lesions. The majority of *in vivo* metastatic mouse models consist in injecting tumor cells either directly into the bloodstream or into the mammary fat pad, but without performing surgery to resect the primary tumor (Shapovalov et al., 2014; Kang et al., 2003). These approaches, especially the first one, do not reflect what happens in HBC patients. Instead, our approach, that have been used by very few studies (Kerbel, 2015; Doornebal et al., 2012) and thoroughly methodologically described by Gast and collaborators (Gast et al., 2017) recapitulates the key biological events of the metastatic cascade and closely mimics the clinical course of metastatic disease in humans. None of the mice used in the studies performed by Kerbel, Doornebal, and Gast developed brain metastases.

As mentioned, all the animals underwent surgery. The surgical technique, as described (Gast et al., 2017), consists in a lumpectomy to remove the primary tumor mass, which should be performed with wide and deep margins (Oglesbee, 2011). Considering the size of these animals, which weight roughly 30 grams, one of the most challenging issues was the ability to perform adequate surgical margins to ensure the removal of all cancer cells. In this regard, one problem we have encountered that should be highlighted with this methodology is regrowth of primary tumor/relapse at the site of surgical resection, as previously found by other authors (Kerbel, 2015). This could be due to inadequate surgical margins. However, local relapse is very common in TNBC (Sharma, 2016), therefore we believe this model truly mimics the HBC behavior in patients.

In addition to that, during the procedure, the tumor should be dissected away from the abdominal wall musculature, keeping the mammary glands intact (Gast et al., 2017). In a low number of mice, at the time of surgery, the tumor was adherent to the abdominal wall, as described by other authors (Gast et al., 2017). When this happened, the abdominal wall with the infiltrating tumor was removed and then sutured. It is important to mention that we cannot exclude that metastasis that occurred in those animals characterized by an infiltration of the abdominal wall could be due to a peritoneal dissemination of cancer cells. Other authors wondered whether metastatic dissemination was exclusively initiated by surgery-induced shedding of cancer cells (Doornebal et al., 2012). In order to rule this out, they performed some experiments and they concluded that metastatic dissemination in their model occurs spontaneously and is not initiated by surgery-induced shedding of cancer cells (Doornebal et al., 2012). However, their data as well as our data do not completely exclude the possibility that surgical manipulation of the primary tumor contributes to metastatic dissemination of cancer cells (Doornebal et al., 2012).

After surgery, *in vivo* bioluminescence has been weekly performed to monitor metastasis development. *In vivo* bioluminescence is a versatile and sensitive tool, based on detection of light emission from cells or tissues, that has been widely used to track tumor cells expressing FLuc, as well as bacterial and viral infections, gene expression, and treatment response (Sato et al., 2004). All the mice were sacrificed when symptoms of distress, such as dehydration, weight loss, apathy, loss of appetite were present. Necropsy has been performed to all the animals and a macroscopic evaluation of the organs revealed metastatic masses, as previously highlighted by *in vivo* bioluminescence. Macroscopic metastases were found in lungs, bone, liver, which are the organs where HBC preferentially metastasize (Minn et al., 2005).

All the metastatic tumors/organs as well as the main organs were collected. In order to confirm the presence of metastatic tumor cells in the collected organs, we performed a PCR amplifying FLuc, which is expressed only in the injected tumor cells. All the organs characterized by the presence of macroscopic metastases showed an amplification of FLuc, confirming that the tumor cells were metastatic tumor cells coming from the injected cell line and not spontaneous tumors. PCR is a highly sensitive technique but its sensitivity is limited. If the sequence of interest is present in a very small number of copies within the sample, it is not able to detect it. Nested PCR involves the use of two primer sets and two subsequent reactions and, therefore, sensitivity and specificity of DNA amplification are significantly enhanced (Carr et al., 2010). In order to detect microscopic metastases, composed of a few cells, we performed a nested PCR for FLuc amplifying

with the first set of primers a sequence upstream from the second set of primers. As a result, we were able to detect an amplification in a few more organs. It is important to mention that when the animals have been euthanized, they have not been perfused with PBS-EDTA to get rid of the blood present within the bloodstream, therefore within the organs. As a result, finding an amplification of FLuc in the collected organs does not completely exclude that the metastatic cells are present within the circulation instead of the organ parenchyma. However, if the amplification came from circulating tumor cells (CTCs), most likely we would have amplified FLuc from all the organs of the same animal. In addition to that, perfusion gets rid of the vast majority of blood but it does not completely remove all the content of blood vessels. Therefore, even if we had perfused the animals, eliminating the vast majority of CTCs, we could have not been completely sure that any amplification came just from the organ parenchyma. Hence, we believe that FLuc amplifications found in the organs are the result of the presence of metastatic cells within the parenchyma.

Considering macroscopic and microscopic metastases, 50% of the WT mice, 100% of the Her2 group, and 82% of the CPL-injected mice developed metastases in many organs, confirming the high aggressiveness of this breast cancer cell line. Moreover, we confirmed the efficacy of the mouse model.

Researchers that used a similar model, therefore injecting tumor cells in the mammary fat pad, performing surgery and seeking for metastases, have never developed brain metastases (Kerbel, 2015; Doornebal et al., 2012; Gast et al., 2017). In our model, one WT mouse, one Her2 mouse, and 5 CPL mice developed brain metastasis, confirming that, especially the cells infected with the CPL, have a high aggressiveness and some sort of predilection to the brain. To the best of our knowledge, this is the first model where mice developed brain metastases from an orthotopic injection of tumor cells, followed by surgical resection of the primary tumor.

In the second part of this metastatic mouse model project we focused on genetic drivers responsible for the colonization of distant organs, with particular attention to the brain. Understanding specific genes or pathways that drive tumor cells to specific metastatic organs is of great interest and would certainly help those patients that develop distant metastasis. Brain metastases are common in TNBC-bearing patients and median overall survival is 5 months (Lin et al., 2008; Niikura et al., 2014). Therefore, targetable genetic alterations in TNBC is an active area of investigation (Brastianos et al., 2014). Recent genomic profiling studies have focused on identifying metastasis specific pathway alterations (Burnett et al., 2015; Salhia et al., 2014). Whole genome sequencing of metastatic TNBC found recurrent mutations in TP53, LRP1B, HERC1, CDH5, RB1, and NF1; while RNA sequencing found a consistent overexpression of FOXM1 gene (Craig et al., 2013). Furthermore, 20% of TNBCs show expression of PDL-1 (Mittendorf et al., 2014), resulting in checkpoint-blockade immunotherapy as an attractive option for patients with TNBC brain metastasis (Berghoff et al., 2014). Also, methylome analyses in TNBC revealed distinct methylation profiles which correlate with prognosis (Stirzaker et al., 2015). Notably, the PI3K-mTOR pathway shows consistent activation in HBC metastasis (Adamo et al., 2011; Wikman et al., 2012) and clinical trials of inhibitors of this pathway for treatment of breast cancer brain metastases are underway.

In veterinary medicine, Hassan and collaborators developed a mouse model of feline mammary cancer metastasis (Hassan et al., 2017). In their study, mice did not develop metastases after subcutaneous dorsal

thoracic skin injection of FMT cell lines, whereas lung, brain, liver, kidney, eye, and bone metastases were found after intratibial and intracardiac injection of FMT cell lines. They found a number of genes that might be relevant to the metastatic process. However, they did not compare gene expression of metastatic tumors with primary tumors (Hassan et al., 2017).

In our study, in order to investigate genetic drivers responsible for distant organ colonization, we used MDA-MB-231 cell line infected with the CPL, as previously described (Martz et al., 2014). We generated a heterogeneous cell population where each cell contained a single viral integration. In order to make sure we injected only those cells that have integrated the vector, the cells have been treated with puromycin. Since the vector contained a puromycin-resistant gene, the cells that did not integrate the vector died after treatment. After surgery performed to remove primary tumors arisen in the mammary fat pad of mice, we performed a PCR on primary tumors amplifying the sequence where the mutant cDNA of the library was contained. Since each gene/mutant cDNA of the library had a different length, we detected multiple bands by PCR, confirming that multiple clones proliferated in the primary tumor of the mammary fat pad.

Sequencing the metastatic organs, we found a few genes that might play a role in the metastatic process: CASP3, HRAS, ER, MAPK9, RHEB, and RalA. It is important to remind that the vast majority of these genes of the CPL were mutated, therefore were probably characterized by a loss of function. The most represented gene was CASP3 and all the brain metastases expressed this gene.

CASP3 is a protein that plays a central role in the execution-phase of cell apoptosis (Julien and Wells, 2017). The mutation in the CASP3 gene of the CPL is in the catalytic domain (Martz et al., 2014), therefore the protein is not functional. Our hypothesis is that the apoptotic process starts but it does not lead to cell death, therefore the cell survives and becomes more resistant. When tumor cells enter the circulation, they can travel along the vessels to other parts of the body. Many cells die while travelling because they find a different environment from the tissue of origin. In order to survive, these cells need to develop some kind of mechanism, such as resistance to apoptosis. A mutation in the CASP3 gene could confer to the cells the ability to evade apoptosis.

It is demonstrated that alterations of caspases participate in tumor development (Kim et al., 2003; Kurokawa et al., 1999; Reed, 2000; Schwartz et al., 1999; Shin et al., 2002; Soung et al., 2003). Somatic mutations of the genes involved in apoptosis, including caspases, have been reported in human cancers (Reed, 2000). Among the caspases, mutations of CASP3, CASP5, CASP7, CASP8, CASP10 have been described in human cancer tissues and cell lines (Kim et al., 2003; Kurokawa et al., 1999; Schwartz et al., 1999; Shin et al., 2002; Soung et al., 2003). Most of the caspase mutations detected in human cancers show reduced apoptosis activity compared to the wild type caspases, suggesting that the inhibition of apoptosis might play a crucial role in tumorigenesis. Although it is a rare event, Soung and collaborators detected CASP3 mutations in several types of tumors such as stomach, lung, colon, rectum, lymphoma, liver, and multiple myeloma (Soung et al., 2004). CASP3-variant alleles have been detected in squamous cell carcinomas of the head and neck (SCCHN) and associated with increased risk of SCCHN (Chen et al., 2008). In addition, CASP3-variant alleles are associated with risk of endometrial cancer (Xu et al., 2009), non-Hodgkin's lymphoma (Lan et al., 2009), and multiple myeloma (Hosgood et al., 2008). It has been reported that CASP3 expression is

significantly reduced in breast cancer cells, cancer tissue, and even in the normal parenchyma surrounding tumors (Devarajan et al., 2002). However, several studies have demonstrated the opposite. Higher levels of CASP3 protein have been found in malignant, compared to nonmalignant breast tissue, and correlated with increased apoptosis (O'Donovan et al., 2003). Indeed, it has been shown that CASP3 is activated in dying tumor cells and causes increased production of PGE2. As a result, tumor cells start proliferating and become resistant to radiotherapy (Huang et al., 2011). This suggests that apoptosis is an essential aspect of tumor growth, and paracrine signals released by apoptotic cells trigger repopulation of these tumor cells that lead to further growth (Shalini et al., 2015). Woenckhaus and collaborators found that the expression of CASP3 in melanoma metastases was higher compared to the expression in primary tumors (Woenckhaus et al., 2003). Similarly, other authors showed a connection between the expression of CASP3 and increasing malignant behavior in some tumors, such as lymphoma, colorectal cancer, and breast cancers (Donoghue et al., 1999; Jonges et al., 2001; Vakkala et al., 1999). Whether it is a CASP3 upregulation or downregulation that is associated with a higher aggressiveness still needs to be elucidated. Other authors demonstrated that modulating CASP3 expression of two tumor cell lines modifies their abilities to metastasize to the lung in mice (Cheng et al., 2008). These authors speculate that there is a delicate balance between death and survival-promoting ability of CASP3 that, as a sum of crosstalk, supports tumor growth and metastasis (Cheng et al., 2008).

In order to test the hypothesis that CASP3 might be involved in the metastatic process and particularly in the colonization of the brain, we performed *in vivo* and *in vitro* experiments. First of all, we successfully infected MDA-MB-231 with the vector that contained the mutant CASP3 (CASP3MT) of the CPL. Then, MDA-MB-231 overexpressing CASP3MT have been injected in the mammary fat pad of three mice to see whether there was a difference in terms of tumor growth as well as to investigate whether these cells were more prone to metastasize to the brain. MDA-MB-231 CASP3MT *in vivo* tumor growth was faster when compared to wild type and CPL, confirming the higher aggressiveness of these cells, as found by other authors (Cheng et al., 2008). After primary tumor surgery, one animal died while waking up after anesthesia. Also, a few animals of the other groups died after the surgery, while recovering from anesthesia and for this reason they have not been considered in the study. For anesthesia, the commonly used anesthetic mixture of ketamine and xylazine was used, as suggested by the Institutional Animal Care and Use Committee (IACUC) and as described (Arras et al., 2001). However, in order to reach surgical tolerance, the drugs might have adverse effects, such as a death rate of roughly 40%, therefore the safety margin of the mixture ketamine/xylazine is low (Arras et al., 2001). The two mice injected with MDA-MB-231 CASP3MT that took part of the study did not develop macroscopic metastases, but did develop microscopic metastases. One out of two developed brain metastasis, confirming that a mutation in the CASP3 gene might play a crucial role in brain colonization. This is certainly a weak conclusion considering the very small number of animals. For this reason, we are planning to repeat the experiment injecting a higher number of mice, in order to get to a stronger outcome.

We also performed *in vitro* experiments comparing MDA-MB-231 overexpressing CASP3MT with a proper control. We evaluated migration as well as proliferation of these cells and we found a higher migration

of cells overexpressing CASP3MT when compared to the control, confirming their higher aggressiveness. We then wondered whether the higher migration was only due to a higher proliferation by these cells, as seen *in vivo*, and not by a real higher migratory ability. To answer to this question we performed a proliferation assay that showed a lower *in vitro* proliferation of CASP3MT cells when compared to the control. This result makes the migration assay results even stronger, suggesting that these cells have a true higher aggressiveness, in terms of migration. Indeed, it is the migratory ability, and not the proliferation rate, that confers to the cells the ability to metastasize (Martin et al., 2013).

Moreover, we performed the same *in vitro* experiments using the HBC MCF7 cell line which is known to be CASP3-deficient (Jänicke, 2009). In order to investigate whether the higher aggressiveness of these cells is due to an overexpression of the functional CASP3 (wild type) or an aberrant expression of the non-functional CASP3 (mutant), we compared cells overexpressing CASP3MT with cells overexpressing CASP3 wild type (CASP3WT) with MCF7 WT, that do not express CASP3 whatsoever (Jänicke, 2009). Intriguingly, the wound healing assay showed different results from the transwell migration assay. In the first assay, MCF7WT showed the highest migration, whereas in the second assay the highest migration has been achieved by MCF7 CASP3MT. The latter result confirms what previously found using MDA-MB-231, so a higher aggressiveness of CASP3MT overexpressing cells.

Cheng and collaborators performed similar experiments looking at the migration of MCF7 versus MCF7 overexpressing CASP3WT (Cheng et al., 2008). The wound healing assay showed a higher migration of MCF7 CASP3WT when compared to the control, which is in contrast with our results. Also, they investigated cell migration of MCF7 overexpressing CASP3MT compared to the control and they found a higher migration of MCF7 CASP3MT, as our transwell migration assay showed, but in contrast to our wound healing assay. We believe, as they speculated, that there is a delicate balance between death and survival-promoting ability of CASP3 that supports tumor growth and metastasis (Cheng et al., 2008). In our study, we also performed a proliferation assay that showed a higher proliferation of MCF7 CASP3MT when compared to the other two cell lines, suggesting a higher aggressiveness of these cells. It is possible that in cells that do not express CASP3, such as MCF7, the apoptotic process is regulated by other caspases. Therefore, it is difficult in this cell line to study the role of CASP3, that certainly need to be investigated with additional experiments.

In addition to CASP3, we found other genes expressed in metastatic cells that might therefore play a role in the metastatic cascade: HRAS, ER, JNK2, RHEB, RalA.

HRAS is a frequently mutated oncogene especially in head and neck cancer, bladder cancer, vulvar squamous cell carcinoma, cutaneous squamous cell carcinoma, and lung cancer (Imielinski et al., 2012; Lawrence et al., 2014; Trietsch et al., 2014). HRAS has been found to be overexpressed in several tumors, such as gastric cancer (Wu et al., 2016). In our study, HRAS has been found in lungs, bone, heart, muscle, and brain metastatic cells.

Estrogen Receptor (ER) is a key element in HBC, especially when it comes to therapy. The most commonly used endocrine therapies inhibit ER activity. Preclinical and clinical studies have elucidated several potential mechanisms underlying endocrine resistance. Recurrent activating missense mutations of ER have

been recently reported by many groups and found in a substantial fraction of endocrine-resistant metastatic ER⁺ breast cancer (Li et al., 2013; Robinson et al., 2013; Fumagalli et al., 2016). In our study, ER has been found in heart and liver metastatic cells.

The c-Jun N-terminal kinase (JNK) family, a subfamily of the MAPKs, participates in a variety of cell responses, including proliferation, differentiation, cell death, and survival (Pan et al., 2016). As a result, abnormal function of JNK leads to diverse diseases, including cancer (Bubici and Papa, 2014). It has been shown that the role of JNK2 in cancer is complicated and controversial. Studies suggest that the role of JNK2 is pro-tumorigenic in multiple myeloma, glioblastoma, epidermal neoplasia, lung cancer, and breast cancer (Barbarulo et al., 2013; Cui et al., 2006; Ke et al., 2010; Nitta et al., 2011; Cantrell et al., 2015). However, in some lung and breast cancer, JNK2 appears to function as a tumor suppressor (Oleinik et al., 2007; Cellurale et al., 2010). In our study, JNK2 has been found in heart metastatic cells.

Ras homolog enriched in brain (RHEB) is a member of the Ras superfamily of small GTPases that are responsible for the activation of numerous important signaling pathways in the cell (Aspuria and Tamanoi, 2004). Studies showed that a mutation in RHEB might be associated with clear cell renal cell carcinoma and endometrial cancer (Lawrence et al., 2014). Additionally, other studies demonstrated that RHEB is overexpressed in various malignant tumors (Lu et al., 2010; Kobayashi et al., 2010) and that in HBC and in head and neck cancer, its overexpression is associated with a worse prognosis (Lu et al., 2010; Kobayashi et al., 2010; Wazir et al., 2013). In our study, RHEB has been found in heart and lungs metastatic cells.

RalA GTPase, a member of the Rab effectors, has been implicated in tumorigenesis, invasion, and metastasis in a variety of solid tumors (Bodemann and White, 2008). Hence, activation of RalA signalin appears to be a critical step in Ras-induced transformation and tumorigenesis (Lim et al., 2005). In our study, RalA has been found in liver and abdominal metastatic cells.

Our study demonstrated that these genes might be involved in the metastatic process. Therefore, their role in HBC progression and metastatization needs to be investigated with further studies.

In summary, during phase III we established a highly clinically relevant mouse model of HBC metastasis. A few mice developed brain metastases, which, to the best of our knowledge, has never been achieved using our approach. Additionally, we found a few genes that might be involved in the metastatic process. Among them, CASP3MT seems to be the most relevant. We believe that CASP3MT might confer to the cells a higher aggressiveness and a higher resistance to apoptosis. It is certainly not the only gene that plays a role in the metastatic dissemination, but its deregulation could help aggressive cells to survive in a foreign environment, such as the blood or a different organ from the tissue of origin, not only in breast cancer, but also in other type of tumors. Further studies are needed to better elucidate its role in cancer progression and metastasis and to explore the value of this model for veterinary medicine as well.

In the **phase IV** of this project, we focused on extracellular vesicles (EVs). EVs have received considerable attention as novel membrane-bound cell-derived cargo systems involved in intercellular communication and microenvironment modulation in many physiological and pathological processes. They exert pleiotropic biological functions via the horizontal transfer of bioactive molecules (proteins, lipids, DNAs,

and RNAs) (Zaborowski et al., 2015). It has been shown that human EVs have an effect at both paracrine and systemic levels (Colombo et al., 2014; Simpson et al., 2009; Rak and Guha, 2012; Tauro et al., 2013; Christianson et al., 2014; Rajendran et al., 2014).

In human cancer, EVs have raised a large interest both as mediators of pathways that lead to tumor progression and as potential novel cancer biomarkers (Maas et al., 2017). In veterinary medicine, very little is known about cancer-derived EVs. To our knowledge, only a few studies have been carried out in veterinary medicine on extracellular vesicles. These studies isolated EVs from equine adipose-derived mesenchymal stromal cells (Pascucci et al., 2015; Pascucci et al., 2014), equine ovarian follicular fluid (da Silveira et al., 2012), equine serum (Rout et al., 2015), bovine milk (Blans et al., 2017; Vaswani et al., 2017), and plasma of sheep, pigs, rats, and rabbits (Johnstone et al., 1989). EVs have never been investigated within the context of veterinary oncology.

In this study, we examined the role that EVs play in tumor angiogenesis. Additionally, we isolated and preliminarily characterized EVs from canine and feline mammary gland carcinoma cell lines.

As previously said, the majority of the experiments of this phase have been performed at the Department of Neurology of the Massachusetts General Hospital during my period abroad, under the supervision of Prof. Xandra O. Breakefield, who has an extraordinary experience on Glioblastoma Multiforme (GBM) and EVs.

GBM is a highly invasive, hypervascular, hypoxic, and therapy-resistant central nervous system neoplasm with a median lifespan from time of diagnosis to death of about 15 months (Stupp et al., 2009; Broekman et al., 2018). GBM is characterized by genetic and epigenetic variations among tumor cells that makes the development of therapies that eradicate all tumor cells challenging and currently impossible (Broekman et al., 2018). GBM growth is supported by a communication with the brain microenvironment, that supports tumor progression and resistance to therapy (Broekman et al., 2018). Tumors are thought to induce changes in normal brain cells, such as endothelial cells, to create a microenvironment that favors tumor success.

In our study, we wanted to investigate the effect of GBM-derived EVs on endothelial cells and how GBM cells, through EVs, recruit new blood vessels. To do so, we performed an *in vitro* tube formation assay where human brain microvascular endothelial cells (HBMVECs) have been exposed for 16 hours to different stimuli: i) endothelial basal medium (EBM); ii) EBM supplemented by growth factors; iii) EBM and GBM8 cell line-derived EVs; iv) EBM and GBM8 supernatant; v) EBM and unconditioned medium (UCM) pellet; vi) EBM and UCM supernatant. GBM8 EVs have been isolated by ultracentrifugation, which is the most popular EV purification technique (Zaborowski et al., 2015; Xu et al., 2016). Phenotypic analysis of tubule formation revealed that the highest values in terms of tubule length, number of tubules, number of branching points, and mesh count were achieved by endothelial cells treated with growth factor, which was the positive control condition. The second highest values were achieved by HBMVECs treated with GBM8-derived EVs, suggesting that they play a crucial role during the angiogenesis process and confirming their ability to stimulate HBMVEC

growth, as previously demonstrated using U251, a human malignant glioblastoma cell line (Giusti et al., 2016) and using two primary GBM stem cell lines (Spinelli et al., 2018).

After 16 hours of treatment, the RNA has been isolated from HBMVECs and sent for total RNA sequencing. Our specific goal is to investigate the transcriptome of HBMVECs, as well as the small RNAs and the long non-coding RNAs. However, this project is part of a biggest study that involves several institutions and the analyses of RNA sequencing are being performed by our collaborators at Baylor College of Medicine in Houston, TX and will be available in the next months. The aim of the whole project is to study the DNA methylation and transcriptional alterations of HBMVECs exposed to GBM-derived EVs. DNA methylation controls gene expression, therefore DNA methylation data, previously obtained by collaborators, will be matched with RNA sequencing data in order to better understand how GBM EVs contribute to angiogenesis.

As mentioned, EVs have never been investigated within the context of veterinary oncology, therefore in this part of the study we isolated and preliminarily characterized EVs from canine and feline mammary gland carcinoma cell lines.

Conventional systems for EVs isolation and characterization have been debated and tentatively standardized by the International Society for Extracellular Vesicles (ISEV) (Lötvall et al., 2014; Van der Pol et al., 2014) and include pelleting by ultracentrifugation of cell culture medium or biological fluids, electron microscopy and analysis of expression of EVs surface markers (Cocucci and Meldolesi, 2015).

EVs can be purified from different body fluids, such as serum, plasma, saliva, urine, milk, effusions, cerebrospinal fluid, as well as from cell culture conditioned medium (They et al., 2006; Colombo et al., 2014). In human medicine, several methodologies are described to isolate EVs: differential centrifugation, density gradient/cushion centrifugation, immune-affinity based capture, size-exclusion chromatography, microfluidic devices, synthetic polymer-based precipitation, and membrane filtration (Xu et al., 2016; Gardiner et al., 2016). In this study, we successfully isolate EVs using differential ultracentrifugation, which is the most popular EV purification technique regardless of the starting material (Zaborowski et al., 2015; Xu et al., 2016). It is a relatively easy and inexpensive method when the ultracentrifuge is available. It requires some expertise in the manual separation of the supernatant from the pellet in the different steps, which is however gained in a relatively short time. The main disadvantage of this method is the co-isolation into the EV-enriched pellet of high molecular weight proteins complexes such as 26S proteasome, HSPG, fatty acid synthase, lipoproteins, and potentially viral particles (Vickers et al., 2011; Tauro et al., 2012). Other methods have been adopted and described for EVs isolation and specific advantages and disadvantages have been discussed (Gardiner et al., 2016). It appears that the selection of the best method relies on several aspects such as the starting material, the importance of the EVs yield versus the purity, specific EVs subtypes to be isolated, and the downstream analysis to be performed with the EVs, as described by the International Society of Extracellular Vesicles (ISEV) (Lötvall et al., 2014).

Different methodologies can be used to measure and quantify EVs. Many studies calculated total EVs-derived proteins to estimate the amount of EVs (Zaborowski et al., 2015). However, this value is often overestimated by the presence of high molecular weight proteins that are present with purified EVs (Xu et al.,

2016). Additionally, different EV subtypes can carry different protein amounts (Zaborowski et al., 2015). Other methods include Nanoparticle Tracking Analyses (NTA), dynamic light scattering, flow cytometry, tunable resistive pulse sensing (tRPS), Transmission Electron Microscopy (TEM), and Raman spectroscopy (Smith et al., 2015). No method alone allows accurate phenotyping, sizing, and measurement for the whole range of EV subtypes. As a consequence, a combination of different techniques has to be used to quantify and characterize EVs. For this reason, in this study we performed TEM and NTA to visualize, measure, and quantitate EVs as well as Immunogold and Western Blot to characterize them.

TEM is used to visualize and to study the physical properties of EVs and can be considered the gold standard (Lawson et al., 2017). Although TEM can accurately measure EV size and morphological features, it is time consuming, requires specialists with experience and is not quantitative. Additionally, the entire procedure (ultracentrifugation, dehydration, and fixation) might alter the size and morphology, producing artifacts, such as the typical "cup shape" morphology of exosomes after fixation (György et al., 2011; They et al., 2006).

In the present study, in EV-enriched pellets TEM highlighted the presence of membrane-bound particles, which size and morphology are similar to that found in many studies on human EVs (Van der Pol et al., 2014; Cizmar et al., 2017; Arraud et al., 2014) and equine EVs (Pascucci et al., 2015). In the UCM pellet no membrane-bound particles were found, confirming the purity of the samples, that can be verified by the absence of growth medium/FBS-derived EVs. It is important to remember that for all the experiments performed in this study, the FBS used in the cell growth media was depleted of EVs by overnight ultracentrifugation and subsequent 0.22 μm filtration. This procedure is necessary to avoid the contamination by vesicles normally present in the FBS (Shelke et al., 2014).

NTA is a highly sensitive method that utilizes the phenomenon that diffusivity of nanoparticles by Brownian motion in a liquid suspension is determined by size, temperature, and viscosity of the liquid in which they are contained (Thayanithy et al., 2017). Particles undergoing Brownian motion are digitally recorded and their motion is analyzed by the software to determine the particle count and size. Our findings confirmed that the most represented population of particles was approximately 100 (\pm 20) nm in diameter, similar to that described in other studies (Sokolova et al., 2011; Dragovi et al., 2011; Vestad et al., 2017). This size range indicates that apparently most of the isolated EVs from feline and canine cancer cells were exosomes. Additionally, fewer larger particles (200 – 600 nm) were present suggesting the presence of other EV subtypes (MVs, apoptotic bodies, and oncosomes), as already reported (Colombo et al., 2014; Baietti et al., 2012). Results from other studies on horse adipose-derived mesenchymal stromal cells vesicles showed similar size range of vesicles (30-200 nm) (Pascucci et al., 2015).

The advantage of the NTA method is that it is a fast and easy way of analyzing large number of particles. However, the method does not differentiate EVs from protein complex aggregates of similar size or any floating particles (e.g. salts) (Colombo et al., 2014). These non-EV particles might be those evidenced by NTA in our UCM samples. Particularly, DMEM showed a relative higher number of particles compared to RPMI and also to NB and EBM. These differences are due to their different composition in terms of proteins, salts and glucose. Also, considering that some instrumental parameters (such as screen gain and camera level) are

still manually determined by the user, the reliability and reproducibility of this technique is strongly based on accuracy of standardization (Colombo et al., 2014).

A comparison of NTA, tRPS, and flow cytometry revealed significant differences among the techniques, suggesting that the absolute EVs quantification is still challenging (Maas et al., 2015). The choice of the method depends on instruments availability and again the specific aims of the study (Colombo et al., 2014).

By Immunogold for Alix and CD63 we could preliminarily characterize EVs produced by mammary carcinoma cell lines. As expected, the UCM presumptive pellet did not show any positivity to these markers, confirming the purity and the absence of EVs in this sample. Western Blot for TSG101 and Alix also showed positivity of cells as well as of EVs, and absence of bands from the UCM sample.

When EV characterization is performed, the markers of choice should be expected to be present in the EVs of interest, especially transmembrane proteins (e.g. CD9, CD63, and CD81) and cytosolic proteins with membrane-binding capacity (e.g. Alix and TSG101) (Lötvall et al., 2014). There is some controversy as to whether some of these markers are exclusively present in specific EV subtypes or are found on all EVs, regardless of their origin and mechanism of biogenesis. It seems that some protein markers such as TSG101, Alix, and CD63 are particularly enriched in exosomes (Xu et al., 2016). However, these proteins have been observed also in other EV subtypes (e.g. apoptotic bodies and microvesicles) (Tauro et al., 2013; Crescitelli et al., 2013) and therefore are, at present, used as common EV markers. In the published studies different isolation techniques, cell types, and culture conditions are used to analyze the EV protein content. Thus, it is difficult to give a conclusive view of the protein composition of the different EV subtypes (Abels and Breakefield, 2016). As a result, standardization of the isolation procedures and more complete experimental data are strongly needed in order to determine if there are specific proteins that can be associated with specific EVs subtypes (Tauro et al., 2013).

EVs are considered to be messengers produced by "donor" cells that play a crucial role in intercellular communication both at paracrine and systemic levels (Xu et al., 2016). EVs carry DNAs, RNAs, and proteins and, acting as *Trojan horses*, are taken up by "recipient" cells inducing changes in their physiology (Zaborowski et al., 2015). It is difficult to visualize the internalization of EVs by recipient cells using optical microscopy, due to their small size. Therefore, we used a technique developed by Lai and collaborators that allows the visualization and tracking of tumor EV delivery, based on palmitoylation of fluorescent proteins (Lai et al., 2015). Palmitoylation enhances the hydrophobicity of proteins and contributes to their membrane association. In other words, it confers on proteins the ability to bind to cell membranes. As a result, palmitoylated fluorescent proteins label all cell membranes and therefore EVs. CYPp-palmtTomato cells produce palmtTomato⁺ EVs that are taken up by recipient cells and can therefore be visualized inside their cytoplasm. The visualization of palmtTomato signal within GFP⁺ cells allowed us to visually confirm EV production by donor cells and uptake by recipient cells, as previously described (Lai et al., 2015), corroborating their role in intercellular communication and the existing need of further studies.

In conclusion, we isolated, measured, and preliminarily characterized canine and feline EVs from mammary gland carcinoma cell lines, using a HBC cell line as a positive control. Moreover, we were able to visualize EV uptake by recipient cells. Further analyses are needed to better characterize EVs with additional markers comparing also different methodologies for isolation and counting. However, this preliminary identification of EVs opens a new interesting unexplored veterinary field with implications not only within the context of cancer but also to many other physiological and pathological processes.

CONCLUSIONS

In this study we focused on different subpopulations of the mammary gland tumors of human, dogs, and cats, with particular attention to cancer stem cells (CSCs), which are thought to be responsible for the tremendous intra-tumor heterogeneity, as well as relapses, resistance to therapy, and metastasis development. We successfully isolated CSC-like cells from well established canine and feline mammary tumor cell lines (CYPp and FMCp, respectively), confirming their $CD44^+/CD24^{-/low}/CD133^+$ phenotype, that however, needs to be verified at both protein and mRNA levels in order to avoid misleading results. Wnt/ β -catenin and Hippo pathways seem to be deregulated in human, canine, and feline mammary tumors. This deregulation is more evident at the protein level, suggesting a possible post-transcriptional regulation of the molecules involved in these pathways, especially β -catenin and YAP/TAZ. The gene expression of EMT-related molecules (SNAIL, TWIST, ZEB) is not significantly different between healthy mammary tissues and HBC, CMT, and FMT, probably due to the complexity of the process as well as the difficulty when working with tissues where different cell populations are present, as in the healthy mammary gland. Phenotypically, we found strong similarities between TNBC and FMTs as well as between HBC ER⁺ and CMTs, suggesting that canine and feline mammary tumors could be certainly used as interesting and valuable spontaneous model of human breast cancer.

Also, we developed a highly clinically relevant *in vivo* mouse model of breast cancer metastasis that resembles the real behavior of this malignant tumor in human patients. According to our results, we believe that caspase 3 could play a role in the metastatic dissemination of cancer cells, particularly in brain metastasis. Further studies will be performed to translate these interesting results within the context of canine and feline mammary tumors.

Furthermore, we investigated the role that tumor-derived EVs play in the microenvironment to support its growth using the human glioblastoma (GBM) model. We detected that GBM-derived EVs indeed are able to induce angiogenesis. Finally, for the first time we isolated EVs from canine and feline mammary tumor cell lines by ultracentrifugation, visualized by Transmissible Electron Microscopy, counted by Nanoparticle Tracking Analysis, and characterized by immunogold and Western Blot. This opens a new interesting unexplored field in veterinary medicine with several diagnostic, prognostic, and therapeutic implications that will certainly be beneficial not only for dogs and cats, but also for humans.

ACKNOWLEDGEMENTS

First of all, I would like to thank Prof. Valentina Zappulli for her help, advice, support, and everything she taught me thus far. She leads the Anatomical Pathology unit, that I consider to be my second house, where I hope I can work as long as possible. Everyone who belongs to our unit is fantastic and contributes to create such a beautiful atmosphere that I am sure everybody would enjoy. I would like to thank Professors, Technicians, Post-Docs, PhD students who make our unit such a great team not only to work and collaborate, but also to hang out with during non-working hours.

Secondly, I would like to thank Prof. Xandra Breakefield and Prof. Christian Badr from the Department of Neurology, Massachusetts General Hospital/Harvard Medical School, Boston, MA, USA, that is where I have been working for a bit more than a year during my period abroad. They gave me the opportunity to work in one of the most important institutions of the world, where I learnt so many things I did not even imagine I would have learnt, before getting there. Xandra and Chris beautifully lead their own lab, where I met many people that have been (and still are!) not only excellent scientists, but also very good friends, who contributed to make my time there definitely the most amazing experience of my life.

Last but not least, I would like to thank my family, who always supports me in everything I do. When it comes to my job, I believe they are even happier than me for what I do. I am sure they are extremely satisfied to see my achievements and what I accomplished during the last years. Making them happy is definitely all I can (and I would say I have to) do to reward them for every single thing they do for me every day.

REFERENCES

- Abdelmegeed SM, Mohammed S. Canine mammary tumors as a model for human disease. *Oncol Lett.* 2018; 15(6):8195-8205.
- Abels E, Breakefield XO. Introduction to Extracellular Vesicles: Biogenesis, RNA Cargo Selection, Content, Release, and Uptake. *Cell Mol Neurobiol.* 2016; 36:301–312.
- Abraham BK, Fritz P, McClellan M, et al. Prevalence of CD44+/CD24-/low cells in breast cancer may not be associated with clinical outcome but may favor distant metastasis. *Clin Cancer Res.* 2005; 11:1154-1159.
- AbuSamra DB, Aleisa FA, Al-Amoodi AS, et al. Not just a marker: CD34 on human hematopoietic stem/progenitor cells dominates vascular selectin binding along with CD44. *Blood Adv.* 2017; 1(27):2799-2816.
- Adamo B, Deal AM, Burrows E, et al. Phosphatidylinositol 3-kinase pathway activation in breast cancer brain metastases. *Breast Cancer Res.* 2011; 13:R125.
- Adega F, Borges A, Chaves R. Cat mammary tumors: genetic models for the human counterpart. *Vet Sci.* 2016; 3(3). pii: E17.
- Aga M, Bentz GL, Raffa S, et al. Exosomal HIF1 α supports invasive potential of exosomes. *Oncogene* 2014; 33(37):4613–4622.
- Ahmad A, Sarkar SH, Bitar B, et al. Garcinol regulates EMT and Wnt signaling pathways in vitro and in vivo, leading to anticancer activity against breast cancer cells. *Mol Cancer Ther.* 2012; 11:2193–2201.
- Aigner K, Dampier B, Descovich L, et al. The transcription factor ZEB1 (Δ EF1) promotes tumour cell dedifferentiation by repressing master regulators of epithelial polarity. *Oncogene.* 2007; 26:6979-88.
- Al-Hajj M, Wicha MS, Benito-Hernandez A, Morrison SJ and Clarke MF. Prospective identification of tumorigenic breast cancer cells. *Proc Natl Acad Sci USA.* 2003; 100:3983-3988.
- Al-Nedawi K, Meehan B, Micallef J, et al. Intercellular transfer of the oncogenic receptor EGFRvIII by microvesicles derived from tumour cells. *Nat Cell Biol.* 2008; 10:619–624.
- Ali HR, Rueda OM, Chin SF, et al. Genome-driven integrated classification of breast cancer validated in over 7,500 samples. *Genome Biol.* 2014; 15(8):431.
- Altin JG, Sloan EK. The role of CD45 and CD45-associated molecules in T cell activation. *Immunol Cell Biol.* 1997; 75(5):430-445.
- Ansieau S. EMT in breast cancer stem cell generation. *Cancer Lett.* 2013; 338(1):63-68.
- Arras M, Autenried P, Rettich A, Spaeni D, Rüllicke T. Optimization of intraperitoneal injection anesthesia in mice: drugs, dosages, adverse effects, and anesthesia depth. *Comp Med.* 2001; 51(5):443-456.
- Arraud N, Linare R, Tan S, et al. Extracellular vesicles from blood plasma: determination of their morphology, size, phenotype and concentration. *J Thromb Haemost.* 2014; 12:614–627.
- Arroyo JD, Chevillet JR, Kroh EM, et al. Argonaute2 complexes carry a population of circulating microRNAs independent of vesicles in human plasma. *Proc Natl Acad Sci USA.* 2011; 108:5003–5008.
- Aspuria PJ, Tamanoi F. The Rheb family of GTP-binding proteins. *Cell Signal.* 2004; 16(10):1105–1112.
- Azzolin L, Panciera T, Soligo S, et al. YAP/TAZ incorporation in the beta-catenin destruction complex orchestrates the Wnt response. *Cell.* 2014; 158:157– 170.
- Baietti MF, Zhang Z, Mortier E, et al. Syndecan – syntenin – ALIX regulates the biogenesis of exosomes. *Nat Cell*

- Biol.* 2012; 14:677–685.
- Bakhshinyan D, Adile AA, Qazi MA, et al. Introduction to cancer stem cells: past, present, and future. *Methods Mol Biol.* 2018; 1692:1-16.
- Balaj L, Lessard R, Dai L, et al. Tumour microvesicles contain retrotransposon elements and amplified oncogene sequences. *Nat Commun.* 2011; 2:180.
- Bao B, Ahmad A, Azmi AS, Ali S, Sarkar FH. Overview of cancer stem cells (CSCs) and mechanisms of their regulation: implications for cancer therapy. *Curr Protoc Pharmacol.* 2013; Chapter 14:Unit 14.25.
- Barbarulo A, Iansante V, Chaidos A, et al. Poly(ADP-ribose) polymerase family member 14 (PARP14) is a novel effector of the JNK2-dependent pro-survival signal in multiple myeloma. *Oncogene.* 2013; 32:4231–4242.
- Barbieri F, Thellung S, Ratto A, et al. In vitro and in vivo antiproliferative activity of metformin on stem-like cells isolated from spontaneous canine mammary carcinomas: translational implications for human tumors. *BMC Cancer.* 2015; 15:228.
- Barbieri F, Wurth R, Ratto A. Isolation of stem-like cells from spontaneous feline mammary carcinomas: Phenotypic characterization and tumorigenic potential. *Exp Cell Res.* 2012; 318(7):847-860.
- Barone R. Mamelles. Tome 4 Splanchnologie II. 1990. Editions vigot, Paris.
- Bartlett J, Mallon E, Cooke T. The clinical evaluation of HER-2 status: which test to use? *J Pathol.* 2003; 199(4):411-417.
- Bartucci M, Dattilo R, Moriconi C, et al. TAZ is required for metastatic activity and chemoresistance of breast cancer stem cells. *Oncogene.* 2015; 34(6):681– 690.
- Batagov AO, Kurochkin IV. Exosomes secreted by human cells transport largely mRNA fragments that are enriched in the 3'- untranslated regions. *Biol Direct.* 2013; 8:12.
- Battle E, Sancho E, Franci C, et al. The transcription factor snail is a repressor of E-cadherin gene expression in epithelial tumour cells. *Nat Cell Biol.* 2000; 2:84-89.
- Bauerschmitz GJ, Ranki T, Kangasniemi L, et al. Tissue-specific promoters active in CD44+CD24-/low breast cancer cells. *Cancer Res.* 2008; 68(14):5533-5539.
- Beffagna G, Sacchetto R, Cavicchioli L, et al. A preliminary investigation of the role of the transcription co-activators YAP/TAZ of the hippo signalling pathway in canine and feline mammary tumours. *Vet J.* 2016; 207:105-111.
- Berghoff AS, Bartsch R, Wohrer A, et al. Predictive molecular markers in metastases to the central nervous system: recent advances and future avenues. *Acta Neuropathol.* 2014; 128:879-91.
- Bezdenzhnykh N, Semesiuk N, Lykhova O, Zhylchuk V, Kudryavets Y. Impact of stromal cell components of tumor microenvironment on epithelial-mesenchymal transition in breast cancer cells. *Exp Oncol.* 2014; 36(2):72-78.
- Bilic J, Huang YL, Davidson G, et al. Wnt induces LRP6 signalosomes and promotes disheveled-dependent LRP6 phosphorylation. *Science.* 2007; 316(5831):1619–1622.
- Birnbaum D, Bertucci F, Ginestier C, et al. Basal and luminal breast cancers: basic or luminous? [review]. *Int J Oncol.* 2004; 25:249–258.
- Blacking TM, Waterfall M, Argyle DJ. CD44 is associated with proliferation, rather than a specific cancer stem cell population, in cultured canine cancer cells. *Vet Immunol Immunopathol.* 2011; 141(1-2):46-57.
- Blacking TM, Waterfall M, Samuel K, Argyle DJ. Flow cytometric techniques for detection of candidate cancer stem

- cell subpopulations in canine tumour models. *Vet Comp Oncol.* 2012; 10(4):252-273.
- Blans K, Hansen MS, Sørensen LV, et al. Pellet-free isolation of human and bovine milk extracellular vesicles by size-exclusion chromatography. *J Extracell Vesicles.* 2017; 6:1294340.
- Blick T, Hugo H, Widodo E, et al. Epithelial mesenchymal transition traits in human breast cancer cell lines parallel the CD44(hi/) CD24(lo/-) stem cell phenotype in human breast cancer. *J Mammary Gland Biol Neoplasia.* 2010; 15(2):235–252.
- Bocker W, Moll R, Poremba C, et al. Common adult stem cells in the human breast give rise to glandular and myoepithelial cell lineages: a new cell biological concept. *Lab Invest.* 2002; 82:737–746.
- Bodemann BO, White MA. Ras GTPases and cancer: Linchpin support of the tumorigenic platform. *Nat Rev Cancer.* 2008; 8:133–140.
- Böing AN, van der Pol E, Grootemaat AE, et al. Single-step isolation of extracellular vesicles by size-exclusion chromatography. *J Extracell Vesicles.* 2014; 3:23430.
- Bongiovanni L, D'Andrea A, Porcellato I, et al. Canine cutaneous melanocytic tumours: significance of b-catenin and survivin immunohistochemical expression. *Vet Dermatol.* 2015; 26(4):270-e59.
- Brastianos PK, Carter SL, Santagata S, et al. Abstract: Genomic characterization of 101 brain metastases and paired primary tumors reveals patterns of clonal evolution and selection of driver mutations. AACR. San Diego, 2014.
- Brunetti B, Asproni P, Beha G, et al. Molecular phenotype in mammary tumors of queens: correlation between primary tumour and lymph node metastasis. *J Comp Pathol.* 2013; 148(2-3):206-213.
- Bubici C, Papa S. JNK signalling in cancer: in need of new, smarter therapeutic targets. *Br J Pharmacol.* 2014; 171:24–37.
- Buess M, Rajski M, Vogel-Durrer BM, Herrmann R, Rochlitz C. Tumor-endothelial interaction links the CD44(+)/CD24(-) phenotype with poor prognosis in early-stage breast cancer. *Neoplasia.* 2009; 11(10):987-1002.
- Burnett RM, Craven KE, Krishnamurthy P, et al. Organ-specific adaptive signaling pathway activation in metastatic breast cancer cells. *Oncotarget.* 2015; 6:12682-12696.
- Caliari D, Zappulli V, Rasotto R et al. Triple-negative vimentin-positive heterogeneous feline mammary carcinomas as a potential comparative model for breast cancer. *BMC Vet Res.* 2014; 10:185.
- Camerlingo R, Ferraro GA, De Francesco F. The role of CD44+/CD24-/low biomarker for screening, diagnosis and monitoring of breast cancer. *Oncol Rep.* 2014; 31(3):1127-1132.
- Campbell LL, Polyak K. Breast tumor heterogeneity: cancer stem cells or clonal evolution? *Cell Cycle* 2007; 6(19):2332–2338.
- Cantin R, Diou J, Bélanger D, Tremblay AM, Gilbert C. Discrimination between exosomes and HIV-1: Purification of both vesicles from cell-free supernatants. *J Immunol Methods.* 2008; 338(1-2):21–30.
- Cantrell MA, Ebel ND, Pfefferle AD, Perou CM, Van Den Berg CL. c-Jun N-terminal kinase 2 prevents luminal cell commitment in normal mammary glands and tumors by inhibiting p53/Notch1 and breast cancer gene 1 expression. *Oncotarget.* 2015; 6:11863–11881.
- Carayon K, Chaoui K, Ronzier E, et al. Proteolipidic composition of exosomes changes during reticulocyte maturation. *J Biol Chem.* 2011; 286:34426–34439.
- Carr J, Williams DG, Hayden TR. Molecular detection of multiple respiratory viruses in molecular diagnostics. 2010. Pp. 289-300.

- Catteau X, Simon P, Vanhaeverbeek M, Noël JC. Variable stromal periductular expression of CD34 and smooth muscle actin (SMA) in intraductal carcinoma of the breast. *PLoS One*. 2013; 8(3):e57773.
- Cellurale C, Weston CR, Reilly J, et al. Role of JNK in a Trp53-dependent mouse model of breast cancer. *PLoS One*. 2010; 5:e12469.
- Chan SW, Lim CJ, Chen L, et al. The Hippo pathway in biological control and cancer development. *J Cell Physiol*. 2011; 226:928–939.
- Chang JC. Cancer stem cells: Role in tumor growth, recurrence, metastasis, and treatment resistance. *Medicine (Baltimore)*. 2016; 95(Suppl 1):S20-S25.
- Charafe-Jauffret E, Ginestier C, Iovino F, et al. Aldehyde dehydrogenase 1-positive cancer stem cells mediate metastasis and poor clinical outcome in inflammatory breast cancer. *Clin Cancer Res*. 2010; 16(1):45–55.
- Chen CH, Shen J, Lee WJ, Chow SN. Overexpression of cyclin D1 and c-Myc gene products in human primary epithelial ovarian cancer. *Int J Gynecol Cancer*. 2005; 15:878–83.
- Cheng CW, Liu YF, Yu JC, et al. Prognostic Significance of cyclin D1, β -catenin, and MTA1 in patients with invasive ductal carcinoma of the breast. *Ann Surg Oncol*. 2012; 19(13):4129–4139.
- Chen DS, Mellman I. Oncology Meets Immunology: The Cancer-Immunity Cycle. *Immunity*. 2013; 39:1-10.
- Chen K, Zhao H, Hu Z, et al. CASP3 polymorphisms and risk of squamous cell carcinoma of the head and neck. *Clin Cancer Res*. 2008; 14:6343–6349.
- Chen N, Nomura M, She QB, et al. Suppression of skin tumorigenesis in c-Jun NH(2)-terminal kinase-2-deficient mice. *Cancer Res*. 2001; 61:3908–3912.
- Chen P, O'Neal JF, Ebel ND, et al. Jnk2 effects on tumor development, genetic instability and replicative stress in an oncogene-driven mouse mammary tumor model. *PLoS One*. 2010; 5:e10443.
- Cheng H, Liang H, Qin Y, Liu Y. Nuclear β -catenin overexpression in metastatic sentinel lymph node is associated with synchronous liver metastasis in colorectal cancer. *Diagn Pathol*. 2011; 6:109.
- Cheng L, Sun X, Scicluna BJ, et al. Characterization and deep sequencing analysis of exosomal and non-exosomal miRNA in human urine. *Kidney Int*. 2014; 86(2):433-444.
- Cheng YJ, Lee CH, Lin YP. Caspase-3 enhances lung metastasis and cell migration in a protease-independent mechanism through the ERK pathway. *Int J Cancer*. 2008; 123(6):1278-1285.
- Chia S, Norris B, Speers C, et al. Human epidermal growth factor receptor 2 overexpression as a prognostic factor in a large tissue microarray series of node-negative breast cancers. *J Clin Oncol*. 2008; 26(35): 5697-5704.
- Chiou SH, Wang ML, Chou YT, et al. Coexpression of Oct4 and Nanog enhances malignancy in lung adenocarcinoma by inducing cancer stem cell-like properties and epithelial-mesenchymal transdifferentiation. *Cancer Res*. 2010; 70(24):10433–10444.
- Christianson HC, Svensson KJ, Belting M. Seminars in Cancer Biology Exosome and microvesicle mediated phen transfer in mammalian cells. *Semin Cancer Biol*. 2014; 28:31–38 (2014).
- Chunthapong J, Seftor EA, Khalkhali-Ellis Z, et al. Dual roles of E-cadherin in prostate cancer invasion. *J Cell Biochem*. 2004; 91(4):649–661.
- Cizmar P, Yuana Y. Detection and Characterization of Extracellular Vesicles by Transmission and Cryo-Transmission Electron Microscopy. *Methods Mol Biol*. 2017; 1660:221–232.
- Clarke RB, Anderson E, Howell A, Potten CS. Regulation of human breast epithelial stem cells. *Cell Prolif*. 2003; 1:45-58.

- Clevers H. The cancer stem cell: premises, promises and challenges. *Nat Med.* 2011; 17:313–319.
- Cocola C, Anastasi P, Astigliano S, et al. Isolation of canine mammary cells with stem cell properties and tumour-initiating potential. *Reprod Domest Anim.* 2009; 2:214–217.
- Cocucci E, Meldolesi J. Ectosomes and exosomes: Shedding the confusion between extracellular vesicles. *Trends Cell Biol.* 2015; 25:364–372.
- Collins LC, Schnitt SJ. Breast. In: Mills SE, ed. *Histology for Pathologists.* 3rd ed. Philadelphia, PA: Lippincott Williams & Wilkins; 2007:57–71.
- Colombo M, Raposo G, Théry C. Biogenesis, Secretion, and Intercellular Interactions of Exosomes and Other Extracellular Vesicles. *Annu Rev Cell Dev Biol.* 2014; 30:255–289.
- Côme C, Magnino F, Bibeau F, et al. Snail and slug play distinct roles during breast carcinoma progression. *Clin Cancer Res.* 2006; 12:5395–5402.
- Comijn J, Berx G, Vermassen P, et al. The two-handed E box binding zinc finger protein SIP1 downregulates E-cadherin and induces invasion. *Mol Cell.* 2001; 7:1267–1278.
- Cordenonsi M, Zanconato F, Azzolin L, et al. The Hippo transducer TAZ confers cancer stem cell-related traits on breast cancer cells. *Cell.* 2011; 147:759–772.
- Crabtree JS, Miele L. Breast cancer stem cells. *Biomedicines.* 2018; 6(3). pii: E77.
- Craig DW, O'Shaughnessy JA, Kiefer JA, et al. Genome and transcriptome sequencing in prospective metastatic triple-negative breast cancer uncovers therapeutic vulnerabilities. *Mol Cancer Ther.* 2013; 12:104–16.
- Crescitelli R, Lässer C, Szabo TG, et al. Distinct RNA profiles in subpopulations of extracellular vesicles: apoptotic bodies, microvesicles and exosomes. *J Extracell vesicles.* 2013; 2:1–10.
- Croce JC, McClay DR. Evolution of the Wnt pathways. *Methods Mol Biol.* 2009; 469:3–18.
- Croker AK, Goodale D, Chu J, et al. High aldehyde dehydrogenase and expression of cancer stem cell markers selects for breast cancer cells with enhanced malignant and metastatic ability. *J Cell Mol Med.* 2009; 13(8B):2236–2252.
- Cui J, Han SY, Wang C, et al. c-Jun NH(2)-terminal kinase 2alpha2 promotes the tumorigenicity of human glioblastoma cells. *Cancer Res.* 2006; 66:10024–10031.
- da Silveira JC, Veeramachaneni DNR, Winger QA, Carnevale EM, Gerrit J. Cell-Secreted Vesicles in Equine Ovarian Follicular Fluid Contain miRNAs and Proteins: A Possible New Form of Cell Communication Within the Ovarian Follicle. *Biol Reprod.* 2012; 86:1–10.
- Damasceno KA, Ferreira E, Estrela-Lima A, et al. Relationship between the expression of versican and EGFR, HER-2, HER-3 and CD44 in matrix-producing tumours in the canine mammary gland. *Histol Histopathol.* 2016; 31(6):675–688.
- Daphu I, Sundstrøm T, Horn S, et al. In vivo animal models for studying brain metastasis: value and limitations. *Clin Exp Metastasis.* 2013; 30(5):695–710.
- de Araújo MR, Campos LC, Ferreira E, Cassali GD. Quantitation of the regional lymph node metastatic burden and prognosis in malignant mammary tumors of dogs. *J Vet Intern Med.* 2015; 29(5):1360–1367.
- de las Mulas JM, Reymundo C, de los Monteros AE, Millán Y, Ordás J. Calponin expression and myoepithelial cell differentiation in canine, feline and human mammary simple carcinomas. *Vet Comp Oncol.* 2004; 2(1):24–35.

- de Menezes-Neto A, Saez MJ, Lozano-Ramos I, et al. Size-exclusion chromatography as a stand-alone methodology identifies novel markers in mass spectrometry analyses of plasma-derived vesicles from healthy individuals. *J Extracell Vesicles*. 2015; 4:27378.
- Debus E, Moll R, Franke WW, Weber K, Osborn M. Immunohistochemical distinction of human carcinomas by cytokeratin typing with monoclonal antibodies. *Am J Pathol*. 1984; 114:121–130.
- Dellmann HD, Carithers JR. Special epidermal structures. In: Goldner B (ed.), *Cytology and Microscopic Anatomy*. 1996. Williams & Wilkins, Media, USA, pp. 338–340.
- Destexhe E, Lespagnard L, Degeyter M, et al. Immunohistochemical identification of myoepithelial, epithelial, and connectivetissue cells in canine mammary-tumors. *Vet Pathol*. 1993; 30:146–154.
- Deugnier MA, Teulière J, Faraldo MM, Thiery JP, Glukhova MA. The importance of being myoepithelial cell. *Breast Cancer Res*. 2002; 4:224–230.
- Devarajan E, Sahin AA, Chen JS, et al. Down-regulation of caspase 3 in breast cancer: a possible mechanism for chemoresistance. *Oncogene*. 2002; 21:8843–8851.
- Di Vizio D, Morello M, Dudley AC, et al. Large oncosomes in human prostate cancer tissues and in the circulation of mice with metastatic disease. *Am J Pathol*. 2012; 181:1573–1584.
- Díaz VM, de Herreros AG. F-box proteins: keeping the epithelial-to-mesenchymal transition (EMT) in check. *Semin Cancer Biol*. 2016; 36:71–79.
- Díaz VM, Viñas-Castells R, de Herreros AG Regulation of the protein stability of EMT transcription factors. *Cell Adh Migr*. 2014; 8:418–428.
- Diaz-Martin J, Lopez-Garcia MA, Romero-Perez L, et al. Nuclear TAZ expression associates with the triple-negative phenotype in breast cancer. *Endocr Relat Cancer*. 2015; 22(3):443-454.
- Dong C, Wu Y, Yao J, et al. G9a interacts with Snail and is critical for Snail-mediated E-cadherin repression in human breast cancer. *J Clin Invest*. 2012; 122(4):1469–148.
- Dong J, Feldmann G, Huang J, et al. Elucidation of a universal size-control mechanism in Drosophila and mammals. *Cell*. 2007; 130:1120–1133.
- Donoghue S, Baden HS, Lauder I, Sobolewski S, Pringle JH. Immunohistochemical localization of caspase-3 correlates with clinical outcome in B-cell diffuse large-cell lymphoma. *Cancer Res*. 1999; 59:5386–5391.
- Dontu G, Abdallah WM, Foley JM, et al. In vitro propagation and transcriptional profiling of human mammary stem/progenitor cells. *Genes Dev*. 2003; 17(10):1253–1270.
- Dontu G, Al-Hajj M, Abdallah WM, Clarke MF, Wicha MS. Stem cells in normal breast development and breast cancer. *Cell Prolif*. 2003; 1:59-72.
- Dontu G, Jackson KW, McNicholas E, et al. Role of Notch signaling in cell-fate determination of human mammary stem/progenitor cells. *Breast Cancer Res*. 2004; 6(6):R605–R615.
- Doornebal CW, Klarenbeek S, Braumuller TM, et al. A preclinical mouse model of invasive lobular breast cancer metastasis. *Cancer Res*. 2013; 73(1):353-363.
- Dragovic RA, Gardiner C, Brooks AS, et al. Sizing and phenotyping of cellular vesicles using Nanoparticle Tracking Analysis. *Nanomedicine*. 2011; 7(6):780–788.
- Dunnwald LK, Rossing MA, Li CI. Hormone receptor status, tumor characteristics, and prognosis: a prospective cohort of breast cancer patients. *Breast Cancer Res*. 2007; 9(1):R6.
- Dupont S, Morsut L, Aragona M, et al. Role of YAP/TAZ in mechanotransduction. *Nature*. 2011; 474(1): 179–183.

- Eger A, Aigner K, Sonderegger S, et al. DeltaEF1 is a transcriptional repressor of E-cadherin and regulates epithelial plasticity in breast cancer cells. *Oncogene*. 2005; 24:2375-2385.
- El Andaloussi S, Mäger I, Breakefield XO, Wood MJA. Extracellular vesicles: Biology and emerging therapeutic opportunities. *Nat Rev Drug Discov*. 2013; 12:347–357.
- Espinosa de Los Monteros A, Fernandez A, Milan MY, et al. Coordinate expression of Cytokeratins 7 and 20 in feline and canine carcinomas. *Vet Pathol*. 1999; 36(3):179-190.
- Espinosa de los Monteros A, Millan MY, Ramirez GA, et al. Expression of maspin in mammary gland tumors of the dog. *Vet Pathol*. 2005; 42:250–257.
- Espinosa de los Monteros A, Millan MY, Ordas J, et al. Immunolocalization of the smooth muscle-specific protein calponin in complex and mixed tumors of the mammary gland of the dog: assessment of the morphogenetic role of the myoepithelium. *Vet Pathol*. 2002; 39:247–256.
- Fan R, Kim NG, Gumbiner BM. Regulation of Hippo pathway by mitogenic growth factors via phosphoinositide 3-kinase and phosphoinositide-dependent kinase-1. *Proc Natl Acad Sci USA*. 2013; 110:2569–2574.
- Fang D, Nguyen TK, Leishear K, et al. A tumorigenic subpopulation with stem cell properties in melanomas. *Cancer Res*. 2005; 65:9328-9337.
- Ferlay J, Colombet M, Soerjomataram I, et al. Cancer incidence and mortality patterns in Europe: Estimates for 40 countries and 25 major cancers in 2018. *Eur J Cancer*. 2018; pii: S0959-8049(18)30955-9
- Fidler IJ, Gersten DM, Hart IR. The biology of cancer invasion and metastasis. *Adv Cancer Res*. 1978; 28:149-250.
- Fidler IJ, Kim SJ and Langley RR: The role of the organ microenvironment in the biology and therapy of cancer metastasis. *J Cell Biochem*. 2007; 101:927-936.
- Fidler IJ, Yano S, Zhang R, Fujimaki T, Bucana CD. The seed and soil hypothesis: vascularisation and brain metastases. *Lancet Oncol*. 2002; 3(1):53–57.
- Fidler IJ. Metastasis: quantitative analysis of distribution and fate of tumor emboli labeled with 125I-5-iodo-2'-deoxyuridine. *J Natl Cancer Inst*. 1970; 45:773-782.
- Fidler IJ. The pathogenesis of cancer metastasis: the "seed and soil" hypothesis revisited. *Nat Rev Cancer*. 2003; 3(6):453-458.
- Fidler IJ. The relationship of embolic homogeneity, number, size and viability to the incidence of experimental metastasis. *Eur J Cancer*. 1973; 9:223-227.
- Florio T, Barbieri F, Spaziante R, et al. Efficacy of a dopamine-somatostatin chimeric molecule, BIM-23A760, in the control of cell growth from primary cultures of human non-functioning pituitary adenomas: a multi-center study. *Endocr Relat Cancer*. 2008; 15(2):583–596.
- Friedl P, Wolf K. Tube travel: the role of proteases in individual and collective cancer cell invasion. *Cancer Res*. 2008; 68:7247-7249.
- Friedrichs K, Ruiz P, Franke F, et al. High expression level of alpha 6 integrin in human breast carcinoma is correlated with reduced survival. *Cancer Res*. 1995; 55(1):901–906.
- Fu V, Plouffe SW, Guan KL. The Hippo pathway in organ development, homeostasis, and regeneration. *Curr Opin Cell Biol*. 2018; 49:99–107.
- Fu YZ, Yan YY, He M, et al. Salinomycin induces selective cytotoxicity to MCF-7 mammosphere cells through targeting the Hedgehog signaling pathway. *Oncol Rep*. 2016; 35(2):912-922.

- Fujimoto A, Neo S, Ishizuka C, et al. Identification of cell surface antigen expression in canine hepatocellular carcinoma cell lines. *J Vet Med Sci.* 2013; 75(6):831-835.
- Fumagalli D, Wilson TR, Salgado R, et al. Somatic mutation, copy number and transcriptomic profiles of primary and matched metastatic estrogen receptor-positive breast cancers. *Ann Oncol.* 2016; 27:1860–6.
- Gama A, Alves A, Gartner F, Schmitt F. p63: a novel myoepithelial cell marker in canine mammary tissues. *Vet Pathol.* 2003; 40(4):412–420.
- Gama A, Alves A, Schmitt F. Identification of molecular phenotypes in canine mammary carcinomas with clinical implications: application of the human classification. *Virchows Arch.* 2008; 453:123–132.
- Gama A, Gartner F, Alves A, et al. Immunohistochemical expression of epidermal growth factor receptor (EGFR) in canine mammary tissues. *Res Vet Sci.* 2009; 87:432–437.
- Gama A, Paredes J, Albergaria A, et al. P-cadherin expression in canine mammary tissues. *J Comp Pathol.* 2004; 130:13–20.
- Gardiner C, Di Vizio D, Sahoo S, et al. Techniques used for the isolation and characterization of extracellular vesicles: results of a worldwide survey. *J Extracell Vesicles.* 2016; 5:32945.
- Gast CE, Shaw AK, Wong MH, Coussens LM. Surgical procedures and methodology for a preclinical murine model of de novo mammary cancer metastasis. *J Vis Exp.* 2017; (125).
- Geiger TR, Peeper DS. Metastasis mechanisms. *Biochim Biophys Acta.* 2009; 1796:293-308.
- Geng SQ, Alexandrou AT, Li JJ. Breast cancer stem cells: Multiple capacities in tumor metastasis. *Cancer Lett.* 2014; 349(1):1-7.
- Geradts J, de Herrerros AG, Su Z, et al. Nuclear SNAIL1 and nuclear ZEB1 protein expression in invasive and intraductal human breast carcinomas. *Hum Pathol.* 2011; 42(8):1125-1131.
- Geyer FC, Lacroix-Triki M, Savage K, et al. B-Catenin pathway activation in breast cancer is associated with triple-negative phenotype but not with CTNNB1 mutation. *Mod Pathol.* 2011; 24(2):209-231.
- Ginestier C, Hur MH, Charafe-Jauffret E, et al. ALDH1 is a marker of normal and malignant human mammary stem cells and a predictor of poor clinical outcome. *Cell Stem Cell.* 2007; 1(5):555–567
- Giuliano A, Swift R, Arthurs C. Quantitative expression and co-localization of Wnt signaling related proteins in feline squamous cell carcinoma. *PLoS One.* 2016; 11(8):e0161103.
- Giusti I, Delle Monache S, Di Francesco M, et al. From glioblastoma to endothelial cells through extracellular vesicles: messages for angiogenesis. *Tumor Biol.* 2016; 37:12743-12753.
- Gjerdrum C, Tiron C, Hoiby T, et al. Axl is an essential epithelial-to-mesenchymal transition-induced regulator of breast cancer metastasis and patient survival. *Proc Natl Acad Sci USA.* 2010; 107(3):1124–1129.
- Gordon MD, Nusse R. Wnt signaling: multiple pathways, multiple receptors, and multiple transcription factors. *J Biol Chem.* 2006; 281(32):22429–22433.
- Green KJ, Bohringer M, Gocken T, Jones JC. Intermediate filament associated proteins. *Adv Protein Chem.* 2005; 70:143-202.
- Griffey SM, Madewell BR, Dairkee SH, et al. Immunohistochemical reactivity of basal and luminal epithelium-specific cytokeratin antibodies within normal and neoplastic canine mammary-glands. *Vet Pathol.* 1993; 30:155–161.
- Guescini M, Genedani S, Stocchi V, Agnati LF. Astrocytes and Glioblastoma cells release exosomes carrying mtDNA. *J Neural Transm.* 2010; 117:1–4.

- Guillemette S, Rico C, Godin P, Boerboom D, Paquet M. In vitro validation of the hippo pathway as a pharmacological target for canine mammary gland tumors. *J Mammary Gland Biol Neoplasia*. 2017; 22(3):203-214.
- Gumbiner BM, Kim NG. The Hippo-YAP signaling pathway and contact inhibition of growth. *J Cell Sci*. 2014; 127(Pt 4):709–717.
- Guo W, Keckesova Z, Donaher JL, et al. Slug and Sox9 cooperatively determine the mammary stem cell state. *Cell*. 2012; 148(5):1015–1028.
- Guo W. Concise review: breast cancer stem cells: regulatory networks, stem cell niches, and disease relevance. *Stem Cells Transl Med*. 2014; 3(8):942-948.
- Gupta GP, Nguyen DX, Chiang AC, et al. Mediators of vascular remodeling co-opted for sequential steps in lung metastasis. *Nature*. 2007; 446(7137):765–770.
- György B, Szabó TG, Pásztói M, et al. Membrane vesicles, current state-of-the-art: Emerging role of extracellular vesicles. *Cell Mol Life Sci*. 2011; 68:2667–2688.
- Hahn KA, Adams WH. Feline mammary neoplasia: biological behavior, diagnosis, and treatment alternatives. *Feline Pract*. 1977; 25:5–11.
- Hahn KA, Bravo L, Avenelli JS. Feline breast carcinoma as a pathologic and therapeutic model for human breast cancer. *In Vivo*. 1994; 8:825–828.
- Hajra KM, Chen DY and Fearon ER. The SLUG zinc-finger protein represses E-cadherin in breast cancer. *Cancer Res*. 2002; 62:1613-1618.
- Han JI, Kim DY, Na KL. Dysregulation of the Wnt/ β -Catenin signaling pathway in canine cutaneous melanotic tumor. *Vet Pathol*. 2010; 47(2): 285-291.
- Han SX, Bai E, Jin GH, et al. Expression and clinical significance of YAP, TAZ, and AREG in hepatocellular carcinoma. *J Immunol Res*. 2014; 2014:261365.
- Han X, Fang X, Lou X, et al. Silencing SOX2 induced mesenchymal-epithelial transition and its expression predicts liver and lymph node metastasis of CRC patients. *PLoS One*. 2012; 7:e41335.
- Harvey KF, Zhang X, Thomas DM. The Hippo pathway and human cancer. *Nat Rev Cancer*. 2013; 13:246–257.
- Hayden DW, Barnes DM, Johnson KH. Morphologic changes in the mammary gland of megestrol acetate-treated and untreated cats: a retrospective study. *Vet Pathol*. 1989; 26:104–113.
- Hebbard L, Steffen A, Zawadzki V, et al. CD44 expression and regulation during mammary gland development and function. *J Cell Sci*. 2000; 113:2619-2630.
- Heijnen BHFG, Schiel AE, Fijnheer R, Geuze HJ, Sixma JJ. Activated Platelets Release Two Types of Membrane Vesicles. *Blood J*. 1999; 94:3791–3800.
- Heijnen HF, Schiel AE, Fijnheer R, Geuze HJ, Sixma JJ. Activated platelets release two types of membrane vesicles: Microvesicles by surface shedding and exosomes derived from exocytosis of multivesicular bodies and alpha-granules. *Blood*. 1999; 94:3791–3799.
- Hellmen E, Lindgren A. The expression of intermediate filaments in canine mammary-glands and their tumors. *Vet Pathol*. 1989; 26:420–428.
- Hemalatha A, Suresh TN, Kumar ML. Expression of vimentin in breast carcinoma, its correlation with Ki67 and other histopathological parameters. *Indian J Cancer*. 2013; 50(3):189–194.
- Herrlich P, Morrison H, Sleeman J, et al. CD44 acts both as a growth- and invasiveness-promoting molecule and

- as a tumor-suppressing cofactor. *Ann N Y Acad Sci.* 2000; 910:106-120.
- Hong D, Fritz AJ, Zaidi SK, et al. Epithelial-to-mesenchymal transition and cancer stem cells contribute to breast cancer heterogeneity. *J Cell Physiol.* 2018. In press.
- Hong JH, Hwang ES, McManus MT, et al. TAZ, a transcriptional modulator of mesenchymal stem cell differentiation. *Science.* 2005; 309:1074–1078.
- Hong W, Guan KL. The YAP and TAZ transcription co-activators: Key downstream effectors of the mammalian Hippo pathway. *Semin Cell Dev Biol.* 2012; 23(7):785–793.
- Hosgood HD 3rd, Baris D, Zhang Y, et al. Caspase polymorphisms and genetic susceptibility to multiple myeloma. *Hematol Oncol.* 2008; 26:148–151.
- Howe LR, Brown AM. *Wnt signaling and breast cancer. Cancer Biol Ther.* 2004; 3(1):36–41.
- Huang Q, Li F, Liu X, et al. Caspase 3-mediated stimulation of tumor cell repopulation during cancer radiotherapy. *Nat Med.* 2011; 17:860–866.
- Huang SF, Cheng SD, Chuang WY, et al. Cyclin D1 overexpression and poor clinical outcomes in Taiwanese oral cavity squamous cell carcinoma. *World J Surg Oncol.* 2012; 10:40.
- Huang X, Yuan T, Tschannen M, et al. Characterization of human plasma-derived exosomal RNAs by deep sequencing. *BMC Genom.* 2013; 14:319.
- Hunter KW, Crawford NP and Alsarraj J. Mechanisms of metastasis. *Breast Cancer Res.* 2008; 10(Suppl 1):S2.
- Hwang MS, Yu N, Stinson SY, et al. miR-221/222 targets adiponectin receptor 1 to promote the epithelial-to-mesenchymal transition in breast cancer. *PLoS One.* 2013; 8(6):e66502.
- Im KS, Kim JH, Kim NH. Possible role of snail expression as a prognostic factor in canine mammary neoplasia. *J Comp Pathol.* 2012; 147(2-3):121-128.
- Imielinski M, Berger AH, Hammerman PS, et al. Mapping the hallmarks of lung adenocarcinoma with massively parallel sequencing. *Cell.* 2012; 150:1107–1120.
- Incassati A, Chandramouli A, Eelkema R, Cowin P. Key signaling nodes in mammary gland development and cancer: beta-catenin. *Breast Cancer Res.* 2010; 12(6):213.
- Isenmann S, Arthur A, Zannettino AC, et al. TWIST family of basic helix-loop-helix transcription factors mediate human mesenchymal stem cell growth and commitment. *Stem Cells.* 2009; 27:2457–2468.
- Jang GB, Kim JY, Cho SD, et al. Blockade of Wnt/beta-catenin signaling suppresses breast cancer metastasis by inhibiting CSC-like phenotype. *Sci Rep.* 2015; 5:12465.
- Jänicke RU. MCF-7 breast carcinoma cells do not express caspase-3. *Breast Cancer Res Treat.* 2009; 117(1):219-221.
- Jemal A, Bray F, Center MM, et al. Global cancer statistics. *CA Cancer J Clin.* 2011; 61:69-90.
- Jeong GO, Shin SH, Seo EJ, et al. TAZ mediates lysophosphatidic acid-induced migration and proliferation of epithelial ovarian cancer cells. *Cell Physiol Biochem.* 2013; 32:253–263.
- Jia S, Zocco D, Samuels ML, et al. Emerging technologies in extracellular vesicle-based molecular diagnostics. *Expert Rev Mol Diagn.* 2014; 14:307-321.
- Jiang W, Hiscox S. beta-catenin-cell adhesion and beyond (review). *Int J Oncol.* 1997; 11:635–641.

- Johnson R, Halder G. The two faces of Hippo: Targeting the Hippo pathway for regenerative medicine and cancer treatment. *Nat Rev Drug Discov.* 2014; 13(1): 63–79.
- Johnstone RM, Bianchini A, Teng K. Reticulocyte Maturation and exosomes release: transferrin receptor containing exosomes shows multiple plasma membrane functions. *Blood.* 1989; 74:1844–1851.
- Jonges LE, Nagelkerke JF, Ensink NG, et al. Caspase-3 activity as a prognostic factor in colorectal carcinoma. *Lab Invest.* 2001; 81:681–688.
- Joyce JA, Pollard JW. Microenvironmental regulation of metastasis. *Nat Rev Cancer.* 2009; 9:239–252.
- Julien O, Wells JA. Caspases and their substrates. *Cell Death Differ.* 2017; 24(8):1380–1389.
- Justice RW, Zilian O, Woods DF, Noll M, Bryant PJ. The Drosophila tumor suppressor gene warts encodes a homolog of human myotonic dystrophy kinase and is required for the control of cell shape and proliferation. *Genes Dev.* 1995; 9(5):534–546.
- Kalra H, Simpson RJ, Ji H, et al. Vesiclepedia: a compendium for extracellular vesicles with continuous community annotation. *PLoS Biol.* 2012; 10(12):e1001450.
- Kang Y, Siegel PM, Shu W, et al. A multigenic program mediating breast cancer metastasis to bone. *Cancer Cell.* 2003; 3(6):537–549.
- Ke H, Harris R, Coloff JL, et al. The c-Jun NH2-terminal kinase 2 plays a dominant role in human epidermal neoplasia. *Cancer Res.* 2010; 70:3080–3088.
- Keller S, König AK, Marmé F, et al. Systemic presence and tumor-growth promoting effect of ovarian carcinoma released exosomes. *Cancer Lett.* 2009; 278:73–81.
- Kerbel RS. A decade of experience in developing preclinical models of advanced- or early-stage spontaneous metastasis to study antiangiogenic drugs, metronomic chemotherapy, and the tumor microenvironment. *Cancer J.* 2015; 21(4):274–283.
- Khoursheed MA, Mathew TC, Makar RR, et al. Expression of E-cadherin in human colorectal cancer. *Surgeon.* 2003; 1(2):86–91.
- Khramtsov AI, Khramtsova GF, Tretiakova M, et al. Wnt/b-catenin pathway activation is enriched in basal-like breast cancers and predicts poor outcome. *Am J Pathol.* 2010; 176(6):2911–2920.
- Kim D-K, Kang B, Kim OY, et al. EVpedia: an integrated database of high-throughput data for systemic analyses of extracellular vesicles. *J Extracell Vesicles.* 2013; 2:1–7.
- Kim HS, Lee JW, Soung YH, et al. Inactivating mutations of caspase-8 gene in colorectal carcinomas. *Gastroenterology.* 2003; 125(3):708–715.
- Klopfleisch R, Gruber AD. Increased expression of BRCA2 and RAD51 in lymph node metastases of canine mammary adenocarcinomas. *Vet Pathol.* 2009; 46(3):416–422.
- Klopfleisch R, Lenze D, Hummel M, Gruber AD. The metastatic cascade is reflected in the transcriptome of metastatic canine mammary carcinomas. *Vet J.* 2011; 190(2):236–243.
- Kobayashi T, Shimizu Y, Terada N, et al. Regulation of androgen receptor transactivity and mTOR-S6 kinase pathway by Rheb in prostate cancer cell proliferation. *Prostate.* 2010; 70:866–874.
- Kohn AD, Moon RT. Wnt and calcium signaling: b-catenin-independent pathways. *Cell Calcium.* 2005; 38(3):439–46.
- Kong D, Banerjee S, Ahmad A, et al. Epithelial to mesenchymal transition is mechanistically linked with stem cell signatures in prostate cancer cells. *PLoS One.* 2010; 5:e12445.

- Kong W, Jarvis C, Mackillop WJ. Estimating the need for palliative radiotherapy for brain metastasis: a benchmarking approach. *Clin Oncol (R Coll Radiol)*. 2015; 27(2):83-91.
- Kontomanolis E, Kalagasidou S, Pouliliou S, et al. The Notch pathway in breast cancer progression. *ScientificWorldJournal*. 2018; 2018:2415489.
- Kowalski PJ, Rubin MA, Kleer CG. E-cadherin expression in primary carcinomas of the breast and its distant metastases. *Breast Cancer Res*. 2003; 5(6):R217–R222.
- Krisnamurthy S, Poornima R, Challa VR, Goud YG. Triple Negative Breast Cancer - Our Experience and Review. *Indian J Surg Oncol*. 2012; 3(1):12-16.
- Kurokawa H, Nishio K, Fukumoto H, et al. Alteration of caspase-3 (CPP32/Yama/apopain) in wild-type MCF-7, breast cancer cells. *Oncol Rep*. 1999; 6:33–37.
- Lacroix M. Significance, detection and markers of disseminated breast cancer cells. *Endocr Relat Cancer*. 2006; 13:1033-1067.
- Lai CP, Kim EY, Badr CE, et al. Visualization and tracking of tumour extracellular vesicle delivery and RNA translation using multiplexed reporters. *Nat Commun*. 2015; 6:7029.
- Lakhani SR, Ellis IO, Schnitt SJ, et al. WHO classification of tumours of the breast. 4th edition. Lyon (France): International Agency for Research on Cancer (IARC) Press; 2012.
- Lamouille S, Xu J, Derynck R. Molecular mechanisms of epithelial–mesenchymal transition. *Nat Rev Mol Cell Biol*. 2014; 15(3):178–196.
- Lan Q, Morton LM, Armstrong B, et al. Genetic variation in caspase genes and risk of non-Hodgkin lymphoma: a pooled analysis of 3 population-based case-control studies. *Blood*. 2009; 114:264–267.
- Larue L and Bellacosa A. Epithelial mesenchymal transition in development and cancer: role of phosphatidylinositol 3' kinase/AKT pathways. *Oncogene*. 2005; 24:7443-7454.
- Lau AN, Curtis SJ, Fillmore CM, et al. Tumor-propagating cells and YAP/TAZ activity contribute to lung tumor progression and metastasis. *EMBO J*. 2014; 33:468–481.
- Lawrence MS, Stojanov P, Mermel CH, et al. Discovery and saturation analysis of cancer genes across 21 tumour types. *Nature*. 2014; 505(7484):495–501.
- Lawson C, Kovacs D, Finding E, Ulfelder E. Extracellular Vesicles: Evolutionarily Conserved Mediators of Intercellular Communication. *YALE J Biol Med*. 2017; 90:481–491.
- Li CCY, Eaton SA, Young PE, et al. Glioma microvesicles carry selectively packaged coding and noncoding RNAs which alter gene expression in recipient cells. *RNA Biol*. 2013; 10:1333–1344.
- Li DM, Feng YM: Signaling mechanism of cell adhesion molecules in breast cancer metastasis: potential therapeutic targets. *Breast Cancer Res Treat*. 2011; 128:7-21.
- Li S, Shen D, Shao J, et al. Endocrine-therapy-resistant ESR1 variants revealed by genomic characterization of breast-cancer-derived xenografts. *Cell Rep*. 2013; 4:1116–30.
- Li Y, Zheng Q, Bao C, et al. Circular RNA is enriched and stable in exosomes: a promising biomarker for cancer diagnosis. *Cell Res*. 2015; 25(8):981-984.
- Liang K, Zhou G, Zhang Q, Li J, Zhang C. Expression of hippo pathway in colorectal cancer. *Saudi J Gastroenterol*. 2014; 20(3):188–194.

- Lim E, Vaillant F, Wu D, et al. Aberrant luminal progenitors as the candidate target population for basal tumor development in BRCA1 mutation carriers. *Nat Med*. 2009; 15:907–991.
- Lim KH, Baines AT, Fiordalisi JJ, et al. Activation of RalA is critical for Ras-induced tumorigenesis of human cells. *Cancer Cell*. 2005; 7:533–545.
- Lin NU, Claus E, Sohl J, et al. Sites of distant recurrence and clinical outcomes in patients with metastatic triple-negative breast cancer: high incidence of central nervous system metastases. *Cancer*. 2008; 113:2638-2645.
- Lin SY, Xia W, Wang JC, et al. Beta-catenin, a novel prognostic marker for breast cancer: its roles in cyclin D1 expression and cancer progression. *Proc Natl Acad Sci USA*. 2000; 97:4262–4266.
- Liu A, Feng B, Gu W, et al. The CD133+ subpopulation of the SW982 human synovial sarcoma cell line exhibits cancer stem-like characteristics. *Int J Oncol*. 2013a; 42:1399-1407.
- Liu J, Ma L, Xu J, et al. Spheroid body-forming cells in the human gastric cancer cell line MKN-45 possess cancer stem cell properties. *Int J Oncol*. 2013b; 42:453-459.
- Liu JB, Feng CY, Deng M, et al. E-cadherin expression phenotypes associated with molecular subtypes in invasive non-lobular breast cancer: evidence from a retrospective study and meta-analysis. *World J Surg Oncol*. 2017; 15(1):139.
- Liu S, Cong Y, Wang D, et al. Breast cancer stem cells transition between epithelial and mesenchymal states reflective of their normal counterparts. *Stem Cell Rep*. 2014; 2(1):78–91.
- Liu S, Wicha MS. Targeting breast cancer stem cells. *J Clin Oncol*. 2010; 28(25):4006-4012.
- Liu TJ, Sun BC, Zhao XL, et al. CD133+ cells with cancer stem cell characteristics associates with vasculogenic mimicry in triple-negative breast cancer. *Oncogene*. 2013; 32(1):544–553.
- Liu W, Moulay M, Willenbrock S. Comparative characterization of stem cell marker expression, metabolic activity and resistance to doxorubicin in adherent and spheroid cells derived from the canine prostate adenocarcinoma cell line CT1258. *Anticancer Res*. 2015; 35(4):1917-1927.
- Liu Y, El-Naggar S, Darling DS, Higashi Y, Dean DC. ZEB1 links epithelial-mesenchymal transition and cellular senescence. *Development*. 2008; 135(3):579–588.
- Llorente A, Skotland T, Sylvanne T, et al. Molecular lipidomics of exosomes released by PC-3 prostate cancer cells. *Biochim Biophys Acta*. 2013; 1831:1302–1309.
- Lombardo Y, de Giorgio A, Coombes CR, Stebbing J, Castellano L. Mammosphere formation assay from human breast cancer tissues and cell lines. *J Vis Exp*. 2015; (97).
- Lötvall J, Hill AF, Hochberg F, et al. Minimal experimental requirements for definition of extracellular vesicles and their functions: A position statement from the International Society for Extracellular Vesicles. *J Extracell Vesicles*. 2014; 3:26913.
- Lu ZH, Shvartsman MB, Lee AY, et al. Mammalian target of rapamycin activator RHEB is frequently overexpressed in human carcinomas and is critical and sufficient for skin epithelial carcinogenesis. *Cancer Res*. 2010; 70:3287–3298.
- Luo Y, Huang W, Zhang H, Liu G. Prognostic significance of CD117 expression and TP53 missense mutations in triple-negative breast cancer. *Oncol Lett*. 2018; 15(5):6161-6170.
- Lyzak JS, Yaremko ML, Recant W, et al. Role of CD44 in nonpalpable T1a and T1b breast cancer. *Hum Pathol*. 1997; 28:772–778.
- Maas SLN, Breakefield XO, Weaver AM. Extracellular Vesicles: Unique Intercellular Delivery Vehicles. *Trends Cell Biol*. 2017; 27:172–188.

- Maas SLN, de Vrij J, van der Vlist EJ, et al. Possibilities and limitations of current technologies for quantification of biological extracellular vesicles and synthetic mimics. *J Control Release*. 2014; 200:87–96.
- MacDonald BT, Tamai K, He X. Wnt/beta-catenin signaling: components, mechanisms, and diseases. *Dev Cell*. 2009; 17(1):9–26.
- MacEwen EG. Spontaneous tumors in dogs and cats: models for the study of cancer biology and treatment. *Cancer Metastasis Rev*. 1990; 9(2):125–136.
- Malhotra GK, Zhao X, Band H, Band V. Histological, molecular and functional subtypes of breast cancers. *Cancer Biol Ther*. 2010; 10:955–960.
- Martin TA, Ye L, Sanders AJ, et al. Cancer Invasion and Metastasis: Molecular and Cellular Perspective. In: Madame Curie Bioscience Database [Internet]. Austin (TX): Landes Bioscience; 2000-2013.
- Martz CA, Ottina KA, Singleton KR et al. Systematic identification of signaling pathways with potential to confer anticancer drug resistance. *Sci Signal*. 2014; 7(357):ra121.
- Marusyk A, Almendro V, Polyak K: Intra-tumour heterogeneity: a looking glass for cancer? *Nat Rev Cancer*. 2012, 12:323–334.
- Marusyk A, Polyak K. Tumor heterogeneity: causes and consequences. *Biochim Biophys Acta*. 2010; 1805(1):105–117.
- Maruyama K, MacLennan DH. Mutation of aspartic acid-351, lysine-352, and lysine-515 alters the Ca²⁺ transport activity of the Ca²⁺-ATPase expressed in COS-1 cells. *Proc Natl Acad Sci USA*. 1988; 85(10):3314-3318.
- Mathivanan S, Fahner CJ, Reid GE, Simpson RJ. ExoCarta 2012: database of exosomal proteins RNA and lipids. *Nucleic Acids Res*. 2012; 40(Database issue):D1241-D1244.
- Mathivanan S, Simpson RJ. ExoCarta: a compendium of exosomal proteins and RNA. *Proteomics*. 2009; 9:4997–5000.
- May CD, Sphyris N, Evans KW, et al. Epithelial-mesenchymal transition and cancer stem cells: a dangerously dynamic duo in breast cancer progression. *Breast Cancer Res*. 2011; 13(1):202.
- Meacham CE, Morrison SJ. Tumour heterogeneity and cancer cell plasticity. *Nature*. 2013;501(7467):328–337.
- Meyer MJ, Fleming JM, Lin AF, et al. CD44posCD49fhiCD133/2hi defines xenograft-initiating cells in estrogen receptor-negative breast cancer. *Cancer Res*. 2010; 70:4624-33.
- Michishita M, Akiyoshi R, Suemizu H, et al. Aldehyde dehydrogenase activity in cancer stem cells from canine mammary carcinoma cell lines. *Vet J*. 2012; 193(2):508-513.
- Michishita M, Akiyoshi R, Yoshimura H. Characterization of spheres derived from canine mammary gland adenocarcinoma cell lines. *Res Vet Sci*. 2011; 91(2):254-260.
- Michishita M, Ezaki S, Ogihara K, et al. Identification of tumor-initiating cells in a canine hepatocellular carcinoma cell line. *Res Vet Sci*. 2014; 96(2):315-322.
- Michishita M, Otsuka A, Nakahira R, et al. Flow cytometric analysis for detection of tumor-initiating cells in feline mammary carcinoma cell lines. *Vet Immunol Immunopathol*. 2013; 156(1-2):73-81.
- Millanta F, Calandrella M, Bari G, et al. Comparison of steroid receptor expression in normal, dysplastic, and neoplastic canine and feline mammary tissues. *Res Vet Sci*. 2005; 79: 225–232.
- Miller ME, Christensen GC, Evans HE, 1964. The mammary gland. *Anatomy of the Dog*. W.B. Saunders, Philadelphia, pp. 789–803.

- Minde DP, Radli M, Forneris F, Maurice MM, Rüdiger SG. Large extent of disorder in Adenomatous Polyposis Coli offers a strategy to guard Wnt signalling against point mutations. *PLoS ONE*. 2013; 8(10): e77257.
- Minn AJ, Kang Y, Serganova I, et al. Distinct organ-specific metastatic potential of individual breast cancer cells and primary tumors. *J Clin Invest*. 2005; 115:44-55.
- Misdorp W, Else RW, Hellme'n E, et al. Histological classification of mammary tumors of the dog and the cat. In: World Health Organization, ed. International Histological Classification of Tumors of Domestic Animals. Second ser. Vol 7. Washington, DC: Armed Forces Institute of Pathology, American Registry of Pathology; 1999:11–56.
- Misdorp W. Tumors of the mammary gland. In: Meuten DJ, ed. Tumors in Domestic Animals. Ames, Iowa: Iowa State Press; 2008: 575–606.
- Mittendorf EA, Philips AV, Meric-Bernstam F, et al. PD-L1 expression in triple-negative breast cancer. *Cancer Immunol Res*. 2014; 2:361-370.
- Mohseni M, Sun J, Lau A, et al. A genetic screen identifies an LKB1-MARK signalling axis controlling the Hippo-YAP pathway. *Nat Cell Biol*. 2014; 16:108–117.
- Moll R, Franke WW, Schiller DL, Geiger B, Krepler R. The catalog of human cytokeratins: patterns of expression in normal epithelia, tumors and cultured cells. *Cell*. 1982; 31:11–24.
- Monteiro J, Gaspar C, Richer W, et al. Cancer stemness in Wnt-driven mammary tumorigenesis. *Carcinogenesis*. 2014; 35:2–13.
- Montserrat N, Gallardo A, Escuin D, et al. Repression of E-cadherin by SNAIL, ZEB1, and TWIST in invasive ductal carcinomas of the breast: a cooperative effort? *Hum Pathol*. 2011; 42(1):103-110.
- Moody SE, Perez D, Pan TC, et al. The transcriptional repressor Snail promotes mammary tumor recurrence. *Cancer Cell*. 2005; 8:197-209.
- Morello M, Minciacchi VR, de Candia P. Large oncosomes mediate intercellular transfer of functional microRNA. *Cell Cycle*. 2013; 12(22):3526–3536.
- Moulay M, Liu W, Willenbrock S, et al. Evaluation of stem cell marker gene expression in canine prostate carcinoma- and prostate cyst-derived cell lines. *Anticancer Res*. 2013; 33(12):5421-5431.
- Nathoo N, Chahlavi A, Barnett G, Toms SA. Pathobiology of brain metastases. *J Clin Pathol*. 2005; 58(3):237–242.
- Nazimek K, Bryniarski K, Santocki M, Ptak W. Exosomes as mediators of intercellular communication: clinical implications. *Pol Arch Med Wewn*. 2015; 125(5):370-380.
- Nelson WJ, Nusse R. Convergence of Wnt, beta-catenin, and cadherin pathways. *Science*. 2004; 303(5663):1483–1487.
- Nickel R, Schummer A, Seiferle E. The anatomy of domestic animals. 1st Edition. Springer-Verlag Berlin Heidelberg GmbH.
- Nielsen SW. The malignancy of mammary tumors in cats. *Mod Vet Pract*. 1967; 33:245–252.
- Nielsen TO, Hsu FD, Jensen K, et al. Immunohistochemical and clinical characterization of the basal-like subtype of invasive breast carcinoma. *Clin Cancer Res*. 2004; 10:5367–5374.
- Nieto MA. The snail superfamily of zinc-finger transcription factors. *Nat Rev Mol Cell Biol*. 2002; 3(3):155–166.

- Niikura N, Hayashi N, Masuda N, et al. Treatment outcomes and prognostic factors for patients with brain metastases from breast cancer of each subtype: a multicenter retrospective analysis. *Breast Cancer Res Treat.* 2014; 147:103-112.
- Niikura N, Saji S, Tokuda Y, Iwata H. Brain metastases in breast cancer. *Jpn J Clin Oncol.* 2014; 44(12):1133-1140.
- Nishikata T, Ishikawa M, Matsuyama T, et al. Primary culture of breast cancer: A model system for epithelial-mesenchymal transition and cancer stem cells. *Anticancer Res.* 2013; 33(7):2867-2873.
- Nitta RT, Del Vecchio CA, Chu AH, et al. The role of the c-Jun N-terminal kinase 2-alpha-isoform in non-small cell lung carcinoma tumorigenesis. *Oncogene.* 2011; 30:234-244.
- Nogués L, Benito-Martin A, Hergueta-Redondo M, Peinado H. The influence of tumour-derived extracellular vesicles on local and distal metastatic dissemination. *Mol Aspects Med.* 2017; 60:15-26.
- Nolte T, Hoen ENM, Buermans HPJ, Waasdorp M, et al. Deep sequencing of RNA from immune cell-derived vesicles uncovers the selective incorporation of small non-coding RNA biotypes with potential regulatory functions. *Nucleic Acids Res.* 2012; 40:9272-9285.
- Nordin JZ, Lee Y, Vader P, et al. Ultrafiltration with size-exclusion liquid chromatography for high yield isolation of extracellular vesicles preserving intact biophysical and functional properties. *Nanomed.* 2015; 11:879-883.
- O'Donovan N, Crown J, Stunell H, et al. Caspase 3 in breast cancer. *Clin Cancer Res.* 2003; 9:738-742.
- Oakman C, Viale G, Di Leo A. Management of triple negative breast cancer. *Breast.* 2010; 19(5):312-321.
- Ogawa Y, Taketomi Y, Murakami M, et al. Small RNA transcriptomes of two types of exosomes in human whole saliva determined by next generation sequencing. *Biol Pharm Bull.* 2013; 36:66-75.
- Oglesbee BL. Blackwell's five-minute veterinary consult: small mammal, 2nd edition. John Wiley & Sons. 2011.
- Oleinik NV, Krupenko NI, Krupenko SA. Cooperation between JNK1 and JNK2 in activation of p53 apoptotic pathway. *Oncogene.* 2007; 26:7222-7230.
- Orozco AF, Lewis DE. Flow cytometric analysis of circulating microparticles in plasma. *Cytometry A.* 2010; 77:502-514.
- Paget S. The distribution of secondary growths in cancer of the breast. *Cancer Metastasis Rev.* 1989; 8:98-101.
- Palmieri D, Chambers A, Felding-Habermann B, Huang S, Steeg PS. The biology of metastasis to a sanctuary site. *Clin Cancer Res.* 2007; 13(6):1656-1662.
- Paltian V, Alldinger S, Baumgärtner W, Wohlsein P. Expression of CD44 in canine mammary tumors. *J Comp Pathol.* 2009; 141(4):237-247.
- Pan CW, Liu H, Zhao Y, et al. JNK2 downregulation promotes tumorigenesis and chemoresistance by decreasing p53 stability in bladder cancer. *Oncotarget.* 2016; 7(23):35119-35131.
- Pan D. The Hippo signaling pathway in development and cancer. *Dev Cell.* 2010; 19(4):491-505.
- Pang LY, Blacking TM, Else RW, et al. Feline mammary carcinoma stem cells are tumorigenic, radioresistant, chemoresistant and defective in activation of the ATM/p53 DNA damage pathway. *Vet J.* 2013; 196(3):414-423.
- Park SY, Gonen M, Kim HJ, Michor F, Polyak K. Cellular and genetic diversity in the progression of in situ human breast carcinomas to an invasive phenotype. *J Clin Invest.* 2010; 120(2):636-644.
- Pascucci L, Dall-Aglio C, Bazzucchi C, et al. Horse adipose-derived mesenchymal stromal cells constitutively

- produce membrane vesicles: a morphological study. *Histol Histopathol.* 2015; 30:549–557.
- Pascucci L, Alessandri G, Dall’Aglio C, et al. Membrane vesicles mediate pro-angiogenic activity of equine adipose-derived mesenchymal stromal cells. *Vet J.* 2014; 202:361–366.
- Payne SJ, Bowen RL, Jones JL, et al. Predictive markers in breast cancer—the present. *Histopathology.* 2008; 52:82–90.
- Pearlman M, Jeudy M, Chelmow D. Practice Bulletin Number 179: Breast Cancer Risk Assessment and Screening in Average-Risk Women. *Obstet Gynecol.* 2017; 130(1):e1-e16.
- Peinado H, Olmeda D, Cano A. Snail, Zeb and bHLH factors in tumour progression: an alliance against the epithelial phenotype. *Nat Rev Cancer.* 2007; 7:415-28.
- Peña L, Gama A, Goldschmidt MH, et al. Canine Mammary Tumors: A Review and Consensus of Standard Guidelines on Epithelial and Myoepithelial Phenotype Markers, HER2, and Hormone Receptor Assessment Using Immunohistochemistry. *Vet Pathol.* 2014; 51(1):127-145.
- Peng Y, Zhang X, Feng X, Fan X, Jin Z. The crosstalk between microRNAs and the Wnt/b-catenin signaling pathway in cancer. *Oncotarget.* 2017; 8(8):14089-14106.
- Pereira CT, Rahal SC, de Carvalho Balieiro JC, Ribeiro AA. Lymphatic drainage on healthy and neoplastic mammary glands in female dogs: can it really be altered? *Anat Histol Embryol.* 2003; 32(5): 282–290.
- Pettersson AT, Mejhert N, Jernas M, et al. Twist1 in Human White Adipose Tissue and Obesity. *J Clin Endocrinol Metab.* 2011; 96(1):133-141.
- Pham PV, Phan NL, Nguyen NT, et al. Differentiation of breast cancer stem cells by knockdown of CD44: Promising differentiation therapy. *J Transl Med.* 2011; 9: 209.
- Piccolo S, Cordenonsi M, Dupont S. Molecular pathways: YAP and TAZ take center stage in organ growth and tumorigenesis. *Clin Cancer Res.* 2013; 19(18):4925–4930.
- Piccolo S, Dupont S, Cordenonsi M. The biology of YAP/TAZ: hippo signaling and beyond. *Physiol Rev.* 2014; 94(4):1287-1312.
- Polyak K, Hu M. Do myoepithelial cells hold the key for breast tumor progression? *J Mammary Gland Biol Neoplasia.* 2005; 10:231–247.
- Polyak K. Breast cancer: Origins and evolution. *J Clin Invest.* 2007; 117(11):3155–3163.
- Ponti D, Costa A, Zaffaroni A, et al. Isolation and in vitro propagation of tumorigenic breast cancer cells with stem/progenitor cell properties. *Cancer Res.* 2005; 65(13): 5506-5511.
- Prasad CP, Gupta SD, Rath G, Ralhan R. Wnt signaling pathway in invasive ductal carcinoma of the breast: relationship between beta-catenin, dishevelled and cyclin D1 expression. *Oncology.* 2007; 73:112–117.
- Prat A, Parker JS, Karginova O, et al. Phenotypic and molecular characterization of the claudin-low intrinsic subtype of breast cancer. *Breast Cancer Res.* 2010; 12(5):R68.
- Provenzano E, Ulaner GA, Chin SF. Molecular classification of breast cancer. *PET Clin.* 2018; 13(3):325-338.
- Psaila B, Kaplan RN, Port ER, Lyden D. Priming the ‘soil’ for breast cancer metastasis: the pre-metastatic niche. *Breast Dis.* 2006; 26:65-74.
- Qiao GL, Song LN, Deng ZF, Chen Y, Ma Lj. Prognostic value of CD44v6 expression in breast cancer: a meta-analysis. *Onco Targets Ther.* 2018; 11:5451-5457.
- Qin H, Blaschke K, Wei G, Ohi Y, Blouin L, Qi Z, Yu J, et al. Transcriptional analysis of pluripotency reveals the

- Hippo pathway as a barrier to reprogramming. *Hum Mol Genet.* 2012; 21:2054–2067.
- Quan Y, Yan Y, Wang X, et al. Impact of cell dissociation on identification of breast cancer stem cells. *Cancer Biomark.* 2012-2013; 12(3):125-133.
- Rajendran L, Bali J, Barr MM, et al. Emerging roles of extracellular vesicles in the nervous system. *J Neurosci.* 2014; 34:15482–15489.
- Rak J, Guha A. Extracellular vesicles – vehicles that spread spread cancer genes. *Bioessay.* 2012; 34:489–497.
- Rakha EA, Reis-Filho JS, Baehner F, et al. Breast cancer prognostic classification in the molecular era: the role of histological grade. *Breast Cancer Res.* 2010; 12(4):207.
- Rakha EA, Reis-Filho JS, Ellis IO. Basal-like breast cancer: a critical review. *J Clin Oncol.* 2008; 26:2568–2581.
- Rasotto R, Caliarì D, Castagnaro M, Zanetti R, Zappulli V. An immunohistochemical study of HER-2 expression in feline mammary tumours. *J Comp Pathol.* 2011; 144(2-3):170-179.
- Reed JC. Mechanisms of apoptosis. *Am J Pathol.* 2000; 39:1415–1430.
- Regidor PA, Callies R, Regidor M, et al. Expression of the CD44 variant isoforms 6 and 4/5 in breast cancer. Correlation with established prognostic parameters. *Arch Gynecol Obstet.* 1996; 258(3):125-135.
- Reis-Filho JS, Tutt AN. Triple negative tumours: a critical review. *Histopathology.* 2008; 52:108–118.
- Restucci B, Maiolino P, Martano M, et al. Expression of β -catenin, E-cadherin and APC in canine mammary tumors. *Anticancer Res.* 2007; 27(5A):3083-3089.
- Reya T, Morrison SJ, Clarke MF, et al. Stem cells, cancer, and cancer stem cells. *Nature.* 2001; 414:105-11.
- Ricardo S, Vieira AF, Gerhard R. Breast cancer stem cell markers CD44, CD24 and ALDH1: expression distribution within intrinsic molecular subtype. *J Clin Pathol.* 2011; 64(11):937-946.
- Rico C, Boerboom D, Paquet M. Expression of the Hippo signalling effectors YAP and TAZ in canine mammary gland hyperplasia and malignant transformation of mammary tumours. *Vet Comp Oncol.* 2018. In press.
- Rismanchi S, Yadegar O, Muhammadnejad S, et al. Expression of vimentin filaments in canine malignant mammary gland tumors: a simulation of clinicopathological features of human breast cancer. *Biomed Rep.* 2014; 2(5):725–728.
- Rivera P, von Euler H. Molecular biological aspects of canine and human mammary tumours. *Vet Pathol.* 2011; 48(1):132-146.
- Robinson DR, Wu YM, Vats P, et al. Activating ESR1 mutations in hormone-resistant metastatic breast cancer. *Nat Genet.* 2013; 45:1446–51.
- Rout ED, Webb TL, Laurence HM, Long L, Olver CS. Transferrin receptor expression in serum exosomes as a marker of regenerative anaemia in the horse. *Equine Vet J.* 2015; 47:101–106.
- Roy SS, Gonugunta VK, Bandyopadhyay A, et al. Significance of PELP1/HDAC2/ miR-200 regulatory network in EMT and metastasis of breast cancer. *Oncogene.* 2014; 33(28):3707–3716.
- Ruivo CF, Adem B, Silva M, Melo SA. The Biology of Cancer Exosomes: Insights and New Perspectives. *Cancer Res.* 2017; 77:6480–6489.
- Runz S, Keller S, Rupp C, et al. Malignant ascites-derived exosomes of ovarian carcinoma patients contain CD24 and EpCAM. *Gynecol Oncol.* 2007; 107(3):563–571.

- Sacchetto R, Testoni S, Gentile A, et al. A defective SERCA1 protein is responsible for congenital pseudomyotonia in Chianina cattle. *Am J Pathol.* 2009; 174:565–573.
- Salhia B, Kiefer J, Ross JT, et al. Integrated genomic and epigenomic analysis of breast cancer brain metastasis. *PLoS One.* 2014; 9:e85448.
- Salomon FV, Geyer H, Gille U, 2008. *Anatomie für die Tiermedizin*, 2nd edn. Enke, Stuttgart, pp. 645–655.
- Sanchez IM, Aplin AE. Hippo: Hungry, hungry for melanoma invasion. *J Invest Dermatol.* 2014; 134:14–16.
- Sanchez-Cespedes R, Suarez-Bonnet A, Millan Y, et al. Use of CD10 as a marker of canine mammary myoepithelial cells. *Vet J.* 2013; 195:192–199.
- Sarli G, Sassi F, Brunetti B, et al. Lymphatic vessels assessment in feline mammary tumours. *BMC Cancer.* 2007; 7:7.
- Sassi F, Benazzi C, Castellani G, et al. Molecular-based tumour subtypes of canine mammary carcinomas assessed by immunohistochemistry. *BMC Vet Res.* 2010; 6:5–13.
- Sato A, Klaunberg B, Tolwani R. In vivo bioluminescence imaging. *Comp Med.* 2004; 54(6):631-634.
- Schabath H, Runz S, Joumaa S, Altevogt P. CD24 affects CXCR4 function in pre-B lymphocytes and breast carcinoma cells. *J Cell Sci.* 2006; 119(Pt 2): 314–325.
- Schackert G, Fidler IJ. Development of in vivo models for studies of brain metastasis. *Int J Cancer.* 1988; 41(4):589–594.
- Scheel C, Weinberg RA. Cancer stem cells and epithelial-mesenchymal transition: concepts and molecular links. *Semin Cancer Biol.* 2012; 22(5-6):296-403.
- Schneider J, Pollan M, Ruibal A, et al. Histologic grade and CD44 are independent predictors of axillary lymph node invasion in early (T1) breast cancer. *Tumour Biol.* 1999; 20:319–330.
- Schwartz S Jr, Yamamoto H, Navarro M, et al. Frameshift mutations at mononucleotide repeats in caspase-5 and other target genes in endometrial and gastrointestinal cancer of the microsatellite mutator phenotype. *Cancer Res.* 1999; 59:2995–3002.
- Shalini S, Dorstyn L, Dawar S, Kumar S. Old, new and emerging functions of caspases. *Cell Death Differ.* 2015; 22(4):526-539.
- Shapovalov Y, Zettel M, Spielman SC, et al. Fluoxetine modulates breast cancer metastasis to the brain in a murine model. *BMC Cancer.* 2014; 14:598.
- Sharma P. Biology and management of patients with triple-negative breast cancer. *Oncologist.* 2016; 21(9):1050-1062.
- Shelke GV, Lässer C, Gho YS, Lötval J. Importance of exosome depletion protocols to eliminate functional and RNA-containing extracellular vesicles from fetal bovine serum. *J Extracell Vesicles.* 2014; 3.
- Shi P, Feng J, Chen C. Hippo pathway in mammary gland development and breast cancer. *Acta Biochim Biophys Sin (Shanghai).* 2015; 47(1):53-59.
- Shi Y, Jin J, Ji W, Guan X. Therapeutic landscape in mutational triple negative breast cancer. *Mol Cancer.* 2018; 17(1):99.
- Shima H, Yamada A, Ishikawa T, Endo I. Are breast cancer stem cells the key to resolving clinical issues in breast cancer therapy? *Gland Surg.* 2017; 6(1):82-88.
- Shin MS, Kim HS, Kang CS, et al. Inactivating mutations of CASP10 gene in non-Hodgkin lymphomas. *Blood.*

- 2002; 99(11):4094–4099.
- Siegel R, Naishadham D, Jemal A. Cancer statistics, 2013. *CA Cancer J Clin.* 2013; 63(1):11–30.
- Silver IA. The anatomy of the mammary gland of the dog and cat. *J Small Anim Pract.* 1966; 7:689–696.
- Simpson RJ, Kalra H, Mathivanan S. ExoCarta as a resource for exosomal research. *J Extracell Vesicles.* 2012; 1.
- Simpson RJ, Lim JWE, Moritz RL. Exosomes: proteomic insights and diagnostic potential. *Expert Rev Proteomics* 2009;6:267–283.
- Singh SK, Clarke ID, Terasaki M, et al. Identification of a cancer stem cell in human brain tumors. *Cancer Res.* 2003; 63:5821-5828.
- Skibinski A, Kuperwasser C. The origin of breast tumor heterogeneity. *Oncogene.* 2015; 34(42):5309–5316.
- Skog J, Würdinger T, van Rijn S, et al. Glioblastoma microvesicles transport RNA and protein that promote tumor growth and provide diagnostic biomarkers. *Nat Cell Biol.* 2008; 10(12):1470–1476.
- Škovierová H, Okajčková T, Strnáděl J, Vidomanová E, Halašová E. Molecular regulation of epithelial-to-mesenchymal transition in tumorigenesis (Review). *Int J Mol Med.* 2018; 41(3):1187-1200.
- Sleeckx N, de Rooster H, Veldhuis Kroeze EJ, Van Ginneken C, Van Brantegem L. Canine mammary tumors, an overview. *Reprod Domest Anim.* 2011; 46(6):1112-1131.
- Smith ZJ, Lee C, Rojalin T, et al. Single exosome study reveals subpopulations distributed among cell lines with variability related to membrane content. *J Extracell Vesicles.* 2015; 4:28533.
- Sneath RJ, Mangham DC. The normal structure and function of CD44 and its role in neoplasia. *Mol Pathol.* 1998; 51:191–200.
- Soares M, Madeira S, Correia J, et al. Molecular based subtyping of feline mammary carcinomas and clinicopathological characterization. *Breast.* 2016; 27:44-51.
- Sokolova V, Ludwig AK, Hornung S, et al. Characterisation of exosomes derived from human cells by nanoparticle tracking analysis and scanning electron microscopy. *Colloids Surf B Biointerfaces.* 2011; 87(1):146–150.
- Song JL, Nigam P, Tektas SS and Selva E. microRNA regulation of Wnt signaling pathways in development and disease. *Cellular signalling.* 2015; 27:1380-1391.
- Soo CY, Song Y, Zheng Y, et al. Nanoparticle tracking analysis monitors microvesicle and exosome secretion from immune cells. *Immunology.* 2012; 136:192–197.
- Sorenmo KU, Rasotto R, Zappulli V, Goldschmidt MH. Development, anatomy, histology, lymphatic drainage, clinical features, and cell differentiation markers of canine mammary gland neoplasms. *Vet Pathol.* 2011; 48(1):85-97.
- Sorenmo KU, Worley DR, Goldschmidt MH. Tumors of the mammary gland. In: Vail D, ed. *Withrow and MacEwen's Small Animal Clinical Oncology.* St Louis, MO: Elsevier; 2013:538–556.
- Soung YH, Lee JW, Kim HS, et al. Inactivating mutations of CASPASE-7 gene in human cancers. *Oncogene.* 2003; 22:6104–6108.
- Soung YH, Lee JW, Kim SY, et al. Somatic mutations of CASP3 gene in human cancers. *Hum Genet.* 2004; 115(2):112-115.
- Spiegelman VS, Slaga TJ, Pagano M, Minamoto T, Ronai ZE, Fuchs SY. Wnt/bcatenin signaling induces the expression and activity of bTrCP ubiquitin ligase receptor. *Mol Cell.* 2000; 5(5):877–882.

- Spinelli C, Montermini L, Meehan B, et al. Molecular subtypes and differentiation programs of glioma stem cells as determinants of extracellular vesicles profiles and endothelial cell-stimulating activities. *J Extracell Vesicles*. 2018; 7(1):1490144.
- Steinhardt AA, Gayyed MF, Klein AP, et al. Expression of Yes-associated protein in common solid tumors. *Hum Pathol*. 2008; 39(11):1582–1589.
- Stewart CJ, Crook ML. Podoplanin and SOX2 expression in CIN 3-like squamous cell carcinoma of the cervix. *Int J Gynecol Pathol*. 2018; 37(1):59–67.
- Stingl J. Detection and analysis of mammary gland stem cells. *J Pathol*. 2009; 217(2):229–241.
- Stirzaker C, Zotenko E, Song JZ, et al. Methylome sequencing in triple-negative breast cancer reveals distinct methylation clusters with prognostic value. *Nat Commun*. 2015; 6:5899.
- Stupp R, Hegi ME, Mason WP, et al. Effects of radiotherapy with concomitant and adjuvant temozolomide versus radiotherapy alone on survival in glioblastoma in a randomised phase III study: 5-year analysis of the EORTC-NCIC trial. *Lancet Oncol*. 2009. 10(5):459–466.
- Sun YF, Yang XR, Zhou J, et al. Circulating tumor cells: advances in detection methods, biological issues, and clinical relevance. *J Cancer Res Clin Oncol*. 2011; 137:1151–1173.
- Svensson KJ, Kucharzewska P, Christianson HC, Sköld S, Löfstedt T. Hypoxia triggers a proangiogenic pathway involving cancer cell microvesicles and PAR-2 – mediated heparin-binding EGF signaling in endothelial cells. *Proc Natl Acad Sci USA*. 2011; 108:13147–13152.
- Szajnik M, Derbis M, Lach M, et al. Exosomes in plasma of patients with ovarian carcinoma: potential biomarkers of tumor progression and response to therapy. *Gynecol Obstet (Sunnyvale)*. 2013; Suppl 4:3.
- Takehara Y, Yamochi T, Nagumo T. Analysis of YAP1 and TAZ expression by immunohistochemical staining in malignant mesothelioma and reactive mesothelial cells. *Oncol Lett*. 2018; 15(5):6825–6830.
- Taketo MM. Shutting down Wnt signal-activated cancer. *Nat Genet*. 2004; 36(4):320–322.
- Talmadge JE, Fidler IJ. AACR centennial series: The biology of cancer metastasis: historical perspective. *Cancer Res*. 2010; 70:5649–5669.
- Tamm C, Bower N, Anneren C. Regulation of mouse embryonic stem cell self-renewal by a Yes-YAP-TEAD2 signaling pathway downstream of LIF. *J Cell Sci*. 2011; 124:1136–1144.
- Tan R, Wang L, Song J, Li J, He T. Expression and significance of Twist, estrogen receptor, and E-cadherin in human breast cancer cells and tissues. *J Cancer Res Ther*. 2017; 13(4):707–714.
- Tanaka K, Tokunaga E, Inoue Y, et al. Impact of expression of vimentin and axl in breast cancer. *Clin Breast Cancer*. 2016; 16(6):520–526.
- Tauro BJ, Greening DW, Mathias RA, et al. Two distinct populations of exosomes are released from LIM1863 colon carcinoma. *Mol Cell Proteomics*. 2013; 12:587–598.
- Tauro BJ, Greening DW, Mathias RA, et al. Comparison of ultracentrifugation, density gradient separation, and immunoaffinity capture methods for isolating human colon cancer cell line LIM1863-derived exosomes. *Methods*. 2012; 56:293–304.
- Taylor-Papdimitriou J, Lane EB. Keratin expression in the mammary gland. In *The Mammary Gland: Development Regulation and Function*, Daniel CW (ed). Plenum Press: New York, 1987; 181–215.
- Teng Y, Wang X, Wang Y, Ma D. Wnt/b-catenin signaling regulates cancer stem cells in lung cancer A549 cells. *Biochem Biophys Res Commun*. 2010; 392(3):373–379.

- Thamm K, Graupner S, Werner C, Huttner WB, Corbeil D. Monoclonal antibodies 13A4 and AC133 do not recognize the canine ortholog of mouse and human stem cell antigen prominin-1 (CD133). *PLoS One*. 2016; 11(10):e0164079.
- Tharp KM, Kang MS, Timblin GA. Actomyosin-mediated tension orchestrates uncoupled respiration in adipose tissue. *Cell Metab*. 2018; 27(3):602-615.
- Thayanithy V, O'Hare P, Wong P, et al. A transwell assay that excludes exosomes for assessment of tunneling nanotube-mediated intercellular communication. *Cell Commun Signal*. 2017; 15(1):46.
- Théry C, Amigorena S, Raposo G, Clayton A. Isolation and characterization of exosomes from cell culture supernatants and biological fluids. Chapter 3, unit 22 in Bonifacino JS, Dasso M, Harford JB, Lippincott-Schwartz J, Yamada KM, eds. *Current Protocols in Cell Biology*. 2006. John Wiley and Sons.
- Thery C, Boussac M, Veron P, et al. Proteomic analysis of dendritic cell-derived exosomes: A secreted subcellular compartment distinct from apoptotic vesicles. *J Immunol*. 2001; 166:7309–7318.
- Thery C, Clayton A, Amigorena S, Raposo G. Isolation and characterization of exosomes from cell culture supernatants. *Curr Protoc Cell Biol*. 2006;m3.22.1-3.22.29.
- Thiery JP, Acloque H, Huang RYJ, Nieto MA. Epithelial-mesenchymal transitions in development and disease. *Cell*. 2009; 139(5):871–890.
- Timmermans-Sprang EP, Gracanin A, Mol JA. High basal Wnt signaling is further induced by PI3K/mTor inhibition but sensitive to cSRC inhibition in mammary carcinoma cell lines with HER2/3 overexpression. *BMC Cancer*. 2015; 15:545.
- Tirino V, Desiderio V, Paino F, et al. Cancer stem cells in solid tumors: an overview and new approaches for their isolation and characterization. *FASEB J*. 2013; 27:13-24.
- Tirino V, Desiderio V, Paino F, et al. Human primary bone sarcomas contain CD133+ cancer stem cells displaying high tumorigenicity in vivo. *FASEB J*. 2011; 25:2022-2030.
- Tomasson MH. Cancer stem cells: a guide for skeptics. *J Cell Biochem*. 2009; 106(5):745–749.
- Tran HD, Luitel K, Kim M, et al. Transient SNAIL1 expression is necessary for metastatic competence in breast cancer. *Cancer Research*. 2014; 74(21):6330–6340.
- Trietsch MD, Spaans VM, ter Haar NT, et al. CDKN2A(p16) and HRAS are frequently mutated in vulvar squamous cell carcinoma. *Gynecol Oncol*. 2014; 135:149–155.
- Urabe F, Kosaka N, Yoshioka Y, Egawa S, Ochiya T. The small vesicular culprits: the investigation of extracellular vesicles as new targets for cancer treatment. *Clin Transl Med*. 2017; 6:45.
- Uyama R, Hong SH, Nakagawa T, et al. Establishment and characterization of eight feline mammary adenocarcinoma cell lines. *J Vet Med Sci*. 2005; 67(12):1273-1276.
- Uyama R, Nakagawa T, Hong SH. Establishment of four pairs of canine mammary tumour cell lines derived from primary and metastatic origin and their E-cadherin expression. *Vet Comp Oncol*. 2006; 4(2):104-113.
- Vakkala M, Paakko P, Soini Y. Expression of caspases 3, 6 and 8 is increased in parallel with apoptosis and histological aggressiveness of the breast lesion. *Br J Cancer*. 1999; 81:592–599.
- Valastyan S, Weinberg RA. Tumor metastasis: molecular insights and evolving paradigms. *Cell*. 2011; 147(2):275-292.
- Van Blitterswijk WJ, De Veer G, Krol JH, Emmelot P. Comparative lipid analysis of purified plasma membranes and shed extracellular membrane vesicles from normal murine thymocytes and leukemic GRSL cells. *Biochim Biophys Acta*. 1982; 688:495–504.

- van der Pol E, Coumans FA, Grootemaat AE, et al. Particle size distribution of exosomes and microvesicles determined by transmission electron microscopy, flow cytometry, nanoparticle tracking analysis, and resistive pulse sensing. *J Thromb Haemost.* 2014; 12(7):1182–1192.
- Vaswani K, Koh YQ, Almughlliq FB, Peiris HN, Mitchell MD. A method for the isolation and enrichment of purified bovine milk exosomes. *Reprod Biol.* 2017; 17:341–348.
- Velasco-Velázquez MA, Popov VM, Lisanti MP, Pestell RG. The role of breast cancer stem cells in metastasis and therapeutic implications. *Am J Pathol.* 2011; 179(1):2–11.
- Vermeulen L, De Felipe, Sousa EM, et al. Wnt activity defines colon cancer stem cells and is regulated by the microenvironment. *Nat Cell Biol.* 2010; 12(5):468–76.
- Vermeulen L. Keeping stem cells in check: A hippo balancing act. *Cell Stem Cell.* 2013; 12(1):3–5.
- Vestad B, Lorente A, Neurauter A, et al. Size and concentration analyses of extracellular vesicles by nanoparticle tracking analysis: a variation study. *J Extracell Vesicles.* 2017; 6(1):1344087.
- Vickers KC, Palmisano BT, Shoucri BM, Shamburek RD, Remaley AT. MicroRNAs are transported in plasma and delivered to recipient cells by high-density lipoproteins. *Nat Cell Biol.* 2011; 13:423–433.
- Vickers KC, Remaley AT. Lipid-based carriers of microRNAs and intercellular communication. *Curr Opin Lipidol.* 2012; 23:91–97.
- Visvader JE, Stingl J. Mammary stem cells and the differentiation hierarchy: Current status and perspectives. *Genes Dev.* 2014; 28(11):1143–1158.
- Waldenström A, Genneback N, Hellman U, Ronquist G. Cardiomyocyte microvesicles contain DNA/RNA and convey biological messages to target cells. *PLoS One.* 2012; 7(4):e34653.
- Wang H, Zhang Y, Du Y. Ovarian and breast cancer spheres are similar in transcriptomic features and sensitive to fenretinide. *Biomed Res Int.* 2013; 2013:510905.
- Wang R, Lv Q, Meng W, et al. Comparison of mammosphere formation from breast cancer cell lines and primary breast tumors. *J Thorac Dis.* 2014; 6(6):829-837.
- Wazir U, Newbold RF, Jiang WG, Sharma AK, Mokbel K. Prognostic and therapeutic implications of mTORC1 and Rictor expression in human breast cancer. *Oncol Rep.* 2013; 29:1969–1974.
- Weigelt B, Peterse JL and van 't Veer LJ. Breast cancer metastasis: markers and models. *Nat Rev Cancer.* 2005; 5(8):591-602.
- Werbeck JL, Thudi NK, Martin CK, et al. Tumor microenvironment regulates metastasis and metastasis genes of mouse MMTV-PyMT mammary cancer cells in vivo. *Vet Pathol.* 2014; 51(4):868–881.
- Wicha MS, Liu S, Dontu G. Cancer stem cells: An old idea—A paradigm shift. *Cancer Res.* 2006; 66(4): 1883–1890.
- Wiese DA, Thaiwong T, Yuzbasiyan-Gurkan V, Kiupel M. Feline mammary basal-like adenocarcinomas: a potential model for human triple-negative breast cancer (TNBC) with basal-like subtype. *BMC Cancer.* 2013; 13:403.
- Wikman H, Lamszus K, Detels N, et al. Relevance of PTEN loss in brain metastasis formation in breast cancer patients. *Breast Cancer Res.* 2012; 14:R49.
- Woenckhaus C, Giebel J, Failing K. Expression of AP-2 α , c-kit, and cleaved caspase-6 and -3 in naevi and malignant melanomas of the skin. A possible role for caspases in melanoma progression? *J Pathol.* 2003; 201(2):278–287.

- Wolff AC, Hammond ME, Schwartz JN, et al. American Society of Clinical Oncology/College of American Pathologists guideline recommendations for human epidermal growth factor receptor 2 testing in breast cancer. *Arch Pathol Lab Med*. 2007; 131(1):18-43.
- Wu D, Pan W. GSK3: a multifaceted kinase in Wnt signaling. *Trends Biochem Sci*. 2010; 35(3):161-168.
- Wu XY, Liu WT, Wu ZF, et al. Identification of HRAS as cancer-promoting gene in gastric carcinoma cell aggressiveness. *Am J Cancer Res*. 2016; 6(9):1935-1948.
- Wu Y, Ginther C, Kim J, et al. Expression of Wnt3 activates Wnt/ β -catenin pathway and promotes EMT-like phenotype in trastuzumab-resistant HER2-overexpressing breast cancer cells. *Mol Cancer Res*. 2012; 10:1597-1606.
- Xiao D, Ohlendorf J, Chen Y, et al. Identifying mRNA, microRNA and protein profiles of melanoma exosomes. *PLoS One*. 2012; 7(10):e46874.
- Xu HL, Xu WH, Cai Q, et al. Polymorphisms and haplotypes in the caspase-3, caspase-7, and caspase-8 genes and risk for endometrial cancer: a population-based, case-control study in a Chinese population. *Cancer Epidemiol Biomarkers Prev*. 2009; 18:2114-2122.
- Xu R, Greening DW, Zhu H, Takahashi N, Simpson RJ. Extracellular vesicle isolation and characterization: toward clinical application. *J Clin Invest*. 2016; 126:1152-1162.
- Xu T, Wang W, Zhang S, Stewart RA, Yu W. Identifying tumor suppressors in genetic mosaics: the *Drosophila* *lats* gene encodes a putative protein kinase. *Development*. 1995; 121(4):1053-1063.
- Yamashita N, Tokunaga E, Kitao H, et al. Vimentin as a poor prognostic factor for triple-negative breast cancer. *J Cancer Res Clin Oncol*. 2013; 139(5):739-746.
- Yang J, Ii M, Kamei N, et al. CD34⁺ cells represent highly functional endothelial progenitor cells in murine bone marrow. *PLoS One*. 2011; 6(5):e20219.
- Yang J, Mani SA, Donaher JL, et al. Twist, a master regulator of morphogenesis, plays an essential role in tumor metastasis. *Cell*. 2004; 117(7):927-939.
- Yano S, Shinohara H, Herbst RS, et al. Expression of vascular endothelial growth factor is necessary but not sufficient for production and growth of brain metastasis. *Cancer Res*. 2000; 60(17):4959-4967.
- Yao M, Wang Y, Zhang P, Chen H, Xu Z, Jiao J, Yuan Z. BMP2-SMAD signaling represses the proliferation of embryonic neural stem cells through YAP. *J Neurosci*. 2014; 34:12039-12048.
- Ye X, Brabletz T, Kang Y, et al. Upholding a role for EMT in breast cancer metastasis. *Nature*. 2017; 547(7661):E1-E3.
- Yu F, Rasotto R, Zhang H, et al. Evaluation of expression of the Wnt signaling components in canine mammary tumors via RT² Profiler PCR Array and immunochemistry assays. *J Vet Sci*. 2017; 18(3):359-367.
- Yu FX, Zhao B, Panupinthu N, et al. Regulation of the Hippo-YAP pathway by G-protein-coupled receptor signaling. *Cell*. 2012; 150:780-791.
- Yu L, Jiao YJ, Zhou L, et al. [Expressions of OCT4, Notch1 and DLL4 and their clinical implications in epithelial ovarian cancer] [Article in chinese]. *Nan Fang Yi Ke Da Xue Xue Bao*. 2016; 37(4):444-450.
- Zaborowski M, Balaj L, Breakefield XO, Lai C. Extracellular vesicles: composition, biological relevance, and methods of study. *Bioscience*. 2015; 65:783-797.

- Zappulli V, De Cecco S, Trez D. Immunohistochemical expression of E-cadherin and β -catenin in feline mammary tumours. *J Comp Pathol.* 2012; 147(2-3):161-170.
- Zappulli V, De Zan G, Cardazzo B, Bargelloni L, Castagnaro M. Feline mammary tumours in comparative oncology. *J Dairy Res.* 2005; 72:98-106.
- Zappulli V, Rasotto R, Caliarì D, et al. Prognostic evaluation of feline mammary carcinomas: a review of the literature. *Vet Pathol.* 2015; 52(1):46-60.
- Zhang C, Yu D. Advances in Decoding Breast Cancer Brain Metastasis. *Cancer Metastasis Rev.* 2016; 35(4):677-684.
- Zhang JM, Wei K, Jiang M. OCT4 but not SOX2 expression correlates with worse prognosis in surgical patients with triple-negative breast cancer. *Breast Cancer.* 2018; 25(4): 447-455.
- Zhang K, Corsa CA, Ponik SM, et al. The collagen receptor discoidin domain receptor 2 stabilizes Snail1 protein to facilitate breast cancer metastasis. *Nat Cell Biol.* 2013; 15(6):677–687.
- Zhou J. An emerging role for Hippo-YAP signaling in cardiovascular development. *J Biomed Res.* 2014; 28:251–254.
- Zhu C, Li L, Zhao B. The regulation and function of YAP transcription co-activator. *Acta Biochim Biophys Sin (Shanghai).* 2015; 47(1):16-28.
- Zidar N, Gale N, Kojc N, et al. Cadherin-catenin complex and transcription factor Snail-1 in spindle cell carcinoma of the head and neck. *Virchows Arch.* 2008; 453(3):267-274.

SUPPLEMENTARY DATA

	DOG	CAT
CD44	F: 5'-TATTTGTGCTGCAAACCATACA-3' R: 5'-CACATCCAATTATTTTGTCTCT-3'	F: 5'-TTTCCGTGACGACTCAGCAG-3' R: 5'-TCTTCCACCTTTGCCATCAGT-3'
CD133	F: 5'-AATATGGGAAGGCGAGGAGC-3' R: 5'-TGGCCACTTTCACCCCTCAAT-3'	F: 5'-GGCTGAGCTGAGTAAAGCCC-3' R: 5'-TGAAGTGTCCAAAGGGATGACT-3'
OCT4	F: 5'-GTGGAGGAAGCTGACAACAA-3' R: 5'-CTCCAGGTTGCCTCTCACTC-3'	F: 5'-GTGGAGGAAGCTGACAACAA-3' R: 5'-CTCCAGGTTGCCTCTCACTC-3'
SOX2	F: 5'-CATGAAGGAGCACCCGGATTAT-3' R: 5'-CATGCTGTAGCTGCCGTTGC-3'	F: 5'-GACAGCTACGCGCATGA-3' R: 5'-GTTTCATGTAGGTTCTGCGAGC-3'
ACTB	F: 5'-TGGCACCACACCTTCTACAA-3' R: 5'-CCAGAGGCGTACAGGGATAG-3'	F: 5'-TGGCACCACACCTTCTACAA-3' R: 5'-CCAGAGGCGTACAGGGATAG-3'

Table S1. Primer sequences used in phase I of the study.

	HUMAN	DOG	CAT
YAP	F: 5'-TGACCCTCGTTTTGCCATGA-3' R: 5'-GTTGCTGCTGGTTGGAGTTG-3'	F: 5'-GCCAGGCAATGCCGAATATC-3' R: 5'-GTGGTAGGTGCCACTGTTGA-3'	F: 5'-CGGATGGGAACAAGCCATGA-3' R: 5'-CCTCTGGTTCACGGCAAAAC-3'
TAZ	F: 5'-TGGACCAAGTACATGAACCACC-3' R: 5'-CTGGTGATTTGGACACGGTGA-3'	F: 5'-AACAAGTCGGCTATGTGGGG-3' R: 5'-GCTGGACAAGACAGAGCAGT-3'	F: 5'-CTACGCTTCAAGTGGGGAATC-3' R: 5'-TTCATTCCTGCAGCACAGTGG-3'
CCND1	F: 5'-ATCAAGTGTGACCCGACTG-3' R: 5'-CTTGGGTCCATGTTCTGCT-3'	F: 5'-AGTGTGATGCGGACTGTCTC-3' R: 5'-CGCACCTCAAATGTTACAG-3'	F: 5'-AGTTCATTTCCAACCCGCT-3' R: 5'-AGACAGTCCCGCTCACACTT-3'
CTNNB1	F: 5'-GACGGAGGAAGGTCTGAGGA-3' R: 5'-CAAATACCCTCAGGGGAACAGG-3'	F: 5'-GGAATGGCTACCCAAGCTGA-3' R: 5'-AAGACTGTTGCTGCCAGTGA-3'	F: 5'-CAGCAGTTTGTGGAGGGAGT-3' R: 5'-GCAGCTGCACAAACATGGA-3'
ANKRD1	F: 5'-GTGTAGCACCAGATCCATCG-3' R: 5'-CGGTGAGACTGAACCGTAT-3'	F: 5'-GGGAGCAGCAGTGGAAAATT-3' R: 5'-TCAAGTCTTCTAGATTTTCAAGCT-3'	F: 5'-GAGAAAAGCGAGAGGGCAGA-3' R: 5'-TTCCTTACGACCGAAACTT-3'
CTGF	F: 5'-GTGGTCTCTCGCCCTCT-3' R: 5'-TCCAGCACGAGGCTCACG-3'	F: 5'-AGGGCCTCTTTGCGACTTC-3' R: 5'-GCTCCGGTACACAGTTCCTC-3'	F: 5'-GGAGCCTTATTGCAAGTGGT-3' R: 5'-CTCAGCATTCCTCCCGTCTG-3'
SNAIL1	F: 5'-TTCTCACTGCCATGGAATTCC-3' R: 5'-GCAGAGGACACAGAACAGAAA-3'	F: 5'-ACTGCAGCCGTGCCTTTG-3' R: 5'-AAGGTTCCGGGAACAGGCTTTG-3'	F: 5'-CACCTGTTTCATGGGCAATTT-3' R: 5'-CATCGGTGAGGCTGAAGCA-3'
SNAIL2	F: 5'-GCACACTGAGTGACGCAATCA-3' R: 5'-AGCACAGGAGAAAATGCCTTTG-3'	F: 5'-TTTTCTGGGCTGGCCAAA-3' R: 5'-CGCCCAGGCTCACGTATT-3'	F: 5'-TGCAGACCCATTCGGATGT-3' R: 5'-CAGCAGCCAGATTCCTCATGT-3'
TWIST1	F: 5'-GTCTAGAGACTCTGGAGCTGGATAACT-3' R: 5'-CGCCCTGTTTCTTTGAATTTG-3'	-	F: 5'-TTAGAAGAGCAGAACCCAAAT-3' R: 5'-CTGCCCGTCTGGGAATCA-3'
TWIST2	F: 5'-AGGACGGTCCCCACATAGG-3' R: 5'-ACATAAGACCCAGAAGAAAATCCA-3'	-	F: 5'-GGAACCGCAGCAGTGTAGT-3' R: 5'-GGAAGCCACAGATGCACTTTG-3'
ZEB1	F: 5'-GATGATGAATGCGAGTCAGATGC-3' R: 5'-ACAGCAGTGTCTTTGTTGT-3'	F: 5'-AAAATGAGCAAAACCATGATCCTAA-3' R: 5'-CCCTGCCTCTGGTCTCTTC-3'	F: 5'-CCCACAGCACCACAGATAAGG-3' R: 5'-TGAATTCATAATCCACAGTTCA-3'
ZEB2	F: 5'-CCAGCTCGAGCGGCATA-3' R: 5'-GCCACACTCTGTGCATTTGAA-3'	F: 5'-TTACCCAGGTCGCCCATA-3' R: 5'-TTAGCCTGAGCGGAGGATCA-3'	F: 5'-CACGATCCAGACCGAGTTA-3' R: 5'-GTCGCGTTCCTCCAGTTTTC-3'
ACTB	F: 5'-TGGCACCACACCTTCTACAA-3' R: 5'-CCAGAGGCGTACAGGGATAG-3'	F: 5'-TGGCACCACACCTTCTACAA-3' R: 5'-CCAGAGGCGTACAGGGATAG-3'	F: 5'-TGGCACCACACCTTCTACAA-3' R: 5'-CCAGAGGCGTACAGGGATAG-3'

Table S2. Primer sequences used in phase II of the study.

